Mitigation of Impulsive Noise for SISO and MIMO G.fast Systems

Israa Ali Al-Neami

Newcastle University

Newcastle Upon Tyne, UK

A thesis submitted for the degree of

Doctor of Philosophy

October 2019

To the soul of my father and my loving husband and children.

Declaration

NEWCASTLE UNIVERSITY

SCHOOL OF ELECTRICAL AND ELECTRONIC ENGINEERING

I,Israa Ali Al-Neami , declare that this thesis is my own work and it has not been previously submitted, either by me or by anyone else, for a degree or diploma at any educational institute, school or university. To the best of my knowledge, this thesis does not contain any previously published work, except where another person's work used has been cited and included in the list of references.

Signature:

Student: Israa Ali Al-Neami

Date:

SUPERVISOR'S CERTIFICATE

This is to certify that the entitled thesis "'Mitigation of Impulsive Noise for SISO and MIMO G.fast Systems' has been prepared under my supervision at the school of Electrical and Electronic Engineering / Newcastle University for the degree of PhD in Electrical and Electronic Engineering.

Signature:

Supervisor: Dr. Martin Johnston

Date:

Acknowledgements

Foremost, I would like to express my sincere gratitude to my advisor Dr. Martin Johnston. This thesis would not have been possible without the direction, leadership, and kind nature of Martin Johnston. Many thanks for his continuous support of my Ph.D study and research, for his patience, motivation, enthusiasm, and immense knowledge. His guidance helped me in all the time of research and writing of this thesis especially he helped me during hard times of my PhD journey. I could not have imagined having a better advisor and mentor for my Ph.D study. A very special gratitude goes out to Dr.Cornelius Healy for his encouragement, insightful comments,and hard questions. He was not only a confidant, but also a consultant on the challenges I faced during my project.

Most importantly, none of this could have happened without him: my loving husband, Ali Adel Alqaisi who believed in me and demanded me to accomplish as much as I possibly could. He was the fuel which kept my engine going throughout my hard PhD journey. it would be an understatement to say that, as a My soul, we have experienced some ups and downs in the first three years. Every time I was ready to quit, you did not let me and I am forever grateful. This dissertation stands as a testament to your unconditional love and encouragement.

My lovely daughter and best friend, Noor and My son, Ayham thanks for you because you were selfishness with me and gave me more than i gave you. Many warm hugs by your little hands that you gave it to me. I owe all of them and hope to make them proud in the years to come. To my life-coach, my second father Haji Adel Alshaikhli, My Mother, and my Aunt Um Mahmood: because I owe it all to you. Many Thanks! My forever interested, encouraging and always enthusiastic: they were always keen to know what I was doing and how I was proceeding, although it is likely that they have never grasped what it was all about!

Who offered their encouragement through phone calls and letters every week – despite my own limited devotion to correspondence. I will miss your screams of joy whenever a significant momentous was reached and also just your general impudence.

My eternal cheerleaders and friends, Harith Fakher and Banfsaj Rasool: I miss your interesting, long-lasting chats and sometime long-lasting fighting! They continuous encouragement throughout my years of study and through the process of researching and writing this thesis. This accomplishment would not have been possible without them. Banfsaj and Harith were there for me like a sister and a brother during the ups an downs and encouraged me never to give up. Thank you!

I am also grateful to my friend, Safaa Awny who accepted me with open arms when I first arrived in our Merz Court school at the university of Newcastle and did everything for me to settle in. Zhen Mei, Wael Abd Alaziz my colleagues at the university of Newcastle, and Khaled M. Rabie, research assistant at the school of engineering in Manchester Metropolitan university thanks for their unfailing support and assistance, for the stimulating discussions. Wael Abd Alaziz thanks for the sleepless night we were working together before deadline.

Last but not the least,I thank all my colleagues who through their kind humour made my PhD journey drops of sunlight where we all eating and laughing together in the kitchen of school, and wishing the best for one another.

I also feel obligated to express my sincere gratitude to the University of Technology for choosing me for their PhD scholarship and The Higher Committee For Education Development in Iraq(HCED) for granting me the funds to study in UK. In addition, there was ample support towards my stay in the UK from the Iraqi Cultural Attaché in London whom I give thanks for.

Abstract

To address the demand for high bandwidth data transmission over telephone transmission lines, International Telecommunication Union (ITU) has recently completed the fourth generation broadband (4GBB) copper access network technology, known as G.fast.

Throughout this thesis, extensively investigates the wired broadband G.fast coding system and the novel impulsive noise reduction technique has been proposed to improve the performance of wired communications network in three different scenarios: single-line Discrete Multiple Tone (DMT)- G.fast system; a multiple input multiple-output (MIMO) DMT-G.fast system, and MIMO G.fast system with different crosstalk cancellation methods. For each of these scenarios, however, Impulsive Noise (IN) is considered as the main limiting factor of performance system.

In order to improve the performance of such systems, which use higher order QAM constellation such as G.fast system, this thesis examines the performance of DMT G.fast system over copper channel for six different higher signal constellations of $M = 32, 128, 512, 2048, 8192$ and 32768 in presence of IN modelled as the Middleton Class A (MCA) noise source.

In contrast to existing work, this thesis presents and derives a novel equation of Optimal Threshold (OT) to improve the IN frequency domain mitigation methods applied to the G.fast standard over copper channel with higher QAM signal constellations. The second scenario, Multi-Line Copper Wire (MLCW) G.fast is adopted utilizing the proposed MLCW Chen model and is compared to a single line G-fast system by a comparative analysis in terms of Bit-Error-Rate(BER) performance of implementation of MLCW-DMT G.fast system. The third scenario, linear and non-linear crosstalk crosstalk interference cancellation methods are applied to MLCW G.fas and compared by a comparative analysis in terms of BER performance and the complexity of implementation.

Contents

List of Figures

List of Tables

Nomenclature

Symbols

$R(f)$	The series resistance parameter of twisted pair
$L(f)$	The series inductance parameter of twisted pair
$C(f)$	The shunt capacitance parameter of twisted pair
f	The frequency
$G(f)$	The shunt conductance parameter of twisted pair
$Z_S(f)$	The longitudinal impedance
Γ	The ratio of Gaussian to impulsive noise power
$Y_P(f)$	The shunt admittance parameter of cable
$\gamma(f)$	The propagation constant parameter
T_b	The blanking threshold
T_c	The clipping threshold
T_h	The fixed threshold value
T^{opt}	The optimal threshold value
μ	The mean of the normal distribution
σ^2, σ_G	The variance of the Gaussian noise
σ_i^2	The variance of the impulsive noise
σ_m^2	The variance of Middleton class A noise
A	The index of Middleton class A noise

B	The channel bandwidth
$Z_0(f)$	the characteristic impedance parameter
$\alpha(f)$	The attenuation constant parameter of twisted pair
$\beta(f)$	The phase constant considered as the imaginary part of a propagation constant $\gamma(f)$
E_b	The energy per bit
E_s	The energy per symbol
N_0	Noise power
$Q(x)$	Q-function of x
R_c	Code rate
$K1$	Constant parameter
$K2$	Constant parameter
$\mathrm{SNR_G}$	Geometric signal-to-noise ratio

Acronyms/Abbreviations

ADC	Analog-to-Digital Converter
ADSL	Asymmetric Digital Subscriber Line
AWGN	Additive white Gaussian noise
BER	Bit Error Rate
BPL	Broadband Power Line
BT	British Telecommunication
CATV	Cable Television Services
CP	Cyclic Prefix
DMT	Discrete Multi-Tone
DSL	Digital Subscriber Line

FD	Frequency Domain
FDD	Frequency Division Duplexing
FEXT	Frequency Division Duplexing
FFT	Fast Fourier transform
FTTH	Fiber TO The Home
4GBB	Fourth Generation Broadband
G.fast	Fast access to subscriber
GF	Galois field
IFT	Inverse Fourier transform
IN	Impulsive Noise
ISI	Inter-Symbol Interference
ITU	International Telecommunication Union
LDPC	Low-density parity-check
MCA	Middleton Class A
MMSE	Minimum Mean-Square-Error
MIMO	Multi-input multi-output
MLCW	Multiple Line Copper Wire
NEXT	Near-end crosstalk
OFDM	Orthogonal frequency-division multiplexing
OT	Optimal Threshold
PL	Power line
QAM	Quadrature amplitude modulation
RS	Reed Solomon
SISO	Single-Input Single-Output

SIC	Successive Interference Symbol
SNR	Signal to noise ratio
TCM	Trellis coded Modulation
4D-TCM	four-Dimensional Trellis coded Modulation
TD	Time Domain
TDD	Time Division Duplexing
VDSL	Very high speed DSL
XDSL	Advanced DSL
ZF	Zero forcing

Chapter 1

Introduction

1.1 Overview

Successive generations of digital subscriber line (DSL) technology combined with the evolution from full copper architecture to fiber-to-the-home (FTTH) has brought fiber closer to the customer and gradually shortened the remaining copper loop [1]. The International Telecommunication Union (ITU) has recently established an advanced xDSL technology which is considered as the fourth generation broadband over copper communications infrastructure under the working name G.Fast, where Fast means Fast Access to Subscriber Terminals [2].

One of the major benefits of DSL technology is the leverage of the existing infrastructure of telephone networks to afford feasible broadband services. This feature means a thorough understanding of the telephony environment is of vital significance for the effective design and deployment of DSL technology [3]. The investigation of the upcoming fast access to subscriber terminals (G.fast.) standard is a niche research area and there is excessive scope for producing novel works in this research area by combining G.fast coded system with signal processing techniques such as equalization, Discrete Multiple Tone (DMT), channel estimation and MIMO, and justify how this improves the quality of communications over copper and help DSL modems to overcome the channel impairment such as path loss, fading, and noise.

In this thesis, the fourth generation of broadband DSL technology over copper will be examined in harsh environments caused by the impact of impulsive noise in combination with signal processing techniques to improve the BER performance of

G.fast system. The thesis begins with, an overview of the state of the art G.fast. Then, we have designed the DMT G.fast coding system model on the Additive White Gaussian Noise (AWGN) channel using six different cross QAM modulation techniques of order 32,128,512, that can reach 2^{15} QAM. And the BER is obtained and compared for all QAM schemes. The proposed MLCW channel model is shown in this work. We have consider a model for 2×2, 4×4, 8×8 and 16×16 MIMO configurations of the G.fast copper channel system using high order QAM techniques. Analogous to the MIMO in the wireless system, MLCW refer to same concept in wired system. Throughout my thesis MLCW and MIMO refer to same concept and can be used interchangeably. Furthermore, two well-known MIMO crosstalk detection,linear and non-linear successive interference cancellation schemes. All these techniques are evaluated and compared in terms of BER performance and complexity criteria.

1.2 Aims and Objectives

The focus of this thesis is the fourth generation broadband system, abbreviated as G.fast, with DMT modulation and concatenated Reed-Solomon(RS) and four-dimensional trellis-coded modulation(4D-TCM) codes RS+4D-TCM. This concatenated coding system plus various signal processing techniques have been evaluated to enhance the BER performance of G.fast system in the presence of impulsive noise on wired copper channels. To achieve this, the following intermediate objectives are addressed:

- To conduct a comprehensive review on the state of the art in DSL broadband communications system.
- To investigate the different existing decoding algorithms such as RS , Viterbi decoding and study methodologies to make them advantageous for impulsive channels.
- To present a simulation analysis of the BER of G.fast coded systems on impulsive noise channels, where time-domain and frequency- domain IN cancellation techniques are studied.
- Employ the well-known twisted pair cable models defined by Chen's model

with, an overview of near-end crosstalk (NEXT) and far-end crosstalk (FEXT) interference.

- To examine the DMT-based G.fast coding system on MIMO channel with Middleton class A noise. MIMO-DMT transmission methods are applied for crosstalk interference cancellation. The computation complexity of interference cancellation techniques required by each detector is estimated and tabulated to provide a reasonable trade-off in the system.

1.3 Statement of Originality

The thesis contributions are focused on the BER performance of G.fast based on the combined RS 4D-TCM coding systems in the presence of IN. The novelty of the thesis is illustrates as follows:

- Chapter 3 presents the BER performance of the G.fast system over a copper channel model for different six cross QAM modulation techniques of order 32,128,512, that can reach 2^{15} QAM. Moreover, in this chapter, the performance of G.fast in the presence of Middleton class A noise is studied. This chapter improves on the performance of impulsive noise (IN) mitigation by proposing and deriving a new threshold-calculation equation for the iterative Zhidkov algorithm, which uses a fixed threshold value. A fair comparison of the signal-to-noise (SNR) performance with an optimal threshold (OT) at different levels of IN using different values of impulsive Index A and the noise ratio Γ, is presented.

- Chapter 4 validates the construction and verification of the proposed MLCW G.fast channel model under the effect of IN. The Zhidkov algorithm using the proposed optimal threshold is proposed as a solution to the IN impact. The contribution of this chapter is a comparative analysis of the bit error probability of a MIMO DMT G.fast system using, firstly, high–order QAM in the presence of Gaussian noise only and the presence of Gaussian and impulsive noise using the Zhidkov algorithm IN cancellation method.

- In chapter 5, the main novelty is implementing a robust MIMO communication system that can mitigate the impact of FEXT which is the dominant limiting

factor on the performance of the twisted-pair based access networks. Then, a performance comparison of linear and non-linear detection techniques are analysed for various MIMO system configurations such as the 4×4, 8×8, 16×16, using high order M-QAM, $32QAM$, $128QAM$ and $512QAM$. Finally, the complexity comparison of crosstalk detection techniques is presented to offer a trade-off between the optimal performance and the reduced complexity implementation.

1.4 Thesis Outline

The thesis is configured as follows:

Chapter 2 begins by providing a theoretical background and literature review of the main aspects that are dealt with in this thesis. Accordingly, a historical overview of the copper access technologies, introduction of coding systems RS and TCM, Middleton's noise model and the state-of-the-art of the fast access to subscriber terminals (G.fast standard) is given. In addition, a general concept of the copper channel models and MIMO system model of wired broadband communication networks is presented.

In chapter 3, a G.fast system model and the encoding and decoding procedures for concatenated $RS + 4D - TCM$ in the presence of Middleton class A impulsive noise are presented. This chapter, gives an overview of the Middleton class A noise channel and the BER performance analysis of the G.fast system on additive Middleton class A noise. Accordingly, a performance comparison between three different IN cancellation methods, Clipping, Blanking, and Zhidkov's algorithm with Middleton Class A impulse noise is presented to investigate the effect of IN on a G.fast system. Finally, an optimal threshold expression is evaluated and applied to Zhidkov's algorithm to accomplish the optimal simulation results of the BER performance of IN cancellation in the frequency domain.

Chapter 4 considers the proposed MIMO copper channel model and explains it in detail with a pair of direct lines, combined with the far-end cross talk (FEXT) effect between the pair of direct lines. Furthermore, a performance analysis comparison between single-line and MLCW G.fast system is introduced. Here different MIMO configurations such as 2×2, 4×4, 8×8, 16×16 are modelled to show the impact in terms of SNR by increasing the number of twisted copper pairs in the same binder

over a 1×1 configuration. An outline of IN cancellation methods for a MIMO G.fast system is studied in this chapter which is used here as a solution to IN mitigation. Finally, the BER is obtained and compared for all MIMO system configurations and it is observed that a significant performance enhancement is provided which mitigates the impact of Middleton Class A noise.

Chapter 5 focuses on studying the behaviour of the MIMO-DMT G.fast system by using linear and non-linear crosstalk cancellation methods under different environments with and without the impact of Impulsive Noise(IN).Then, the effect of increasing the order of cross QAM on the BER performance of the system is also accomplished in this chapter.

Three different MIMO configurations 4×4, 8×8, 16×16 with 32, 128 and 512 cross QAM constellations are used to calculate the BER performance comparison between linear and non-linear MIMO cancelling schemes. Next, the computational complexity for these detection techniques on different MIMO configurations are explained. Finally, it is clearly understood that the balance between the BER performance and the complexity criteria can be accomplished by using the Succsesive Interference SIC ZF and SIC MMSE as a MIMO detectors.

Chapter 6 presents the thesis conclusion and suggestions for upcoming investigation in this field study.

1.5 Publications Related to the Thesis

1. I. Al-Neami, G. Al-Rubaye, M. Johnston and C. Tsimenidis, "Optimal threshold calculation for improved impulsive noise mitigation in the frequency domain", in Proc. IEEE 11th International Symposium on Communication Systems, Networks & Digital Signal Processing (CSNDSP), Budapest, 2018,pp.1-5.

2. I. Al-Neami, C. Healy, M. Johnston and C. Tsimenidis, "Investigation into Impulsive Noise Techniques for a G.fast System", in Proc. IEEE 11th International Symposium on Communication Systems, Networks& Digital Signal Processing (CSNDSP),Budapest,2018, pp.1-5.

3. Israa Al-Neami, Ali J. Al-Askery, Martin Johnston, Charalampos Tsimenidis, "Performance of Coded Multi-Line Copper Wire for G.fast Communications

in the Presence of Impulsive Noise", in Proc. International Conference on Broadband Technologies and Digital Communication Systems (ICBTDCS), Barcelona, 2019.

Chapter 2

Background and Literature Review

2.1 Background

Chapter 2 gives a general background and literature review on DMT based G.fast coding systems in the presence of Impulsive Noise. The next sections will present the basic principles of wired communication system using DMT techniques that are employed in this work. Accordingly, a brief overview of wireline access network technologies such as DSL will be introduced with DMT transmission technology. Historical overview of the various generations of the most pertinent twisted pair access technologies are shown in table 2.1 [4].

During the last three decades, two generation of broadband access systems were employed:The first generation, is considered as the start of data communication voice-band modems and it is based on integrated service digital networks(ISDN)with data rates of 56kb/s that achieved by using a voice band bandwidth of only $3kHz$ (developed by Bell Labs in 1958 [5]). And the second generation, which started with the ADSL(asymmetric digital sub-scriber line)technology that overcomes the basic limitation of the voice band channel by extending the bandwidth and shortening the loops($< 5km$). This gradual increase in bandwidth(up to 1.1MHz in ADSL1 and ADSL2, and 2.2MHz in ADSL2plus)and loop distance led to increase the data rates of the order of 10-20Mb/s [5], [4].

The very high speed DSL(VDSL) which is the third generation that provided customer data rate up to 10Mb/s over shorter loop lengths that is below kilometres.

Generation	*Technology*	*Standards Approved*	*copper loop length*	*Aggregate Rates (bit/s)*
G1	V.32	1984	>10 km	10 k (DS) + 10 k (US)
	V.90	1998	>10km	56 k (DS) + 43 k (US)
G2	ADSL	1999	5km	8 M (DS) + 1 (US)
	ADSL2+	2003	5km	24 M (DS) + 1.3 M (US)
	ADSL2 17a	2006	2km	100 M (DS+US)
G3	ADSL2 17a vectored	2010	1km	150 M (DS +US)
	ADSL2 35b vectored	2014	500 m	350 M (US + DS)
G4	G.fast 106	2015	250 m	1 G (DS + US)
	G.fast 202	expected 2016	250 m	2 G (DS + US)
G5	XG.FAST single pair	expected 2020	70 m	4 G (DS + US)
	XG.FAST two pair	expected 2020	70 m	10 G (DS + US)

Table 2.1: Historical overview of the copper access technologies

This chapter describes the fundamental theory behind the concatenated coding method and the modulation used for G.fast. Furthermore, the concepts of copper access models used with wired communications, Middleton's Noise model, MIMO G.fast and different models of MIMO Detectors are discussed. Finally, a survey on previous works related to the systems are presented.

2.2 Broadband Access Network

Generally, the term broadband refers to high-speed data communications. Broadband targets numerous high-speed transmission technologies such as:

- Digital Subscriber Line (DSL)
- Cable Modem
- Fiber
- Wireless
- Satellite
- Power Lines (PL)

However, the focus in this work will be on upcoming DSL technologies named G.fast (fast access to subscriber terminals) standard system. Wired broadband essentially means there is a physical connection to a physical location (a home or business) through a cable. Mainly, DSL is one of Broadband wireline access networks that targeted high speed internet services by providing a stable bandwidth to the user. These targeted high services such as teleconferencing, e-mail, web browsing, video-on-demand, voice over IP over the Copper telephone lines already installed to homes and businesses [6]. The DSL transmission medium to user can be coaxial cable, optical fiber, twisted pair, or hybrid of fiber and copper [7].

Traditionally, broadband or cable television services (CATV) is delivered via coaxial cables which carry radio frequency signals. The fiber optic technology are comprised of glass fiber strands over which electrical signals are converted to light pulses (on/off) and then optical (light) pulses are sent through these glass fibers around the diameter of a human hair. Another well-established network for wired broadband is Broadband over Power Lines (BPL). Wired Broadband services also

are delivered over the existing low- and medium-voltage electric power distribution network.

2.3 Concept and Review of Twisted Pair Cable Model

Alexander Graham Bell, the pioneer of telecommunications, invented the Copper twisted pair cable in 1881, and which are still important in broadband access networks. During the end of the 19th century, the copper access network found their way with the deployment of telephone lines. Each telephone line is composed of two identical copper wires which are twisted together in order to decreases the electromagnetic leakage between lines [8].

The twisted pair cable is dedicated for the edge part of the telephone network topology, where as particular the broadband access network are connect customers to the central office or street cabinets and the remaining distance to the user is joined with optical fibre transmission. Each twisted pair consists of two identical copper wires, which are twisted together as a single circuit. The twisted pair cable mainly relies on balanced signal circuit principle, where two wires have the same conductor length and same impedance [8]. In particular, electromagnetic coupling signals that increase continuously with frequency in DSL systems and then, the twisting between each pair is not sufficient and all DSL systems have to cope with the electromagnetic leakage between lines [9].

2.4 Modelling of Twisted Pair

Nowadays, there are two essential existing twisted pair models , the first is focused on modelling of the primary line coefficients of series resistance $R(f)$, series inductance $L(f)$, shunt capacitance $C(f)$ and shunt conductance $G(f)$ or their combination, the longitudinal impedance $Z_S(f)$ and the shunt admittance $Y_P(f)$, while the second group estimates the secondary line coefficients of twisted copper pairs which consist of the propagation constant $\gamma(f)$ and the characteristic impedance $Z_0(f)$. Essentially, attenuation constant $\alpha(f)$ is the most significant line frequency characteristic which is considered as a real part of a propagation constant $\gamma(f)$ besides the

a phase constant $\beta(f)$, which denotes the imaginary part of a propagation constant $\gamma(f)$ as given by [10], [11]:

$$\gamma(f) = \alpha(f) + j\beta(f) \quad [dB/k_m, rad/k_m] \tag{2.1}$$

Propagation delay measures the amount of the time required to spread a signal from one end of the circuit to the other. While attenuation measures the amount of energy, which is lost as a result of travelling the Electrical signals along the cabling link. It is important to mention here that all of reference models which equivalent in frequency domain, are exhibiting unrealistic (non-real) behaviours when applied to studies in time domain.

In addition to providing an overview of modelling of twisted pair, in the sections a short review of the most well-known types of cable models; British Telecom (BT), G.fast ITU-T G.9701, Simple Square Root and Chen Models are given. Particularly, the main motivation of these cable models is to achieve good accuracy over the entire frequency range for numerous types of twisted pair cables whereas keeping low complexity and low number of essential parameters. In this thesis, the mathematical model named Chen's model has been applied for the advanced XDSL technology, G.fast. This model is exhibiting very useful presentation when implemented in frequency domain-based computer simulations for performance evaluation of twisted-pair [12]. These reference models have been explained briefly bellow.

2.4.1 British Telecom BT Model

The most often used model is a British Telecom model (BT). This model is based on demonstrating of the primary line coefficients by using 13, 11 or 7 parameters in all. The simplified versions of BT model with 11 or 7 parameters can be provided a less complex but lower accuracy, while the full version of BT model with 13 parameters is commonly suitable for frequency band up to tens or hundreds of MHz and is specified as [10], [12], [13]:

$$R(f) = \frac{1}{\frac{1}{\sqrt{4r_{0C}^4 + a_C \times f^2}} + \frac{1}{\sqrt{4r_{0S}^4 + a_S \times f^2}}}, \quad [\Omega/k_m],$$

$$L(f) = \frac{l_0 + l_\infty \times (\frac{f}{f_m})^b}{1 + (\frac{f}{f_m})^b}, [H/k_m],$$

$$C(f) = c_\infty + c_0 \times f^{-c_e}, [F/k_m],$$

$$G(f) = \mathrm{g}_0 \times f^{\mathrm{g}_e}, \quad [S/k_m]. \tag{2.2}$$

Where $R(f)$, $L(f)$, $C(f)$, and $G(f)$ are the primary line coefficients of series resistance, series inductance, shunt capacitance and shunt conductance respectively. Each one of 13 parameters in the equations above, r_{0C}, a_C, r_{0S}, a_S, l_0, l_∞, f_m, b, c_∞, c_0, c_e, g_0 and g_e, is pointed out separately one type of metallic cable.

2.4.2 G.fast ITU-T G.9701 Model (KPN)

The model presented in recently presented G.fast recommendation G.9701 is based on modified KPN model, which is represented by the primary line coefficients, the longitudinal impedance $Z_S(f)$ and the shunt admittance$Y_P(f)$ as given by:

$$Z_{S(jw)} = jw \times L_{S\infty} + R_{S0} \times \left(1 - q_s q_{\mathrm{x}} + \sqrt{q_s^2 q_{\mathrm{x}}^2 + 2\frac{jw}{ws}\left(\frac{q_s^2 + \frac{jw}{w_s \times q_Y}}{\frac{q_s^2}{q_{\mathrm{x}}} + \frac{jw}{w_s \times q_Y}}\right)}\right), \tag{2.3}$$

$$Y_P(jw) = jw.C_{P0}.(1 - q_C).\left(1 + \frac{jw}{w_D}\right)^{\frac{-2\phi}{\pi}} + jw.C_{P0}.q_C \tag{2.4}$$

This model following the individual 9 parameters, $L_{S\infty}$, R_{S0},C_{P0},q_s, q_{x}, q_Y, q_C,w_D and w_s, which is supplied accurate G.fast channel approximation as a minimum up to 212 MHz. Nevertheless, this model is depended on the large number of parameters which led to its overall complexity, and therefore not adopted in practice applications [10], [12].

2.4.3 Simple Square Root Model

The simplest attenuation constant model is described by a square root of a frequency $\sqrt{f}$ as given by:

$$\alpha(f) = k_1 \times \sqrt{f} \tag{2.5}$$

It is clear from above equation, the model is based only on k_1 which is the parameter specified individually for each type of metallic line and $\sqrt{f}$ the simple square root of frequency. It is able to provide a fast attenuation approximation for selected type of twisted pair cables, particularly for UTP cat.5, 6 and 7 cables at higher frequencies. So, unfortunately, such simplification is constrained and inaccurate for star-quad telecommunication Type cables and cables with higher dielectric constant. Therefore, it is not suitable for several types of metallic cables. Also, make its practical application difficult: this is the reason behind the modification as will be presented in the following section [12], [13], [10].

2.4.4 Chen Model

In the previous model, a fundamental limitations are that low accuracy for telecommunication cables using quad internal configuration as well as higher dielectric constant. Due to that, simple square root model was not very accurate for star-quad (the proportions of pairs) telecommunication type lines and cables with higher dielectric constant.

To successfully deal with this difficulty, Chen [12], [13] advised a modification of simple square root model by adding an additional mathematical term $k_2 \times f$ for simulating linear frequency dependence of attenuation as in:

$$\alpha(f) = k1 \times \sqrt{f} + k_2 \times f \tag{2.6}$$

This model became one of the most used twisted pair cable attenuation models. This is due to the fact, Chen's model typically provides adequate accuracy with attenuation constant $\alpha(f)$ approximation over wide frequency band for numerous types of telecommunication cables. Additionally, The validity of the model was also provided through mathematical derivations presented by Acatauassu et al. [11], where the causality of the model was also corrected and a modification was proposed by adding a phase constant $\beta(f)$ to be suitable with time domain application in the future.

2.5 Wireline DMT Technology

For numerous years, DMT technique has been candidate for DSL systems. Over wide-bandwidths, the DSL channel is frequency selective and has lengthy transmission bands. DMT technique, as well known as Orthogonal Frequency Division Multiplexing (OFDM) technique in the area of wireless communications can effectively divide a broadband frequency selective channel into a large number of frequency-flat narrowband sub-carriers (also known as tones or subchannels). On the other hand, due to long transmission taps the frequency selective channel exhibits frequency dependent attenuation and delay and as a result the transmission symbols are extended and overlap each other. This influence is known as inter-symbol interference(ISI). With a sufficient long cyclic prefix inserted in each symbol, the majority of the ISI impact can be already removed [9].

Originally, ADSL presented in two versions before discrete multi-tone (DMT) was selected for the first ITU-T ADSL standards, G.992.1 and G.992.2. ADSL and VDSL are applicants for modern broadband access. Consequently, all today's installations of DSL are based on the DMT modulation structure [7]. G.fast uses a common building block of DMT modulation scheme and is similar to the DSL technologies such as ADSL/ADSL2. However in contrast to ADSL and VDSL2, G.fast uses time division duplexing(TDD) rather than frequency division duplexing(FDD) to separate upstream and downstream transmission [14]. Basically, the idea of DMT system is to perform signal processing in the frequency domain where the data is carried by N orthogonal subcarriers as showed in Fig. 2.1, G.fast uses $n = 2048$ carriers for the 106 MHz profile and $n = 4096$ carriers for the 212 MHz profile [14]. At the transmitter, a data stream is parallelized into K parallel symbols by the serial to parallel (S/P) block. Typically, the symbols (also called subcarriers) are mapped into complex values C_n according to an M-ary quadrature amplitude modulation (QAM) where k is the subcarrier (subchannel) number, $n = 0, 1, 2, ..., N - 1$. It should hereby be mentioned that DMT is a real modulation format that is the modulated signal can be made real by imposing the Hermitian symmetry in the frequency-domain signal [15], [16], [6]. More details about Hermitian symmetry will be discussed in the next chapter, section 3.3.1.

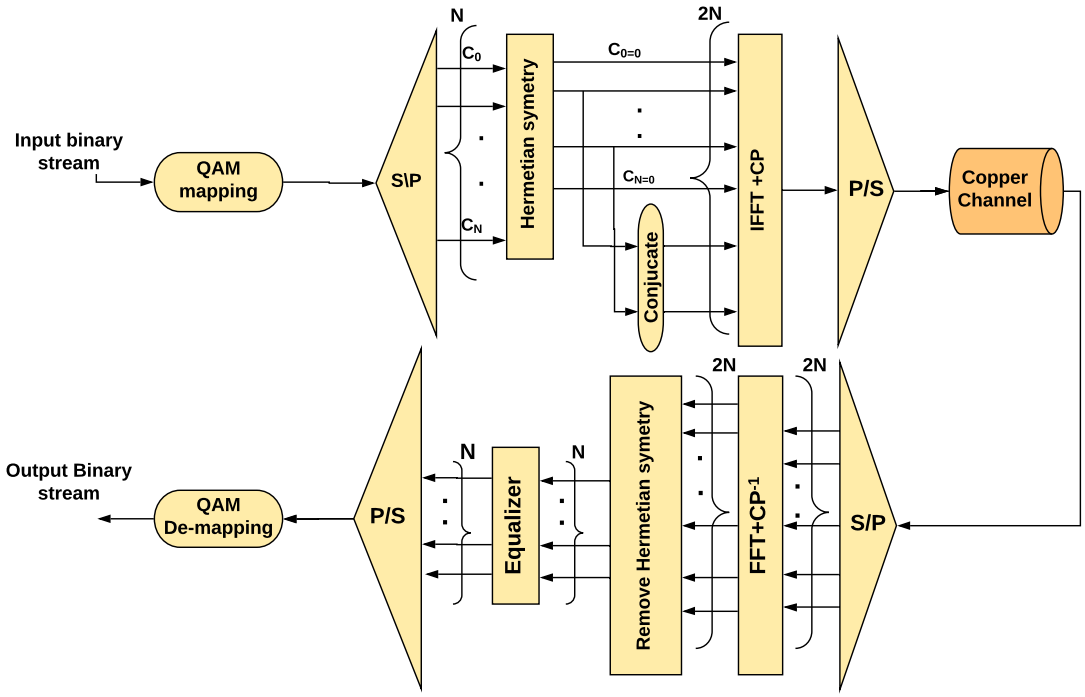

Figure 2.1: The block diagram of DMT transformation over copper channel

After that, each subcarrier is multiplexed and converted to a time-domain DMT symbol by applying the inverse fast Fourier transform (IFFT) such that: [16]

$$c_k = \frac{1}{\sqrt{2N}} \sum_{n=0}^{2N-1} C_n e^{j2\pi k \frac{n}{2N}}, \quad k = 0, 1, ..., 2N-1 \tag{2.7}$$

where c_k ia a real valued time domain signal which Followed by a cyclic prefix effect. A cyclic prefix (CP) is appended to each time domain DMT symbol before transmission to avoid ISI and to maintain effect of the FFT and keep the channel estimation, equalization and time synchronization as simple as possible. At the receiver side, the received signal is digitized by an analog-to-digital converter (ADC). The digital signal is then time synchronized and converted from S/P before being converted to a frequency-domain DMT symbol by fast Fourier Transformation (FFT). The CP is removed first, followed by FFT, and the signal is frequency synchronized and equalized [15], [16], [6].

2.6 FEXT and NEXT Crosstalk

The interfering crosstalk from adjacent copper twisted-pair in the broadband access network is considered as one of the most impairments for high-speed DSL system. This destructive crosstalk between neighbouring DSL systems arises from inherent electromagnetic coupling between the twisted pair cables in the same copper access binder. This crosstalk is classified as far-end crosstalk (FEXT) or near-end crosstalk (NEXT) [9].

FEXT is the interference between upstream lines of different pairs or between downstream lines of different pairs as seen in Fig. 2.2. FEXT depends on the physical properties of the copper cable. The original signal at the transmitters affected by the essential propagation loss of the cable and will be attenuated. In a real network uses a worst case model, FEXT is consider as a function of the crosstalk in the cable and the cable topology [2], [17]:

$$|H_{FEXT,99}(f)|^2 = X_{fext}.l.\,|H(f)|^2\,.f^2 \tag{2.8}$$

where X_{fext} is a a scaling factor whose value depends on the characteristics of the line, $|H(f)|^2$ indicates the attenuation(insertion loss) of the line under Consideration,and $H(f)$ is the direct channel transfer function of the victim line. f is the central frequency of the measured tone $[Hz]$ and l is the coupling length of the disturbing line [9]. Interestingly, studies in[3] have presented that the FEXT effect is much stronger in short cables than in longer ones. The crosstalk originate from the transmitters on the same end is referred to the near end crosstalk (NEXT) as shown in Fig. 2.3. NEXT is thus interference between upstream lines and downstream lines from different pairs [8], [9]. The transfer function for a 99 worst-case NEXT channel is given as:

$$|H_{NEXT,99}(f)|^2 = X_{next}.f^{1.5} \tag{2.9}$$

where X_{next} is a constant. Particularly, the DSL lines are used in a multi-user perception by involve a multi-user or cable binder channel considered as a multiple-input multiple-output (MIMO) channel model. Here the cable binder which contains N number of lines (i.e., users) equipped with DSL Transceivers. each wire pair (i.e. tranceveier) of the cable binder employs DMT as the transmission technique with K

independent parallel subchannels(tones) per line. A large electromagnetic couplings occurs when large number of closely packed twisted pairs are in a typical binder, which lead to significant "crosstalk" [18]. In chapter five, the FEXT impact in detected MIMO-DMT transmission schemes is studied.

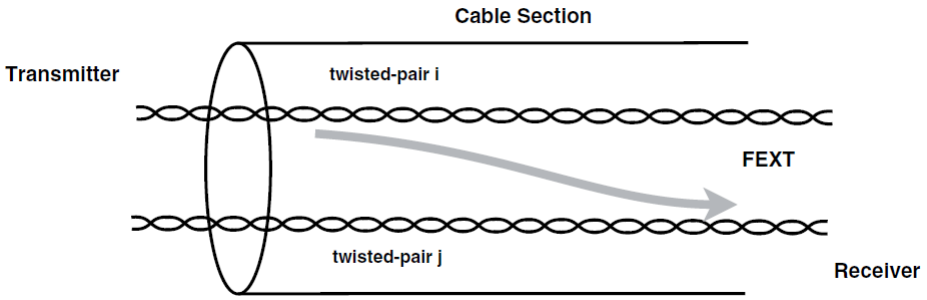

Figure 2.2: FEXT crosstalk in a copper cable binder for a 2×2 DSL network system

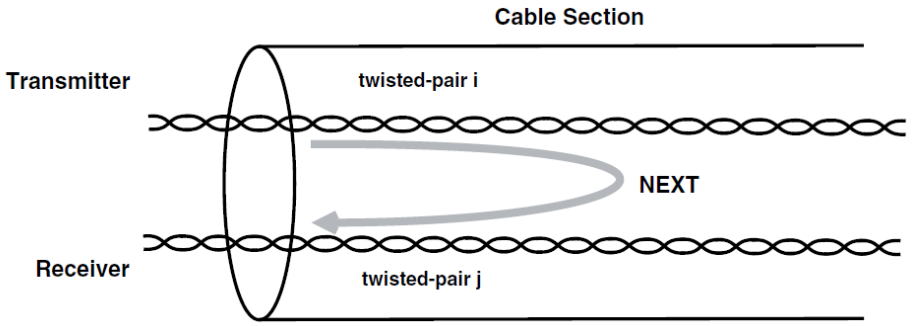

Figure 2.3: NEXT crosstalk in a copper cable binder for a 2×2 DSL network system

2.7 Middleton Class A Distributions

Three statistical noise classes for non-Gaussian channels have been introduced by Middleton. These models are; class A, class B, and class C. Middleton class A was first introduced in 1977, which characterises narrowband noise, while class B, that defines broadband noise. Class C, which is the sum of class A and B models. Since Middleton class A is well known and important factor to describe the channel behaviour in a communications environment, it will be introduced in details in this section. [19, 20].

Middleton class A distributions are commonly used to represent the impulsive noise of wired communication channels [20] and their PDF is defined as:

$$p(X) = \sum_{s=0}^{\infty} \frac{e^{-A} A^s}{s!} . \frac{1}{\sqrt{2\pi\sigma_s^2}} \exp\left(-\frac{|X|^2}{2\sigma_s^2}\right), \tag{2.10}$$

where the variance σ_s^2 is defined as:

$$\sigma_s^2 = \sigma_t^2 \left(\frac{\frac{s}{A} + \Gamma}{1 + \Gamma}\right) \tag{2.11}$$

and

$$\sigma_t^2 = \sigma_G^2 + \sigma_I^2, \qquad \Gamma = \frac{\sigma_G^2}{\sigma_I^2}. \tag{2.12}$$

The parameters σ_G^2 and σ_I^2 are the variances of Gaussian noise and impulsive noise, respectively. Γ is the background to impulsive noise ratio parameter, which indicates the strength of impulsive noise compared to Gaussian noise. A is the impulsive index, which increases the impulsive behavior as it becomes larger that takes values $\leqslant 1$ and becomes Gaussian when A is small. Fig. 2.4 illustrates the Middleton class A noise PDF vs random variables for various values of A. It also compares AWGN and the impulsive PDFs.

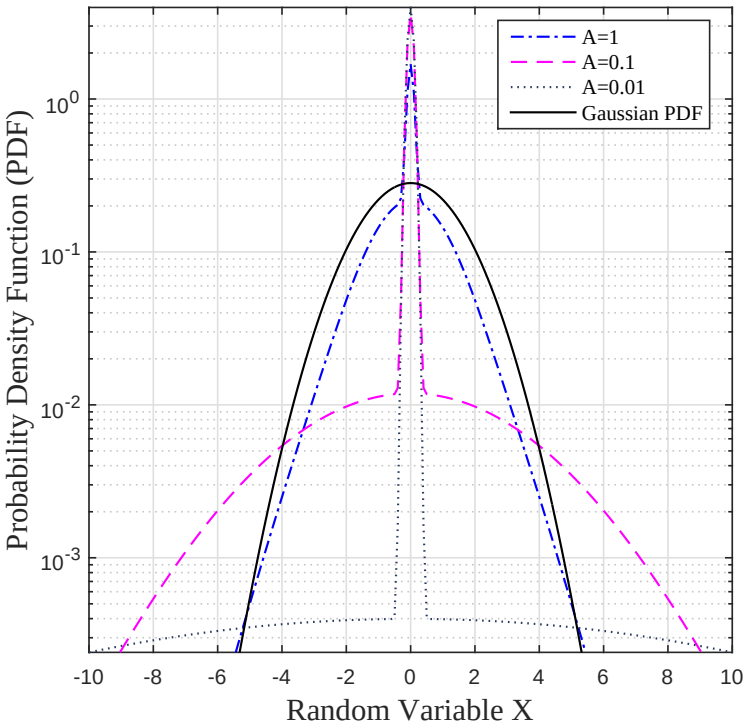

Figure 2.4: PDF Middleton class A distribution.

For more detail about Middleton class A impulsive noise model, which is extensively studied and employed in the literature, please refer to chapter 4, and 5 and [21–26].

2.8 Impulsive Noise Cancellation Methods

Generally, various techniques for impulsive noise mitigation have been discussed in the literature. An overview of simple nonlinearity techniques including blanking and clipping is given in the following subsection. A frequency-domain method for impulsive noise cancellation that was proposed by Zhidkov [6] is also described briefly here.

2.8.1 Time Domain Methods

The function of these techniques is replacing the received time domain affected samples before demodulation by either zero(nulling) or clipping these samples if the peak exceeds a paticular threshold. These traditional approaches are based on the time domain signal r_k which received before the demodulation process using FFT,

i.e., $y_k = f(r_k)$.

$$y_k = \begin{cases} r_k, & |r_k \leq T_c| \\ T_c e^{jarg(r_k)}, & |r_k > T_c| \end{cases}, k = 0, 1, 2, ..., N-1. \tag{2.13}$$

where T_c is the clipping threshold.

$$y_k = \begin{cases} r_k, & |r_k \leq T_b| \\ 0, & |r_k > T_b| \end{cases}, k = 0, 1, 2, ..., N-1. \tag{2.14}$$

where T_b is the blanking threshold.

2.8.2 Frequency Domain Methods

Whereas traditional approaches for impulsive noise cancellation are employed in a time domain before OFDM demodulation. Another approaches compensate impulsive noise in a frequency domain after OFDM demodulation and channel equalizer. This method is discussed in widely overview, and Zhidkov Compensation Algorithm is applied to DMT-based G.fast broadband system and its performance is considered by means of simulation in section 3.3.4 in chapter 3.

2.9 Wireline Multi-Input Multi-Output

Employing more than one twisted pair as a binder at the receiver of the broadband wired accesss networks has the potential of boosting coverage and capacity. Now a whole cable binder is considered as a transmission channel with MIMO. The considered cable binder consists of n wire pairs and therefore a (n, n) MIMO transmission system arises.

Fig. 2.5 illustrates a general block diagram of the wired communication system with multiple transmitting lines Tx and multiple receiving lines Rx on copper twisted pair channels. Here the multi-pair binder which contains U number of lines (i.e. users) equipped with DSL Transceivers. each wire pair (i.e. tranceveier) of the cable binder employs DMT as transmission technique with K independent parallel subchannels (tones) per line.

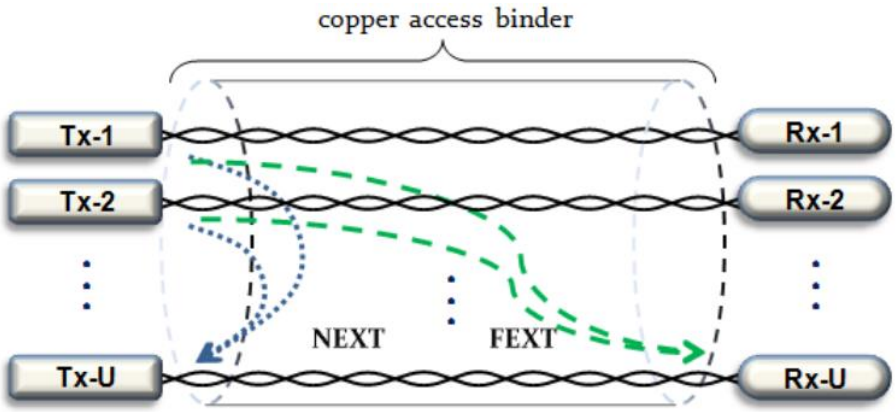

Figure 2.5: General block diagram of wired MIMO system .

In this case the received signal $R\mathrm{x}$ can be calculated at each uth line is given by:

$$R\mathrm{x}^k = \boldsymbol{H}^k T\mathrm{x}^k + w^k \tag{2.15}$$

where

- $T\mathrm{x}^k = [T\mathrm{x}_1^k, T\mathrm{x}_2^k, ..., T\mathrm{x}_U^k]^T$ is the transmitted signal vector on tone k for all N users;
- $w^k = [w_1^k, w_2^k, ..., w_U^k]^T$ is the additive noise vector on tone k including the extrinsic network impairment, e.g., impulse noise, radio frequency interference (RFI), thermal noise and alien crosstalk
- $\boldsymbol{H}^k$ corresponds to a $U \times U$ is the MIMO channel matrix representing the channel transfer functions on tone k.

In order to eliminate the effect of MIMO channel crosstalk there are several types of channel estimations. [27–31]

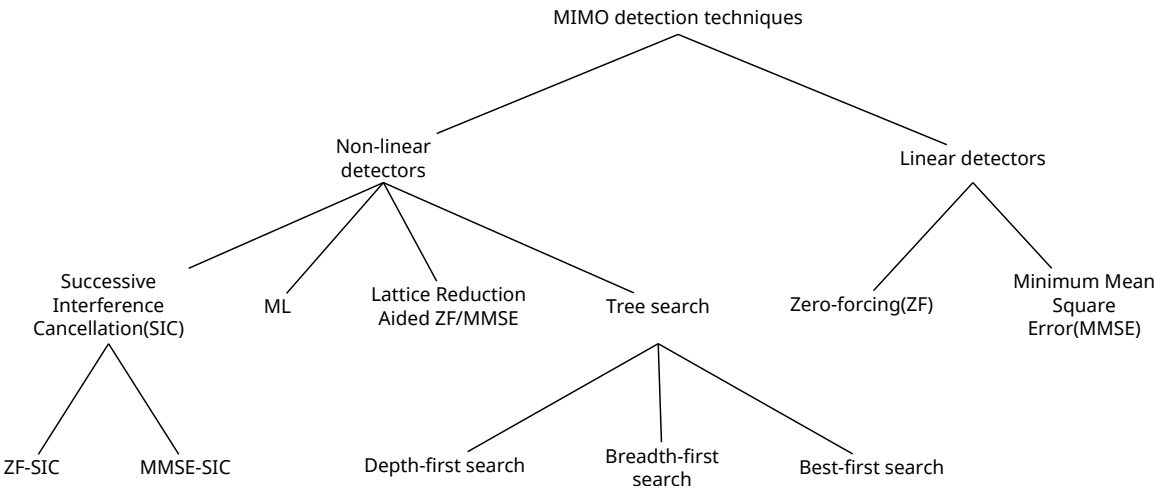

Figure 2.6: The flow chart of MIMO detection techniques

What can be clearly seen in Fig. 2.6 is the continual development of MIMO detection techniques [32]. Detection methods are generally classified into two main approaches, linear detectors such as Zero Forcing (ZF), Minimum Mean-Square-Error Detector (MMSE), and non-linear detectors such as ZF, MMSE, and Maximum Likelihood Detector(ML). The two main approaches, linear and non-linear currently being adopted in this research.

- Zero Forcing Detector (ZF)

  ZF applies the inverse of the channel frequency response, and the weight matrix W_{zf} of ZF detector can be expected as:

$$W_{zf} = \frac{H^*(k)}{|H(k)^2|} \tag{2.16}$$

  where H is the frequency response of channel.

- Minimum Mean-Square-Error Detector (MMSE). The weight matrix W_{mmse} of MMSE detector that is selected to minimize the mean error, can be estimated as:

$$W_{mmse} = (HH^H + \sigma^2 \boldsymbol{I})h_i, \tag{2.17}$$

  where $\boldsymbol{I}$ is the $N_t \times N_r$ identity matrix, H is the frequency response of channel and σ^2 is the variance of noise.

- Maximum Likelihood Detector (ML)

  ML detector is considered as the optimum non-linear detector for a MIMO system. At the receiver, ML detector estimates the transmitted signal vector x_n from the received signal y_m successfully based on the Subsequent minimum distance criterion, which is given by:

$$\hat{x_i} = \sum_{m=1}^{N_r} \left| \boldsymbol{y}_m - \sum_{n=1}^{N_t} h_{mn} x_n \right|^2 \tag{2.18}$$

  where $\hat{x_i}$ is the estimated transmitted signal.

  ML provides optimal error performance but also it suffers from high complexity. ML detector has an exponential complexity increases with M^{N_t}, where M is the number of constellation size. For example, for 128-QAM and 4 transmit antennas, a total of 128^4= 268435456 comparisons per symbol should be executed for each transmitted symbol. Consequently, for high modulation order M which is considered with advanced 4th generation (4G) broadband communications targeting high data rate, ML becomes usefulness. Due to this, ML has been already excluded in this work.

2.10 Introduction of Coding

Currently the demand for development of reliable communication and wireless systems is increasing [33]. Hence detection and correction errors in the information that received over communication channels take in account. Therefore error control coding is essential in communication system design for different applications [33] and then, Channel coding supports the communication system designers to reduce the effects of a noisy communication channel [34].

Since 1940s particular attention is paid to error control coding theory and now being vastly used in communication systems. As clarified by Shannon in his paper published in 1948 [35], there is a parametric quantity called the channel capacity C that is a function of input output characteristics for each physical channel. Shannon displayed that there exist error control codes such that arbitrary small error probability of the data to be conveyed over the channel can be accomplished as long as the data transmission rate is less than the capacity of the channel [34]

, [35]. Performance value is generally determined by BER (Bit–Error-Rate) during digital data transmission and storage processes. BER is explained with Number of error bits/Number of total bits. Forward error correction coding can be classified into two main types: linear block coding and convolution encoding. Reed-Solomon codes derive below the class of linear block codes [34], [36]. An optimum design of coding system is depended on a profound understanding of the channel and noise environment [37].

A widely used channel encoding method is (Error Correcting Code) ECC, ECC is belong to the method of transmitting information from a source to a destination with minimum error. In this system, sequence of digital information data sent to an encoder; the encoder adds a parity(redundant)bits, so a longer sequence of the coded bits called a codeword. Then, the codeword is transmitted to a receiver. Finally, the original data sequences are then recovered by a suitable decoder [34]. Fig. 2.7 shows a generic diagram of typical communication system with channel coding [38].

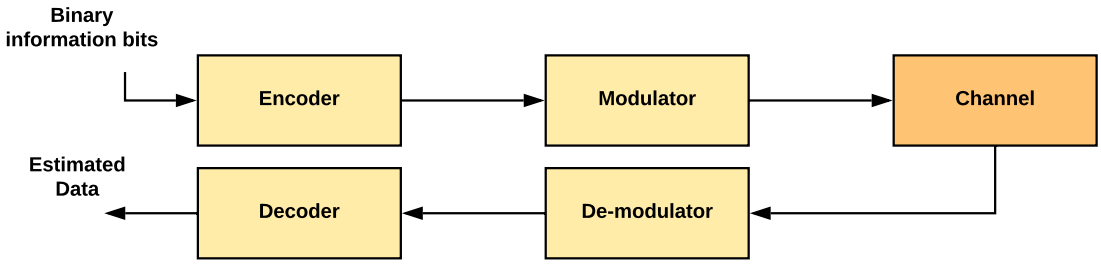

Figure 2.7: A Generic Diagram of Typical Communication System with Channel Coding.

2.10.1 Reed-Solomon code(RS):

RS codes are best for correcting both burst and random errors, so these are more particularly used in digital communication and data storage systems. RS codes are non-binary linear error correcting codes invented in paper by Irving Reed and Gus Solomon On January 2, 1959 [34].

2.10.1.1 Represantation of Reed-Solomon Code

The RS codes are represented as RS (n, k) with s-bit symbols, where n is the code word length and k is the number of original data symbols. Number of parity symbols can be considered by subtracting original data symbols from code word length which is presented as $n - k = 2t$ [39]. Fig. 2.8 depicts the representation of RS codeword. This means that the encoder adds parity symbols to k data symbols of s bits each and make an n symbol code word. There are n-k parity symbols of s bits each. A Reed-Solomon decoder can correct up to t symbols that contain errors in a code word, where $2t = n - k$ [34].

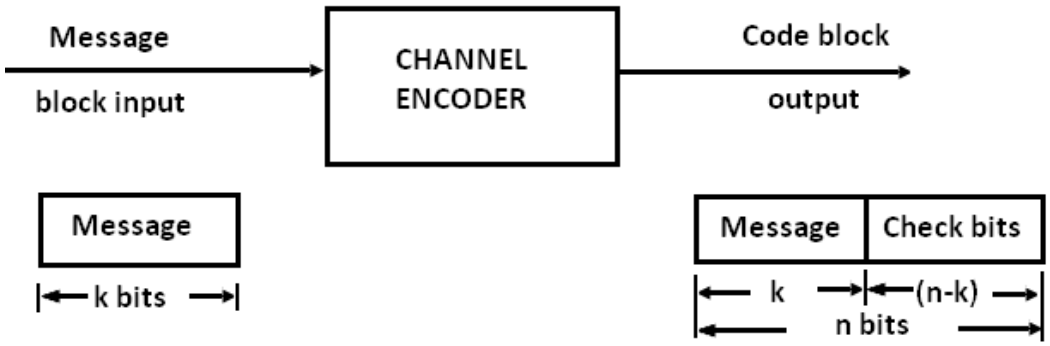

Figure 2.8: The general structure of RS codeword

The relationship between the symbol size, s, and the size of the codeword n, is given by: $n = 2^{s-1}$. For example, known a symbol size (s), the maximum codeword length (n) for a Reed-Solomon code is $n = 2^{s-1}$. For example, the maximum length of a codeword with 7-bit symbols (s=7) is 127 symbols [34], [39].

2.10.1.2 Architectures of RS Encoder and Decoder

Reed-Solomon codes are based on a specialist area of mathematics known as Galois fields or finite fields. A finite field has the property that arithmetic operations (+,-, x, / etc.) on field elements always have a result in the field. A Reed-Solomon encoder or decoder needs to carry out these arithmetic operations. These operations require special hardware or software functions to implement [34], [40].

A Reed-Solomon codeword generation is responsibility of generator polynomial, which has a unique Property that all valid codewords are accurately divisible by the

generator polynomial:

$$g(x) = (x + \alpha)(x + \alpha^2)(x + \alpha^3)...(x + \alpha^{2t}) \tag{2.19}$$

$$= g_0 + g_1 x^1 + g_2 x^2 + ... + g_{2t-1} x^{2t-1} + x^{2t} \tag{2.20}$$

where α is a primitive element in GF (2^m), and $g_0, g_1, g_2, \ldots, g_{2t-1}$ are the coefficients from GF (2^m) [34]. And the codeword c(x) is constructed using: $c(x) = g(x)m(x)$ where c(x) is the codeword polynomial, m(x) is message polynomial [39], [34].

2.10.1.3 RS Encoder:

The $2t$ parity symbol $p(x)$ is the remainder which is generated by dividing message block with the generator polynomial and it is represented as:

$$p(x) = x^{2t} m(x) mod g(x) \tag{2.21}$$

During RS encoding process, the RS codes are encoded by adding the parity symbols at the end of k-symbols message $m(x)$ which is together named codeword $c(x)$ as shown in figure below [41]:

$$c(x) = x^(2t)m(x) + p(x) \tag{2.22}$$

2.10.1.4 RS Decoder:

The RS decoder comprises of a digital circuits and processing components to adopt the following steps [41]:

1. Syndrome calculations.
2. Finding the error location polynomial $\sigma(x)$.
3. Find the error positions (the root of the polynomial).
4. Finding the error values.
5. Correct the received codeword r(x) with the error locations and value found.

The syndrome accumulate is considered the first step in the decoding process, it is done to verify if there is an error in the received codeword. The received codeword r(x) is related to the codeword message c(x) which is transmitted and affected by noise and error polynomial e(x) as:

$$r(x) = c(x) + e(x) \tag{2.23}$$

The syndromes can be accumulated by substituting 2t roots of the generator polynomial $g(x)$ into $r(x)$ and can be represented as below:

$Si = r(\alpha^i), i = 1, 2, 3, ..., 2t$

where $\alpha, \alpha^2, \alpha^3, ..., \alpha^{2t}$ are the roots of $g(x)$ [41], [34].

According to an equation below: $e(x) = e_{j_1}x^{j_1} + e_{j_2}x^{j_2} + ... + e_{j_v}x^{j_h}$ where $e(x)$is the error polynomial, it is contains h $\leq$ t non-zero elements. It means that there are h errors arises through the transmission process, placed at positions $x^{j_1}, x^{j_2}, ..., x^{j_h}$. where $0 \leq j_1 < j_2 < j_3 < \ldots < j_h \leq (n-1)$. The index 1 refer to first error ,. . . , h refer to h^{th} error while the index j refer to error location. To correct the corrupted the received codeword, error locations x^{j_i} and error values e_{j_i} should be determined.

The error location number can be defined as:

$\lambda_l = \alpha^{j_l}$ where l=1,2,...,v.

Then, 2t syndromes can be accumulated by substituted α^i into the received codeword r(x) where i=1,2, . . . ,2t. Afterward, the roots of this polynomial is calculated using Chien search algorithm. Finally, Forney algorithm is used to find the error values. Hence the received codeword can be correct from the positions and values of errors which are obtained from the above two algorithms by XORing with the error vector.

2.10.2 Trellis Coded Modulation (TCM)

In communication systems, ECC reduces the power utilization by adding extra (redundant) bits to the transmitted signal. This procedure requires a high-order modulation scheme, which requires a wider bandwidth and additional signal power would be demanded to achieve the same BER level of system [42]. In order to obtain improved reliability of a digital transmission environment without increasing transmitted power or required bandwidth, TCM is applied to solve the conflict of value efficiency between transmitted power and channel bandwidth [42]. Therefore, TCM

is well suited to use as an attractive scheme that combining error correction coding with modulation in digital communication systems, in particular, the systems having limitations in their transmission bandwidth requirements [43], [44] .

TCM first introduced by Ungerboeck in 1976 [45]. According to Ungerboeck, channel coding and modulation techniques are merged by using high-order signal constellations. Thereby, maximize the minimum Euclidean Distance(ED) between signal codes. The key idea behind TCM is that channel coding and modulation are joined together in order to achieve significant coding gain over uncoded modulation without any bandwidth expansion requirement [46], [38]. As a result, channel coding and modulation are treated as a single entity in TCM scheme [47], [44]. The functional diagram of TCM is depicted in Fig. 2.9 as below [38].

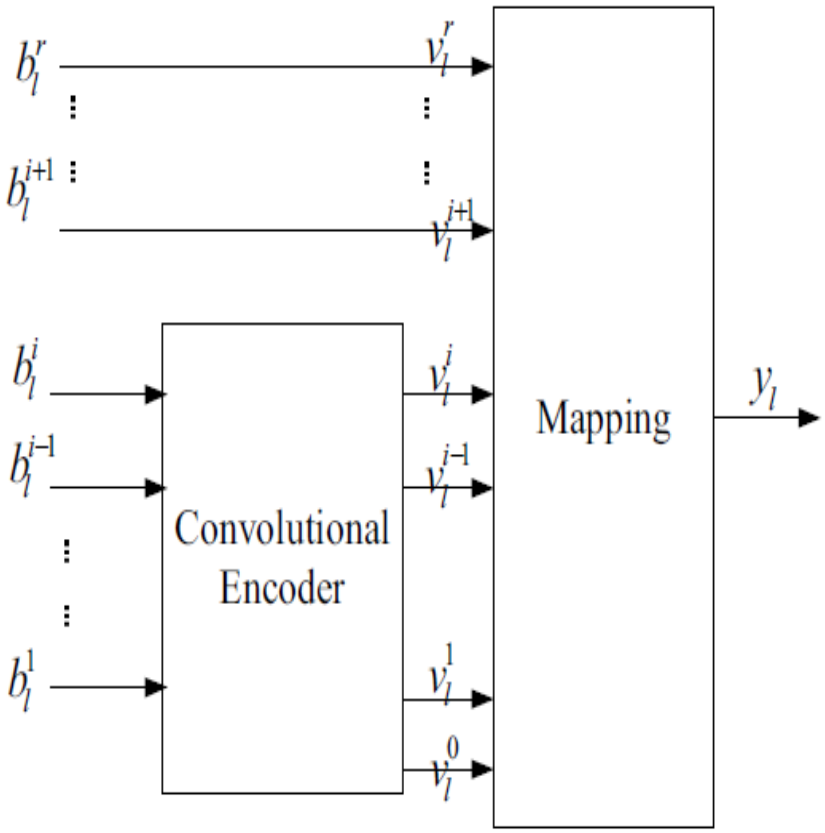

Figure 2.9: General digram of TCM coding system

It is importantly to note, as shown in Fig. 2.9 the TCM encoding system has

the following input/output relationship: $b_l^r = v_l^r, ..., b_l^{i+1} = v_l^{i+1}, b_l^i = v_l^i, ..., b_l^1 = v_l^1$ and v_l^0 represents the parity bit which is generated by the convolutional encoder. Actually, the TCM system is separated into prominent parts: an encoder and a mapper. The uncoded bits $(v_l^r \dots v_l^{k+1})$ are used to choose one subset (partition) in the constellation map which is segmented into $2^r - k$ partitions as stated by Ungerboeck's set partitioning set principle [45]. Whereas the coded bits $(v_l^k \dots v_l^0)$ are used to choose one of the 2^{k+1} points in a partition which is previously selected by uncoded bits. Finally, the TCM symbol $(v_l^r, \dots, v_l^{k+1}, \dots, v_l^0)$ is mapped to a point with specific amplitude and phase in the constellation map [38]. It is significantly to mention that a memoryless mapper following the encoder creates a one-to-one correspondence between the k+1 coded bits and a constellation with 2^{k+1} signals. The particular mapping of the subset signals by coded bits is not particularly important [48].

2.10.2.1 Set Partitioning

In TCM, set partitioning is a significant process after convolutional encoder [42]. The basic to integrate modulation and coding method is to invent a current method for mapping the coded bits into appropriate signal points so that the minimum Euclidean distance is maximized. In 1982, Ungerboeck developed such method, based on the principle of mapping by set partitioning [47], [49]. It is important to remember that is to get the best TCM schemes, the set partitioning method follows three Ungerboeck rules [42]:

- U1: parallel transitions are assigned members of the same partition;
- U2: neighboring transitions are assigned members of the next partition, i.e. transitions stemming from, or merging into the same node;
- U3: make all the signals are used equally often.

According to the set partitioning rules, the M-ary constellation is sequentially partitioned into 2, 4, 8, ..., $2^{(log_2 M)-1}$ subsets, with size M/2, M/4, M/8, ..., 2 with gradually larger minimum distances.

A set partitioning method of the 16-points QAM constellation is explained in the Fig. 2.10 [49].

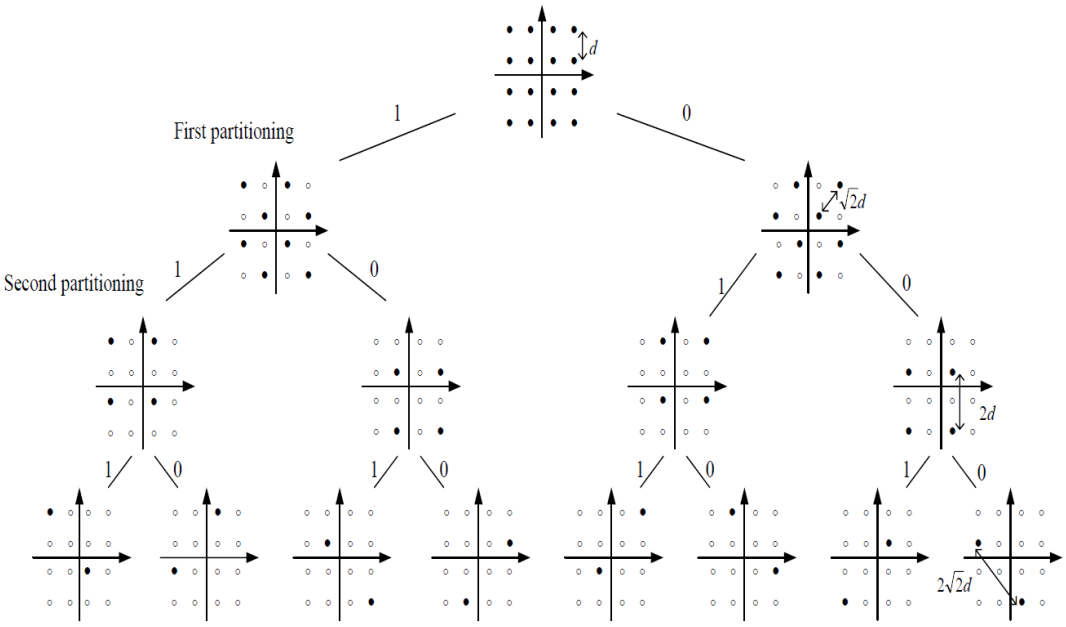

Figure 2.10: Partitioning of the 16-points QAM constellation

In QAM constellation, each level of partitioning increases the minimum Euclidean distance gradually by $\sqrt{2}$ [42]. In Fig. 2.10, the $d$min between points in the subsets is increased by at least a factor of $\sqrt{2}$ with each partitioning. In the first partitioning, the 16-points constellation is partitioned into two 8-point subsets. The square of the minimum Euclidean distance d increases to $\sqrt{2}d$ from d. In the second partitioning, each of the two 8-point subsets is subdivided into two subsets of 4-point, and the square of the minimum Euclidean distance d is increased to 2d. This process continues on the subsets until each subset has only two points, and the square of minimum Euclidean distance d is now increased to $2\sqrt{2}d$.

2.10.2.2 Viterbi Algorithm

In 1967 [50], Andrew Viterbi suggested a standard way to decode convolutional codes and this became the Viterbi Algorithm. A critical feature of this algorithm is the complexity of the decoding process grows linearly with the number of symbols being transmitted, rather than exponentially with the number of the transmitted

symbols.

According to Viterbi algorithm, if a codeword sequence of length K is transmitted, and the received sequence $r_0, r_1, ..., r_{k-1}$ is Detected at the output of the AWGN channel, then the ML receiver looks for the sequence $x_0, x_1, ..., x_{k-1}$ that diminishes as:

$$\sum_{i=0}^{k-1} |r_i - x_i|^2 \tag{2.24}$$

The branch metrics to be used are obtained as follows: firstly, if there are no parallel transitions then the branch in the trellis of the convolutional encoder used for coding is labelled by signal x, so at discrete time i the metric associated with that branch is calculated by $|r_i - x|^2$. While if there are presence of parallel transitions (because of uncoded bits), the branches have labels $x', x'', ...$ in the set x, then the decoder selects the signal among x',x'' ,..., with the minimum distance from r_i (this is a "demodulation" process), then and based on the signal selected, the decoder structures the metric that is $\min_{x^i \epsilon x} |r_i - x^i|^2$.

2.10.2.3 Multi-Dimensional Trellis Coding Modulation (TCM)

The performance improvement of TCM can be achieved by increasing the number of states in trellis coding, this involves the number of shift registers which is used in the convolutional code). On the other hand, the coding gain saturates at the higher number of states (the increase of coding gain is more slowly). To solve this conflict and accomplish higher coding gain, the constellation should be changed. Multi-dimensional constellations signal model is presented in the TCM as an attractive solution for this problem [51], [52]. The fundamental concept of multi-dimensional TCM lies in the fact that it is increasing the number of symbols created in one process period. Multi-dimensional signals can be transmitted as sequences of constituent one (1-D) or two-dimensional (2-D) signals [47]. Hence 2K-D TCM methods are considered, m bits are transmitted per integral 2D signal, and hence mK bits per 2K-D signal are transmitted.

Use of multidimensional constellations in TCM offers a number of advantages, spaces with larger dimensionality have more room for the signals, which can accordingly be spaced at larger Euclidean distances. Hence, an increased noise immunity may achieved from the multidimensional constellation itself. An essential cost with

1-D and 2-D constellations is that when the size of the constellation is doubled over that of an uncoded scheme. The reason behind that lies in the fact that a redundant bits which is generated through convolutional encoder are added every signalling interval. The decoding process of multidimensional TCM begins with comparing received N -dimensional point pairs then building the accrued error metric for each states branch and path. As a primary step, the point in each of the multidimensional subset that is closest to the received point is determined and estimate its linked metric (the squared Euclidean distance between the two points). Fig. 2.11 shows the decoding process of 4-D TCM, it is illustrate how to get the closest point in the 4-D signal constellation and its associated metric [49].

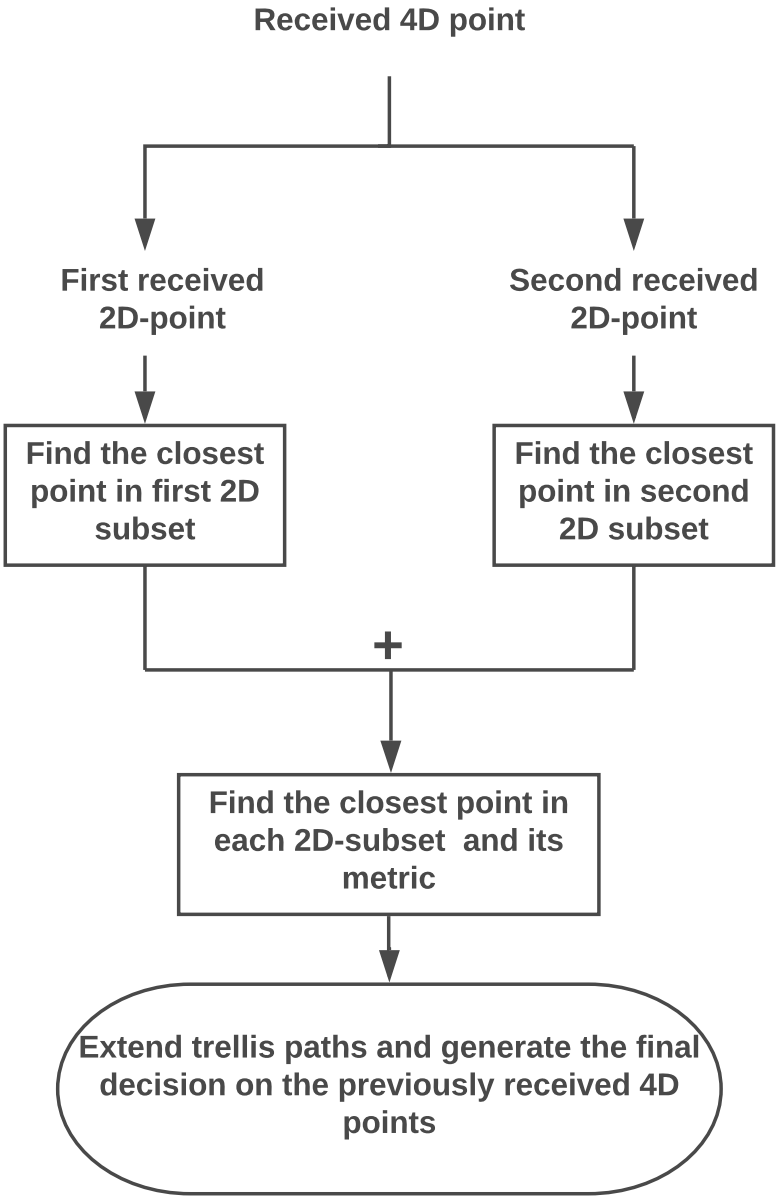

Figure 2.11: Decoding process of 4-D received point in 4-D TCM system

On account of the way a multidimensional constellation is partitioned, the closest point in each multi-dimensional subset and its linked metric may be achieved as follows:

- Each received $2N$-dimensional point is divided into a pair of N-dimensional points;
- The closest point in each $2N$-dimensional subset and its associated metric are found based on the point in each of the N-dimensional subsets that is closest to the corresponding received N-dimensional point;
- The previous procedure may be used iteratively to get the closest point in each 2N-dimensional subset and its associated metric based on the closest point in each of the basic 2D subsets and its associated metric. Based on these metrics, Viterbi decoder will recover the original signal(i.e., the input of the convolutional encoder) [42], [51], [53].

2.11 Concatenated Coding Schemes

As stated by Forney in 1966 [54], a "concatenated" code is designed by combining two different codes, it works to encounter the obstacle of decoding complexity by breaking the essential calculation into manageable sections. The concatenated coding scheme proposed by Forney [54] is an error correcting coding scheme that accomplishes a significant immunity against noise and comparatively high coding gain by using codes that are relatively easy to decode [55], [56]. Coding scheme using the convolutional coding with Viterbi decoding for the inner code and the Reed-Solomon (RS) code for the outer code is a special case of the general concatenated coding scheme proposed by Forney. Fig. 2.12 below shows general concatenated coding scheme [42].

An attractive approach of increasing coding gain in systems using TCM is by concatenating the TCM codes with an outer Reed Solomon code [57]. In Fig. 2.13, a Reed-Solomon block code and TCM code decoded with the Viterbi algorithm are concatenated [58]. It is interesting to note that the concatenated coding system using the 4-D TCM with Viterbi decoding for the inner code and the reed Solomon code used over GF(2^8) for the outer code will be used in this project.

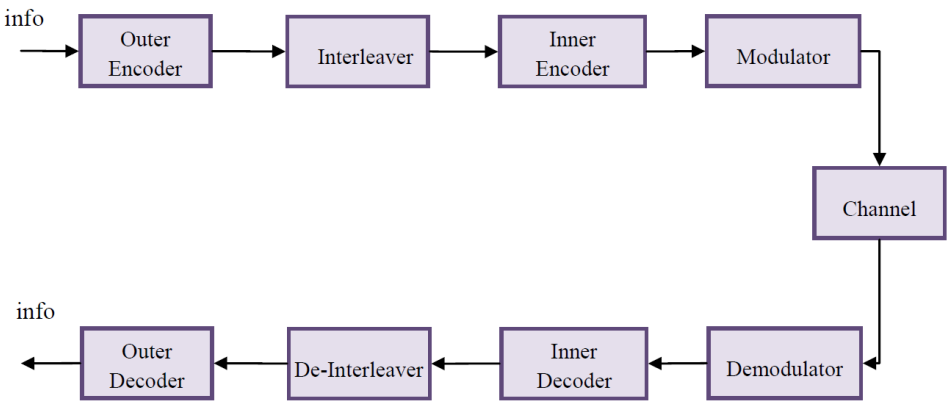

Figure 2.12: General concatenated coding scheme

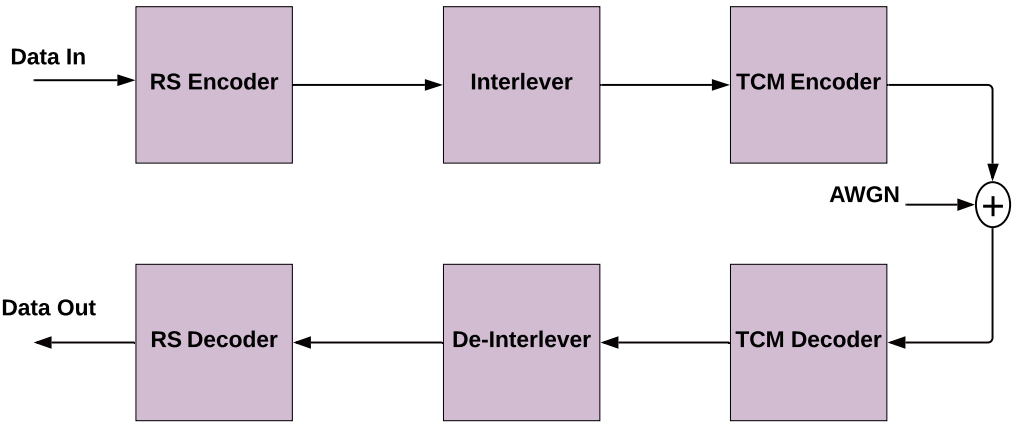

Figure 2.13: Concatenated TCM+RS system scheme

2.12 Literature review

This section surveys previous work related to the DSL Broadband Access System Networks. The survey covers the forth generation DMT-based G.fast standard over copper channel in two different scenarios: single-line DMT based G.fast and MIMO DMT based G.fast systems in the presence of impulsive noise.

2.12.1 DSL Broadband Access System Networks Wireline DMT Technology

The purpose of this section is to review recent research into the upcoming generations of broadband access network. The fast internet access and video on demand services paved the way to 4th generation G.fast. In order to reach the target date rates up to 1G/bs used with broadband services, the fourth-generation(G.fast)was developed and specified in ITU-T G.9700 and G.9701 standards [59]. In which the used frequency(spectrum)is extended to 106MHz and will expected to 212MHz. This broadband system will be the interest of this thesis.

VDSL is being developed to work on high frequencies above ADSL and to meet the rapid growing demand for higher data rates. In 2010, the vectoring is taking into account and led to creating a vectored VDSL2 which is reach the data rates to 150Mb/s for upstream and downstream(US+DS)over short distance up to 1km [4], [60]. Vectoring technology suppresses crosstalk interference limitation and enables VDSL2 rates to crosstalk-free rates. The vectored VDSL2 paved the way to the fourth-generation G.fast [4], [61]. G.fast is a new standard from the International Telecommunication Union, which targets 1Gb/s over short copper loops using frequencies up to 212MHz [4]. While gradually transitioning to FTTH architecture network, many efforts and researches mainly resulted in hybrid fiber-copper architectural solutions(FTTx)used with broadband technologies [5], [59], [62], [63], [64], [65], [33] as in Fig 2.14 [66].

In [33] G.fast-based FTTdp(Fiber To The distributed point)deployment is emerging and provide fiber-like speed (up to 1Gb/s). This work points out that strong Far-End crosstalk(strong FEXT)is the key limiting factor in G.fast environment. This explains the need to an approach which reduce the PSD(Power Spectral Density)of the transmitted signal to fillfull the Power Spectral Denisity(PSD)mask and maximum Aggregate Transmit Power(ATP). This approach also discussed in [67]. The authors in [67]extend the previous studies which considered the power optimization algorithms in VDSL2 to G.fast.

A similar idea has been proposed in [62], this paper highlights the coexistence of G.fast-based FTTdp with VDSL2-based FTTC. This mixed-scenario uses G.fast copper link between DP and CPE(Customer Premise Equipment). As in [33], the Self-FEXT also play a key bottleneck and it reduced by crosstalk cancellation (Vec-

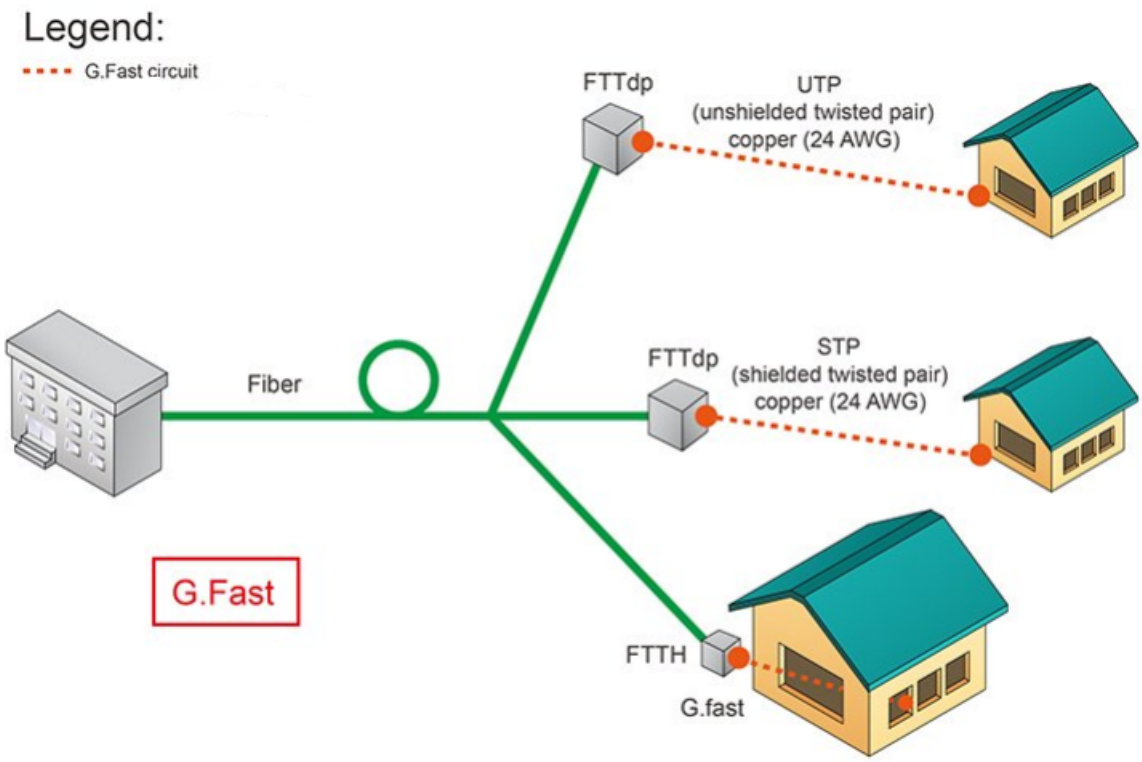

Figure 2.14: G.fast technology

toring).

Another architectural solution which introduced in [64], Pre-G.fast which is considered a solution to paved the way towards the fourth generation broadband network G.fast. Downstream Power Back-Off(DPBO)procedure has been presented to achieve equal aggregate bit rates in the(0-17)MHz band between vectored FTTC and non-vectored FTTdp terminals(mixed scenario). It is important to mention that data rates over twisted copper pairs is limited by the electromagnetic impairment(crosstalk) [68]. Besides that, Dynamic Spectrum Management(DSM)is considered an important strategy which aims to cancel the impact of Self-FEXT(that is caused by the vectored line in the same cable binder) [68]. Vectoring(DSM level3), as defined by ITU-TG.993.5 standard, can achieve the performance of bit rates of VDSL2 lines [69], [70].

In the situation of mixed scenario as that mentioned in [64], [62], the coexistence of vectored lines with the non-vectored lines or in a separate vector lines led to emergence of alien crosstalk(crosstalk arise from non-vectored lines or lines that outside the vectored group) [69], [71]. According to [69], the issue of ensuring the compatibility of vectoring in the presence of alien crosstalk has been addressed.System

Level Vectoring (SLV), cross-DSLAM Level Vectoring (xDLV)are introduced in [69] as a solutions to limit the generation of alien crosstalk. Recently in [71] DSM is also presented as a tool aimed to mitigate the effect of alien crosstalk and ensure the compatibility between vectored and non-vectored lines over cable containing two twisted pairs exploiting that essential dimensions (bonding, phantom, MIMO).

A well-know recent studies (by Coomans et al., 2014 and 2015) demonstrated a system concept of XG.FAST using frequency bandwidth of 500MHz and using Time Division Duplexing (TDD) as duplexing method and Discrete Multiple Tones(DMT) modulation. It was shown that it is possible to achieve multi-gigabit data on twisted pairs or coax, and reach 10 Gb/s [4], [72].

G.Fast just like VDSL2, also specifics concatenated Reed Solomon and Trellis Coded Modulation (RS+TCM) for forward error correction code (FEC) [33]. Shannon in 1948 first introduced his famous paper, "A Mathematical theory of communication " , [73], [74] showed that R is the transmission rate of information (in bits per second) and C is the channel capacity(in bits per second). R required of a communication is less than C by a data transmission code. Shannon tell us no coding method can fulfill reliable performance if R is greater than C [73], [74].

Since then, other researchers have expanded on this work by finding good coding schemes and different decoders design to improve the implementation of the scheme in hardware and software. The first proposed of concatenated codes is introduced by Forney in 1966. As reported by Forney, concatenated is an approach of building long codes from out the shorter ones. The representation of system as inner and outer codes is simplified the complexity of decoding [75] , [74].

Viterbi in 1967 first developed an effective algorithm to find code word with minimum distance (Euclidean Distance), to the received sequence in a trellis. This algorithm is presently the most efficient decoding procedure for convolutional code [42]. In 1989, concatenating of multiple convolutional code, was introduced and implemented with Soft Output Viterbi Algorithm (SOVA)by Berrue, et.al. In 1993 first introduced the recent devolvement of channel coding is turbo codes, specifically two or more, constituent codes and an interleaver i.e.,(parallel concatenated convolutional codes) PCCC [74], [76], [77].

According to [74, 78] turbo code namely (serially concatenated convolutional code) SCCC which was investigated in 1966, it has better performance than PCCC. There are two types of convolutional code depend on the presence of information bits

in the output sequence: NSC(non-systematic code), in which the information bits is not represent in the encoder output. While the second type called RSC(recursive systematic code), in which the information bits is directly presented in the encoder output sequence.

In recent years, A large and growing body of literature has investigated on channel coding schemes. These schemes are like turbo product codes (TPC) [79], [58], low density parity check (LDPC) [80], [81], [74] and product accumulate(PA) codes [74]. In 2010 [42], [74] K.Byun, et,al. proposed the performance comparison of RS code with recursive systematic code RSC and non-systematic convolutional code. In [82] , [74], a key study comparison of these coding schemes towards plain TCM is achieved.

Besides, a comparison between the PCC turbo codes and the TCM concatenated with RS coding is conduct for systems requiring high spectral efficiency and low delay [74]. Moreover, during 10 years ago, other performance comparisons have presented in many publishing. In 2010 [38] introduced a new iterative decoding approach with low-complexity based on soft value modification (SVD) algorithm which consists of RS code concatenated with TCM scheme with an interlever in between. In this modified technique, the RS decoder is based on Berlekamp-Massey (BM) algorithm, and the TCM decoder is based on Viterbi (VB) algorithm which combined with SVM algorithm to make the soft value more reliable and increase the VB and RS decoder's correction capacity.

Other studies [74, 83] in 2014 focus on the performance comparesion of RSC-RSC and RS-RSC concatenated codes with Viterbi algorithm. According to [34], it was shown that RSC-RSC concatenated code have best performance rather than RS-RSC. Recently, in 2015 [38] shows that the performance of serially concatenated (RSC-RSC) codes system gives better BER (bit error rate) than the non-systematic convolutional (NSC) code system. Also compared its performance with RSC-RSC concatenated codes which was introduced in [83], [74]. It is interesting to note that in 2015 [84], a performance comparison between RS+TCM and low-density parity-check (LDPC) codes for copper twisted pairs in light of current G.fast standard. According to [84], the LDPC codes have good error performance more than convolutional interleaved RS with TCM.

In addition to concatenated coding with TCM, multi-dimensional TCM is considered an important innovation in TCM technology and introduced in 1984 [85],

[86], [42]. Many researches have been working on multi-dimensional TCM with 2-dimensional and 4-dimensional modulation mapping using set partitioning rules. Mapping by set partitioning first introduced in famous paper of Ungerboeck in 1981 [47], which aim was to maximize free Euclidean distance ED between constellation points in each subset. [86], [87] have searched for the first 4-D TCM code, called GCS (Gallager – Calderbank –Sloane) code that can transmit only an un integral number of bits in each 2-D signaling interval [88].

2.12.2 Digital Subscriber Line Communications in the Presence of IN

Throughout the literature,A major problem in several communication systems is the presence of IN, which is a limiting factor in many applications such as power lines, digital subscriber line (DSL) and some wireless communication systems [89].

A traditional technique to mitigate the effects of IN on many communication systems has been proposed in [90], [91]. The concept of time domain (TD) mitigation methods is to identify high signal amplitudes and then apply clipping or nulling (Blanking) to these peaks when they are above a fixed threshold value. However, the literature also proposes using IN cancellation depending on the frequency domain (FD) signal processing after the multi-carrier demodulator [92], [93], [94]. The idea of IN frequency domain mitigation is to compensate for the IN samples and subtract them from the output of the equalizer. In [92], the authors described an iterative process where the information is exchanged between estimators that operate on the signal in the FD and TD. Similar work also has appeared in [93] where sub-carriers with extreme values are identified to detect the impulses in the FD. Furthermore, in [94] pilot tones are used to identify the position of noise impulses. Recent work in this topic is described in [95], [96].

The estimation process of the effects of IN are based on preliminary decisions on the transmitted signals. By using a fixed threshold value, the amplitude of IN sample exceeding a FT are considered to be an impulse noise pulse, otherwise the amplitudes are assumed to be noise pulses and then blanked. A FT value does not always make the correct decision for all assumed IN occurrences. Selecting a very high value of FT may blank the true IN samples and a very low value of FT may not blank all the AWGN noise samples. Even so, there is a little volume of published

studies investigating the effect of IN on the performance of G.fast communications system. Besides, most work on this topic, which is based on IN mitigation methods which assume a fixed threshold (FT). Therefore, finding a novel equation of OT value and mitigate the effect of IN will be essential issue in this work to reach the best performance of G.fast system in terms of BER. [97], [98].

2.12.3 Wired MIMO Communications

In recent years, there has been an increasing amount of literature on wired MIMO Communication networks. Of late, the demand for high data rate communication network has been increasing. Channel's available bandwidth is a limiting factor of a maximum bit rate in single-channel wireline communications systems. Therefore, a single-channel communication system may not be adequate for high data-rate applications. An effective solution is introduced in this thesis to increase the data rate by employ multiple transceivers(pairs of wires) communicating over multiple channels which are usually in close [99].

Researchers in [100], have shown the earliest references to MIMO methods in the DSL literature, where two sets of transceivers were considered. The concept of the vectoring method was presented in [101] as a crosstalk reduction technique. In the DSL literature, it is common to describe DSL systems employing such methods as a vectored system. Most of these methods are based on multiple twisted pairs which are represented as a MIMO channel in a vectored system. In [102], discrete multi-tone modulation (DMT) with orthogonal frequency-division multiplexing (OFDM) was considered over MIMO cable bundles and was presented alongside a mathematical description of the transmission line.Partial cancellation method in MIMO based system with simplified vectoring techniques have shown to provide excellent performance results as presented in [103], [104].

Furthermore, general theory of alien crosstalk cancellation, and an overview of such MIMO methods are given in [105]. An alternative approach towards MIMO signal processing was presented in [106], [107]. Thereby, near-end crosstalk (NEXT) and far-end crosstalk (FEXT) become the dominant limiting disturbances, limiting the performance of the twisted-pair based access networks. [108], [109]. Crosstalk cancellation is one technique to moderate the impact of crosstalk. Several crosstalk cancellation techniques have been suggested in [102], [110], [111], [112], [104]. Dif-

ferent techniques existed for different applications need, With the advent of Multiuser signal processing technology, referred to as vectoring proposed by Ginis and Cioffi in [70], [113] numerous MIMO detection techniques have been developed to cancel crosstalk in MIMO wireline systems [114]. These techniques include linear detectors such as zero-forcing (ZF) [104], [115] and minimum mean squared error (MMSE) [116], [108], and non-linear based detectors such as the ZF generalized decision feedback equalizer (ZF-GDFE) [117], MMSE-GDFE [118] and ML [119], [120].

Generally, Maximum Likelihood (ML) Detector is considered as the Optimum receiver for a MIMO channel. Although ML reaches the best performance, it experiences an exponential complexity in the number of signal dimension N and constellation size [119]. Interestingly, investigations in [104], [115] by Cendrillon et al. have shown that the optimal receiver in typical DSL channels is ZF due to the diagonal dominance of the channel matrix. Hence, through the years, the ZF processing has become well known for upstream decoding as in [117], [114], and downstream precoding in DSL systems [111], [121].

2.13 Summary

This chapter presented a theoretical background of concepts, such as the basic knowledge on non-Gaussian noise model MCA and its applications. In this chapter, the essential information for wired channel modelling, concatenated system coding systems, RS + TCM ,DSL broadband access networks and wired MIMO communications explained. Then, a brief knowledge of wired copper G.fast channel models construction gave, as well as a comparison between G.fast coded system over copper channel with and without impulsive noise. Three different IN cancellation methods proposed to reduce the impact of impulsive noise. Additionally, an introduction to channel coding and concatenated coding system clarified. Since trellis and Reed Solomon codes are the main interest of this thesis, the decoding and encoding procedure of these codes illustrated. Finally, MIMO–G.fast communication system with proposed copper channel model carried out.

Chapter 3

G.fast-state of the art and standardisation

3.1 Introduction

The subject of this chapter is the fourth generation broadband system, abbreviated as G.fast, with DMT modulation and concatenated RS code and 4D-TCM with an interleaver in between. This aims to achieve data rates of up to 1 Gb/s over very short copper loops up to 250 metres. To reach these data rates, the bandwidth has been extended to 106 MHz [122]. One of the most serious problems in communications systems is the presence of IN which can be considered as a limiting factor in many circumstances such as in power lines, DSLs and wireless communication systems [89], [123].

Middleton's model, which is a Gaussian-mixture distribution or a Poisson-Gaussian process [124], can be utilised to model IN. Unlike AWGN, impulse noise has very high instantaneous power and a wide frequency spectrum, which leads to high BER and prevents a receiver from correcting and making decisions on the transmitted symbols [125]. Two possible forms of impulse noise exist in DSLs, which are internally or externally induced. Indicators of externally induced impulses include high-voltage devices, railways, fluorescent tubes and lighting, while internally induced impulses are caused by dialling pulses, busy signals or ringing [126].

IN typically originates from electromagnetic and electronic equipment and affects transmission in the form of random bursts of relatively short duration and very high instantaneous power [127]. The most well-known of the traditional IN

mitigation methods in OFDM-based communication systems are blanking and clipping techniques, as considered by Zhidkov [91], and these have been employed in this work as a benchmark for performance comparisons. The application of nonlinearity techniques to the received time-domain (TD) signal is a simple and widely employed technique to reduce the effect of IN, involving clipping or blanking (replacing with zeros) high signal amplitudes above a selected threshold value. However, the unimpaired amplitude of the original signal may be clipped or blanked due to the imperfect identification of IN components, resulting in a BER degradation, which is a disadvantage of this technique [128], [91].

This is particularly likely to happen when the order of the QAM constellation is high, as is the case for G.fast and motivates us to propose an alternative method of impulse noise mitigation. The implementation of iterative methods has been suggested to estimate IN in the TD [124], [129]. It can then be subtracted from the signal received in the TD or in the FD after the operation of the FFT at the receiver, by means of either an adaptive or a non-adaptive threshold detector. This chapter quantifies the BER performance of a G.fast system over a copper channel in the presence of IN modeled as a Middleton's class A noise source. We focus on a practical algorithm for IN mitigation in OFDM receivers proposed by Zhidkov [95] which is applicable in G.fast systems. The key point of this algorithm is the compensation of impulsive noise in FD after OFDM demodulation and channel equalization rather than its implementation in the time domain before OFDM demodulation as in conventional methods.

This chapter proves that the performance of a mitigation noise system is threshold-dependent. Therefore, the main contribution of this chapter is to propose an optimal threshold calculation method to enhance the capability of IN cancellation in the frequency domain. A direct relationship between two parameters,namely, impulsive Index A and the noise ratio Γ, is derived. The proposed method can be applied, for example, to the G.fast standard and successive generations of Digital Subscriber Line (DSL) technology, which aim to achieve data rates up to 1 Gb/s over very short copper loops up to 250 meters [122].

The chapter is organized as follows. In Section II, the G.fast standard is introduced. Section III gives a description of the system model and explains the iterative Zhidkov algorithm and its application in G.fast system. Section IV shows simulation results. Finally, Section V concludes the chapter.

3.2 System Model of G.fast Standard

Firstly, error correction and detection methods, such RS coding, Galois Field (GF), convolutional code and 4D-TCM are investigated during this study. The general system block diagram of G.fast standard is given in Fig. 3.1.

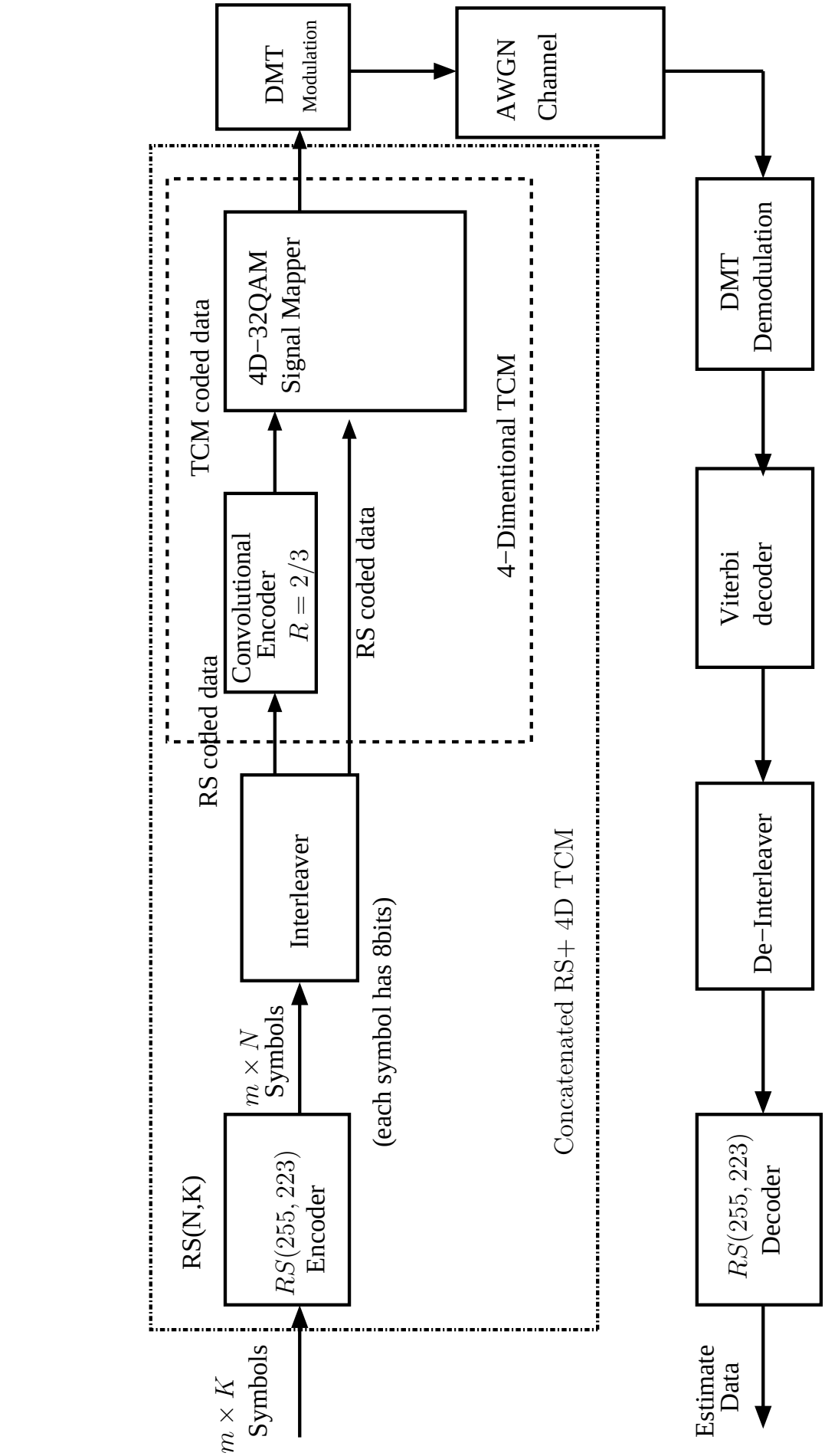

Figure 3.1: G.fast standard system

The first block in Fig. 3.1 is (N,K) RS code with symbols which are non-binary elements belonging to Galois field GF (2^s), where s is a positive integer, each code symbol of RS code is represented by s binary bits based on a definite basis of GF (2^s). The RS (255,223) encoder will considered in this study as an outer code with N=255 symbols in the code word produced from K=223 information symbols. The channel will be considered to be an AWGN channel. While $t = (N - K)/2$, it can be note that RS(255,223) code has the capability of correcting $t = 16$ symbol errors in each block of length N=255.

As described in Fig. 3.1, the encoding operation is achieved in two stages. Primarily, the message stream is divided into $m \times K$ blocks of symbols which are applied to the RS(255,223) encoder as an input. Then, the codeword is formed by attaching the $N - K$ redundancy symbols to the data symbols. The output of the encoder is a code word of N symbols (each symbol has 8 bits). It is important to mention that the $m \times N$ encoded codewords by the outer (RS) code are read into a block interleaver Π, row-by-row, where each row contains of an RS codeword. Then, the codewords are being fed to the inner 4-Dimensional TCM encoder which is consists of 2/3 binary convolutional encoder and 4-D 32 QAM signal mapper (it being discussed in details in the following section 3.2.1)

$m \times N$ encoded symbols have been passed to 4-D TCM are converted to complex symbols which are selected according to 4-D 32 QAM constellation points. Then, these set of complex symbols are fed as the input to the DMT modulation and transmitted through the AWGN channel. The basic idea of DMT is to split the available bandwidth into a large number of subchannels. DMT is able to allocate data so that the throughput of every single subchannel is maximized.

It can be seen that decoding process is accomplished in the reverse order. Firstly, Ncomplex numbers have been received are passed as the input to The Viterbi decoder, Viterbi decoding algorithm is used to decode them and resulting in $m \times N$ decoded codewords. After that, for each of $m \times N$ codewords are passed to the RS decoder, the Redundant bits $(N - K)$ are discarded from each N inner codeword symbols and the resulting is K decoded codewords of the RS decoder.

3.2.1 Design of four-dimensional TCM with Cross 32-QAM constellation

A block diagram of four-dimensional TCM with 32-QAM constellation in Fig. 3.2 is employed as inner encoder in G.fast coding system. It can be seen that The simulated TCM encoder comprises from the convolutional trellis encoder with 2/3 rate, the bit converter, and a memoryless signal mapper [130], [48].

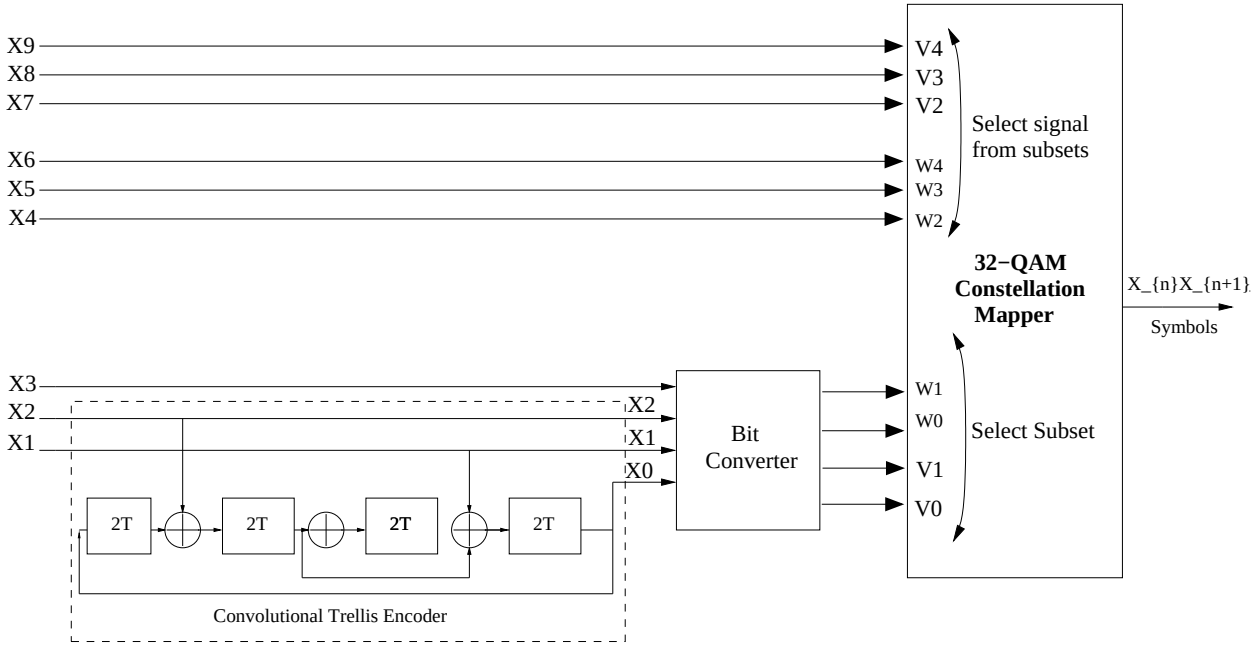

Figure 3.2: Partitioning of the 16-points QAM constellation

The TCM encoder works as follows, it receives n=9 information bits at one even time instance $2t$, and generates $n+1$ information bits which are define two symbols. Then, the two selected symbols are sent over the channel at times $2t$ and $2t+1$. The symbols are presented as complex numbers. As cleared from Fig. 3.2, three stages are needed With the purpose of create the four-dimensional TCM with 32 QAM constellation code:

1. Define a master constellation;
2. Constellation mapper;
3. Partitioning the master constellation into four subsets.

3.2.1.1 Define a master constellation

To construct higher 2^m-Quadrature Amplitude Modulation (2^m-QAM) constellations used with G.fast coding system, a defined algorithmic constellation mapper is employed here with a minimum number of bits equal to five and a maximum number of bits equal to 15 for all values of m. Each constellation point is symbolised as a pair (Real, Imag). The valid values of Real and Imaginary points are odd integers ±1,±3,±5, etc. Figure 3.3 shows the result which obtained from constructing a 5-bit constellation(i.e., m=5), represents a cross 32-QAM Master constellation which is used to calculate the BER performance of G.fast coding system.

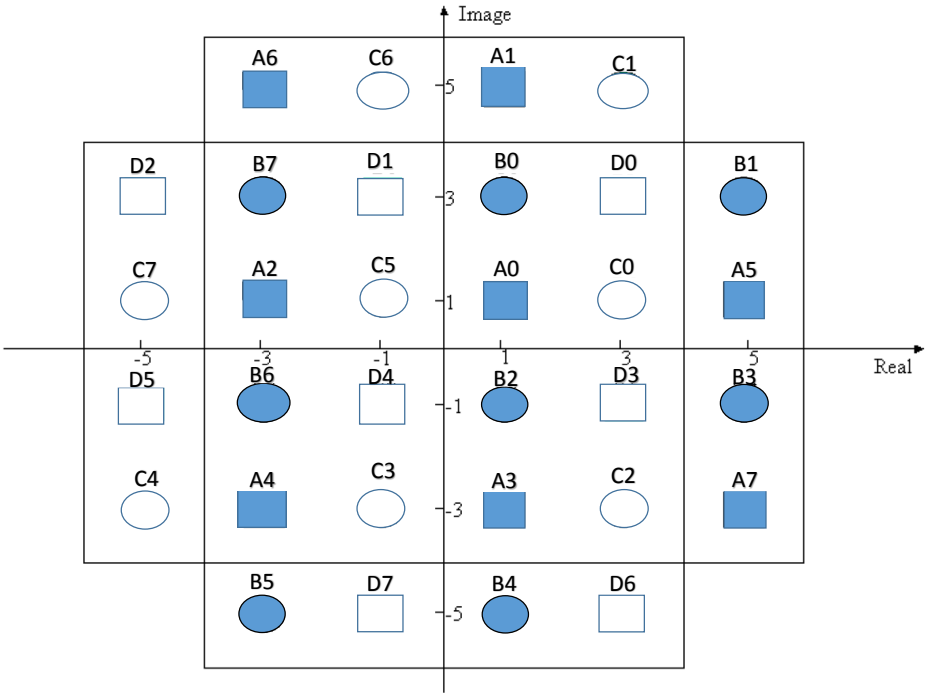

Figure 3.3: Mapping result of $M = 32$ points 2D master QAM constellation

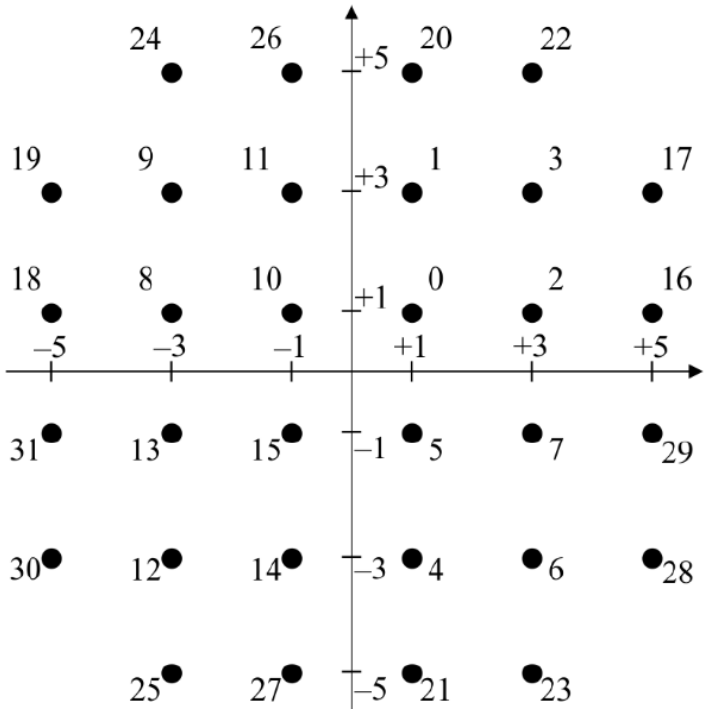

Figure 3.4: Constellation labels for 32-QAM master constellation

For perfection of representation, each constellation point in Figure 3.3 is labelled by an integer whose unsigned binary representation is (V_{m-1} V_{m-2} ... V_1 V_0), where m=5. The signal points are labelled according to their distance. The smaller number corresponds to the signal point that has the shorter distance. When the distance is the same, the point with the greatest imaginary point is taken first as seen in Figure 3.4. It is significant to comment here that the 7-bit constellation is achieved from the 5-bit constellation by replacing each label **r** with the 2×2 block of labels and extend the constellation-size to a 7-bit constellation:

$$\begin{matrix} \mathbf{4r+1} & \mathbf{4r+3} \\ \mathbf{4r} & \mathbf{4r+2} \end{matrix}$$

Formerly, the same process is used to build the larger m-bit constellations recursively for odd and even values of m. Basically, all the constellations defined for odd values of m are cross in shape, while the constellations defined for even values of m are square in shape. The process of the constellation mapping is be considered in the following subsection.

3.2.1.2 Constellation Mapper

Referring to the block diagram of four-dimensional TCM with 32-QAM constellation in Fig. 3.2, the constellation mapping process of the three encoded bits and the remaining 6 non-encoded information bits into the 4D constellation symbols are as follows. The three output bits X_0, X_1 and X_2 of the trellis encoder collected with third information bit X_3 to represented the input to the bit converter. the bits (V_0, V_1) and (W_0 and W_1) are computed on the basis of (X_3, X_2, X_1, X_0) by using the linear equations shown below:

$$\begin{aligned} \mathrm{W}_1 &= \mathrm{X}_1 \oplus \mathrm{X}_3, \\ \mathrm{W}_0 &= \mathrm{X}_3, \\ \mathrm{V}_1 &= \mathrm{X}_0 \oplus \mathrm{X}_1 \oplus \mathrm{X}_2 \oplus \mathrm{X}_3, \\ \mathrm{V}_0 &= \mathrm{X}_2 \oplus \mathrm{X}_3. \end{aligned} \tag{3.1}$$

It is can be seen from Fig. 3.3, that the master 2D 32-QAM constellation is consists of four subsets of signal points such as A,B,C and D, each one of these 2D subsets has eight complex symbols. On the basis of Table 3.1, each one of the pairs (V_0, V_1) and (W_0 , W_1) are used to select a pair of the four 2D subsets A,B,C and D matching to a 2D subsets in accordance with Table **??**. Then, the Signal Mapper shall select a first point (X, Y) from the constellation based on the v-bits word (V_{m-1} V_{m-2} ... V_1 V_0) and the second point is selected based on the w-bits word (W_{m-1} W_{m-2} ... W_1 W_0) as outlined in Fig. 3.2.

2D Subset	***W0, W1***	***V0, V1***
A	00	00
B	01	01
C	10	10
D	11	11

Table 3.1: Relation between W_0, W_1 and V_0, V_1 and four 2D subsets A, B, C, D

Then, the remaining 6 uncoded bits are separated into two groups (each group has three bits) renamed as W_2, W_3, W_4 and V_2, V_3, V_4. Related to the mapping Table below, the first group W_2, W_3, W_4 is used to choice a 2D point from the

first 2D subsets which is Decided by the W_0, W_1, and generate the first symbol X_n (represent as a complex number). While the second group V_2, V_3, V_4 which according to the same mapping table, select the second 2D point from the second 2D subset decided by the V_1, V_0 and generate the second complex symbol X_{n+1}.

Table 3.2: Mapping table result for M=32

2D Subset A

Index	Real	Image
0	-3	5
1	-3	1
2	-3	-3
3	1	5
4	1	1
5	1	-3
6	5	1
7	5	-3

2D Subset B

Index	Real	Image
0	-3	3
1	-3	1
2	-3	-5
3	1	3
4	1	-1
5	1	-5
6	5	3
7	5	-1

2D Subset C

Index	Real	Image
0	-5	1
1	-5	-3
2	-1	5
3	-1	1
4	-1	-3
5	3	5
6	3	1
7	3	-3

2D Subset D

Index	Real	Image
0	-5	3
1	-5	-1
2	-1	3
3	-1	-1
4	-1	-5
5	3	3
6	3	-1
7	3	-5

3.2.1.3 Subset Partitioning

In a trellis coded modulation system, each expanded constellation is labelled and partitioned into four subsets(A,B,C and D) using a method named set-partitioning which is illustrated in expanded manner in the previous chapter in section 2.10.2.1.

For example, The four basic 2-dimensional subsets, indicated by 0, 1, 2 and 3 for A, B, C, D correspondingly, are shown in Figure 3.5.

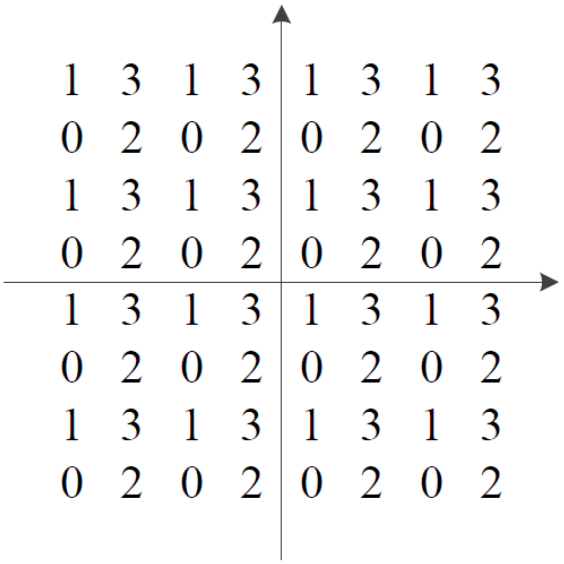

Figure 3.5: Mapping of 2-dimensional subsets of QAM constellation

According to the constellation mapping process, each one of the two LSBs, (V1, V0) and (W1, W0) of constellation points is representing the ith 2-dimensional subset S_2^i in which the constellation point exists. The bits (V1, V0) and (W1, W0) are in fact the binary representations of four values of index i as 0,1,2 and 3 as mentioned before in section 3.2.1.2, see Table 3.1. Each 4-dimensional subset can be written as the union of two 2-dimensional subsets as $S_2^i \times S_2^i$ as cleared from Table 3.2. The three bits (X2, X1, X0) are used to determine which one of the eight possible 4-dimensional subsets S_4^i is chosen . Where i is the integer with binary representation (X2, X1,X0). While the bit X3 (see Figure 3.2) decides which one of the two 2-dimensional subsets is selected from the 4-dimensional subset. The relationship is presented in Table 3.2.

Table 3.3: Correspondence relation between 4-dimensional and 2-dimensional subsets

4-D Subset	X3	X2	X1	X0	V1	V0	W1	W0	2-D subsets
S_4^0	0	0	0	0	0	0	0	0	$S_2^0 \times S_2^0$
	1	0	0	0	1	1	1	1	$S_2^3 \times S_2^3$
S_4^4	0	1	0	0	0	0	1	1	$S_2^0 \times S_2^3$
	1	1	0	0	1	1	0	0	$S_2^3 \times S_2^0$
S_4^2	0	0	1	0	1	0	1	0	$S_2^2 \times S_2^2$
	1	0	1	0	0	1	0	1	$S_2^1 \times S_2^1$
S_4^6	0	1	1	0	1	0	0	1	$S_2^2 \times S_2^1$
	1	1	1	0	0	1	1	0	$S_2^1 \times S_2^2$
S_4^1	0	0	0	1	0	0	1	0	$S_2^0 \times S_2^2$
	1	0	0	1	1	1	0	1	$S_2^3 \times S_2^1$
S_4^5	0	1	0	1	0	0	0	1	$S_2^0 \times S_2^1$
	1	1	0	1	1	1	1	0	$S_2^3 \times S_2^2$
S_4^3	0	0	1	1	1	0	0	0	$S_2^2 \times S_2^0$
	1	0	1	1	0	1	1	1	$S_2^1 \times S_2^3$
S_4^7	0	1	1	1	1	0	1	1	$S_2^2 \times S_2^3$
	1	1	1	1	0	1	0	0	$S_2^1 \times S_2^0$

3.3 G.fast Implementation and Channel Model

The following sections will show DMT G.fast System over IN copper channel in the presence of Middleton class A and introduce the proposed method of threshold calculation.

3.3.1 DMT-based G.fast System Over Impulsive Noise Copper Channel

The block diagram for a DMT-based G.fast system over a copper channel with a blanking non-linear compensator is illustrated in Fig. 3.6. It can be seen that the G.fast system model is constructed using a concatenated RS code and 4-D TCM code, which are separated by an interleaver. The information data is first encoded by the outer RS code and then fed to the inner 4-D TCM encoder which comprises a 2/3 binary convolutional encoder and 4-D 32 QAM signal mapper. Then the coded sequence is passed to the DMT modulator. For a standard DMT system, the FFT algorithm for modulation and demodulation is used. Subsequently, each subcarrier stream is mapped into complex quadrature amplitude modulation (M-QAM) symbols S_k (M= 1, 4, 8, ..., 64) , where k=1,2,... $K-1$ denotes the subcarrier number and K-1 is the total number of data-carrying subcarriers used for transmission.

It should hereby be mentioned that a modulated symbols Sk are a complex values. Thus, by applying Hermitian symmetry to the modulated symbols S_K that is setting half of it as the mirrored and conjugated copy of the others. The resulting is a real-valued signals. The Hermitian symmetry property is satisfied as:

$$S_{2K-k} = S_k^* \tag{3.2}$$

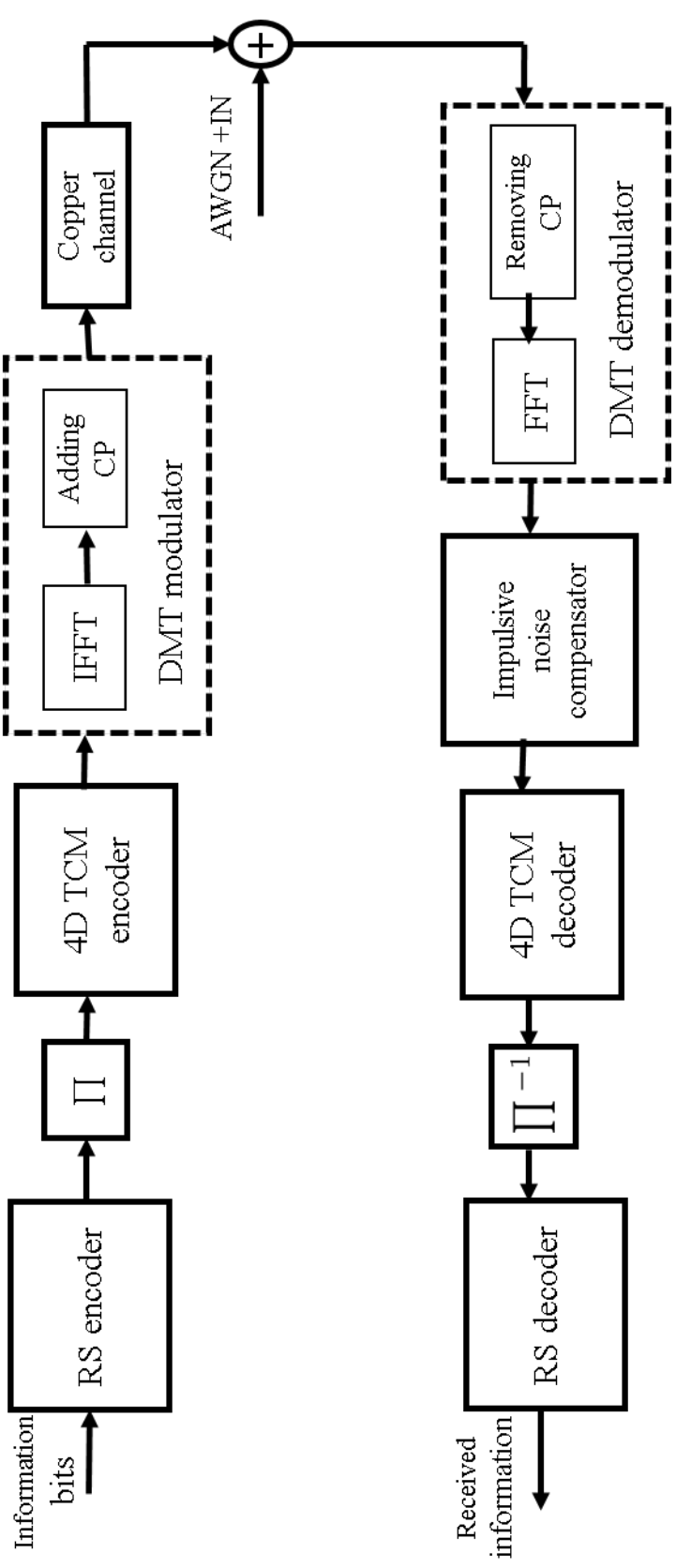

Figure 3.6: Block diagram of DMT based G.fast system over an IN copper channel with an IN compensator at the receiver

Moreover, when the K-1 information symbols Sk, where S_k are complex symbols and K is the number of sub carriers ($k = 1, 2, \ldots, K-1$) are employed as input values for a 2K-point inverse FFT (IFFT), where the DC components S0, and are set to zero (). The discrete output time-domain signal s_n generated by means of an inverse fast Fourier transform (IFFT) and The Hermitian symmetry can be written as

$$s_n = \frac{1}{\sqrt{2K}} \sum_{k=0}^{2K-1} S_k e^{j2\pi n \frac{k}{2K}}, \quad n = 0, 1, ..., 2K-1 \tag{3.3}$$

where S_k are complex symbols and K is the number of sub carriers and The resulting s_n is a real-valued, time domain discrete signal containing of 2k sample points [126, 131].

The effect of using parallel transmission of the data is the signal period is much longer than in the situation of ordinary serial transmission. Hence, only a small fraction of a time domain signal period effected by ISI. Besides, the use of a cyclic prefix reduced this ISI and orthogonality among the subcarriers is guaranteed. Then, parallel to serial converted symbol is Prefixing with a cyclic prefix of length μ which inserted to the each of DMT symbols, resulting in [126].

$$\tilde{s} = [s_{N-\mu}, s_{N-\mu+1}, ..., s_0, s_1, s_{N-1}]^T \tag{3.4}$$

where μ is the length of the cyclic prefix, which should obey the constraint $\mu \Delta t \geq \tau_{max}$,

The DMT signal $\tilde{s}$ is transmitted over an IN copper channel modeled by a Middleton Class A (MCA) distribution [97, 132, 133] and the received signal r (in TD) is given by:

$$r = h\tilde{s} + i + w \tag{3.5}$$

where the received signal r is a $(N + \mu) \times 1$ vector. The impulse response channel h is an $(N + \mu) \times 1$ vector, while i and w are the $(N + \mu) \times 1$ IN and AWGN noise vectors.

As shown in [132,133], various cable models have been described for DSL copper channels, such as the BT0H model, Chen's model and KPN1. The twisted pair copper channel model used in this chapter is Chen's model which is suitable in frequencies up to 200 MHz and causal impulse responses as defined in [13], [134]:

$$\alpha = K_1\sqrt{f} + K_2 f \tag{3.6}$$

$$\beta = K_3 f \tag{3.7}$$

The propagation constant γ is modelled as $\gamma = \alpha + j\beta$, where α is the attenuation constant, β is the phase constant and f is the frequency. Figure 3.7 show the transfer functions and impulse response of the Chen copper channel model.

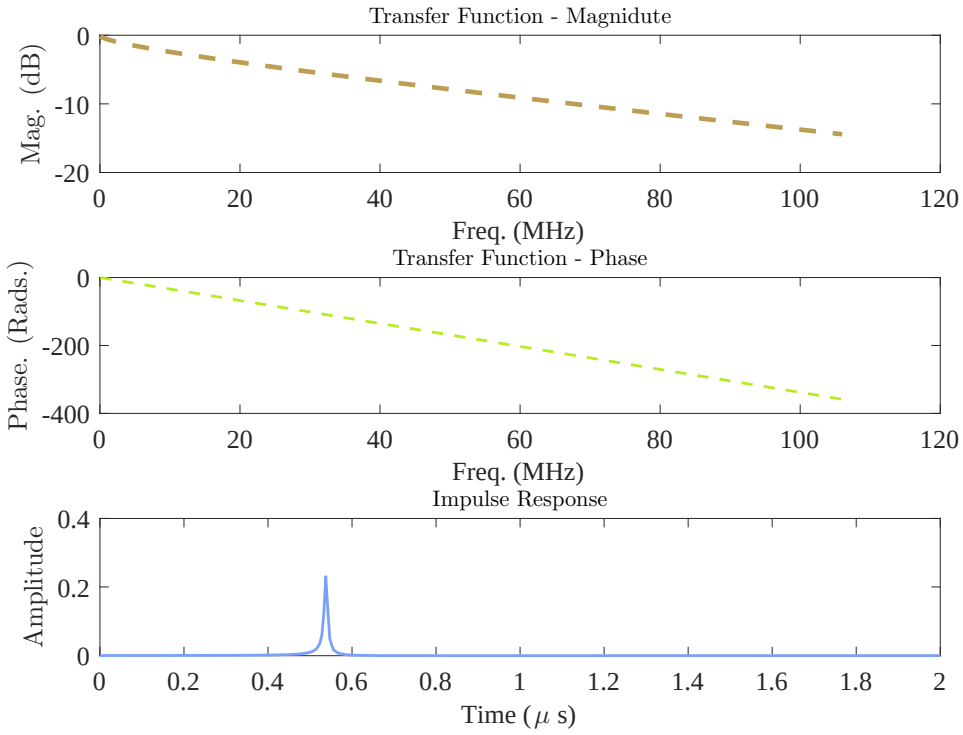

Figure 3.7: The transfer functions and impulse response of the Chen copper channel model.

At the receiver, the cyclic prefix is removed, the received symbols after a FFT can be recovered as:

$$R = HX + I + W \tag{3.8}$$

where H is an $M \times 1$ vector made up of the FFT of the channel impulse response h, X is an $M \times 1$ vector which represents the DFT of the transmitted signal x, W is the FFT of w and represents the background noise in the frequency domain and I is the DFT of the impulsive noise i, respectively.

In order to develop the receiver, we assume ideal channel estimation (i.e. $\tilde{H} \equiv H$). Now, the received signal R can be equalized by the frequency-domain channel equalizer (FEQ) and expressed as:

$$R^{eq} = R\hat{H^{-1}} = X + W\hat{H^{-1}} + I\hat{H^{-1}} \tag{3.9}$$

3.3.2 Middleton Class *A* Distribution

This section considers a well-known impulsive noise model called a Middleton Class A distribution [97, 132, 133], which is widely used in communication systems. This model employed here to represent the effects of IN on the BER performance of G.fast coding system. For a further demonstration of Middleton class A parameters influence on the noise pattern, Fig. 3.8 shows Middleton class A random variables vs samples pattern for a few scenarios and for 10000 samples.

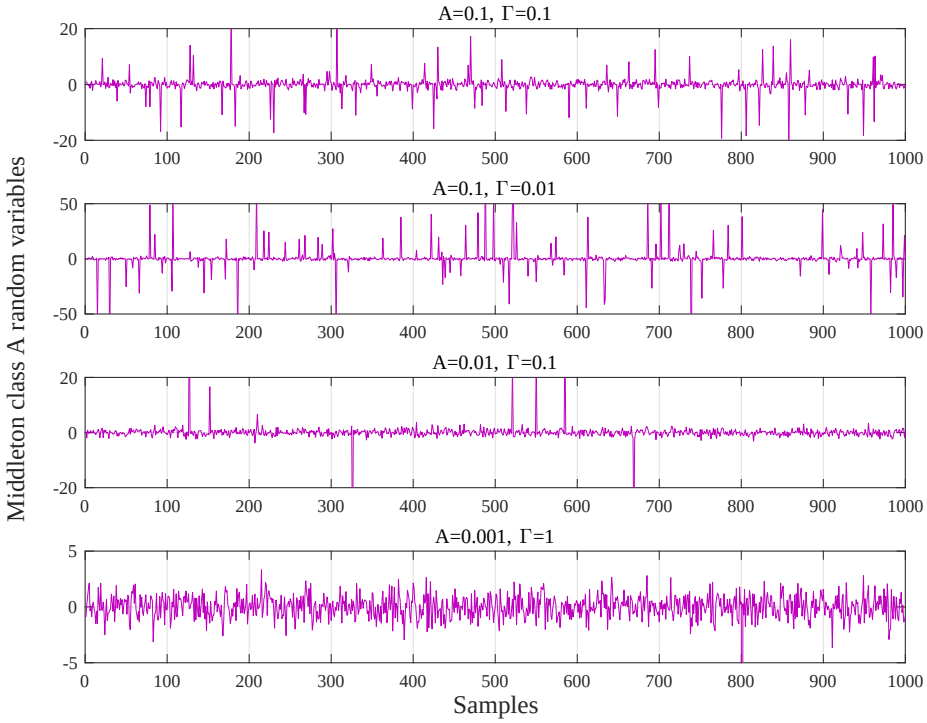

Figure 3.8: Simulation of 1000 samples of independent Middleton class A noise channel, for various values of Asand Γ.

It is worth to mention that Using Middleton Class A means that construction and simulation of an equivalent noise source from real world measured data is possible. This is a significant benefit, thus providing the opportunity to quantify noise characteristics based on real world measurements on various devices.

3.3.3 Frequency Domain Method

Impulsive noise mitigation methods in the frequency domain have been presented in [95, 96, 135]. The basic principle behind this method is to estimate the positions and amplitudes of IN in the frequency domain after the OFDM demodulator and the channel equalizer output, then subtract them from the received signal. This method is very effective for higher-order QAM constellations, such as those used in the G.fast system. In this work, the Zhidkov algorithm is considered as IN cancellation FD method.

The received OFDM signal over a copper channel in the presence of IN can be expressed as [95]:

$$R_k = H_k X_k + W_k + I_k, \quad k = 0, 1, \ldots, N-1, \tag{3.10}$$

where W_k is the DFT of the AWGN samples and I_k is the DFT of the IN samples. Based on the algorithm presented in [95], the received signal at the zero forcing equalizer (ZFE) output can be expressed as:

$$R_k^{(eq)} = \frac{R_k}{H_k} = X_k + \frac{W_k}{H_k} + \frac{I_k}{H_k}, \quad k = 0, 1, \ldots, N-1, \tag{3.11}$$

The main idea is based on the estimation of the equalized IN samples $\frac{I_k}{H_k}$ and then to subtract this from the equalized received signal samples $R_k^{(eq)}$. This operation can provide the estimated DFT of the transmitted signal $\hat{X}_k$ by utilizing the Maximum Likelihood (ML) criterion based on the minimum Euclidean distance computation. The total noise samples $D_k = W_k + I_k$ in the frequency domain can be estimated as:

$$\hat{D}_k = H_k(R_k^{(eq)} - \hat{X}_k), \quad k = 0, 1, \ldots, N-1, \tag{3.12}$$

Therefore, we need to estimate the IN samples $\hat{I}_k$ from the estimated total noise samples $\hat{D}_k$. That can be achieved by transforming $\hat{D}_k$ into the time domain $\hat{d}_k$ by utilizing an IDFT as

$$\hat{d}_n = \mathcal{F}^{-1}\left\{H_k(R_k^{(eq)} - \hat{X}_k)\right\}, \quad n = 0, 1, \ldots, N-1, \tag{3.13}$$

Then, the variance as given by:

$$\sigma^2 = \frac{1}{M}\sum_{l=0}^{M-1}\left|\hat{d}_l\right|^2 \tag{3.14}$$

After that, vector $\hat{i}$ can be formed based on following rule :

$$\hat{i} = \begin{cases} \hat{d}_l, \text{ if } \left|\hat{d}_l\right| > T_h\hat{\sigma}^2, l = 0, 1, \cdots, M-1, \\ 0, Otherwise \end{cases} \tag{3.15}$$

where T_h is threshold value that corresponds to small probability of false detection.

Vector $\hat{i} = [\hat{i_0}, \hat{i_1}, \cdots, \hat{i_{M-1}}]$ is transformed into $\hat{I} = [\hat{I_0}, \hat{I_1}, \cdots, \hat{I_{M-1}}]$ by means of DFT. The final step of the compensator process can be done by multiplied vector $\hat{I} = [\hat{I_0}, \hat{I_1}, \cdots, \hat{I_{M-1}}]$ by $\hat{H^{-1}} = [\hat{H_0^{-1}}, \hat{H_1^{-1}}, \cdots, \hat{H_{M-1}^{-1}}]$, which represents inverse channel frequency response h=h[H0,H1]. Then ,subtracted from equalizer output $R^{(Req)}$ as follow:

$$R^{(comp)} = R^{(eq)} - \hat{I}\hat{H^{-1}} \tag{3.16}$$

where the compensated signal $R^{(comp)}$ is M-element vector represented in FD by means of FFT. The block-scheme of impulsive noise Zhidkov Compensation algorithm is demonstrated in Fig. 3.9. Here, peak detector is achieves procedures termed by (3.14) and (3.15).

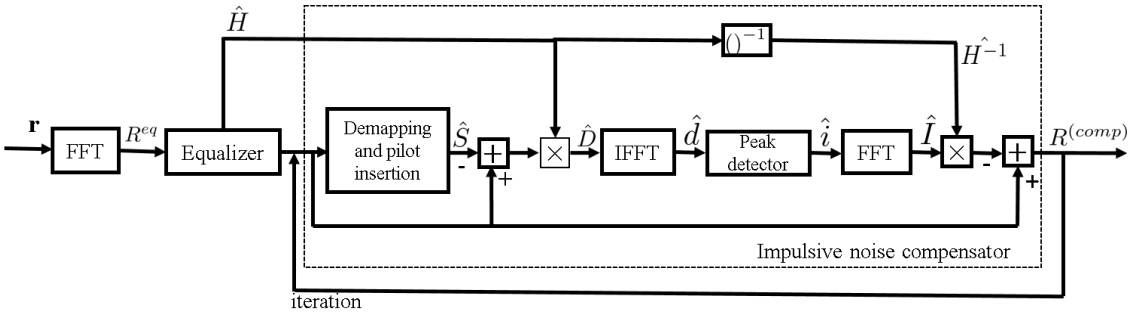

Figure 3.9: Block diagram of impulsive noise Zhidkov compensator

As a final point of this procedure, the previous steps are then repeated in order to improve IN cancellation and get best performance in term of BER. Then the IN samples in the TD can be estimated using the following condition:

$$\hat{i}_n = \begin{cases} \hat{d}_n, & \text{if } |\hat{d}_n| > T_h\hat{\sigma}^2 \\ 0, & \text{otherwise} \end{cases}, n = 0, 1, \cdots, N-1, \tag{3.17}$$

where T_h is the Fixed Threshold (FT). This is a crucial factor in impulsive noise compensation process as it is responsible for deciding which amplitude $|\hat{d}_n|$ is to be blanked [136] (i.e., whether the amplitude $|\hat{d}_n|$ belongs to the AWGN noise or to the IN). However, one FT value is not suitable for all the SNR values for different probabilities of IN. Therefore, an optimal estimation threshold exists which is derived in the next section.

3.3.4 The Proposed Threshold-Calculation Method for Frequency Domain IN Mitigation Method

We propose that instead of fixing a threshold, blanking will take place at higher SNRs if it is implemented at an OT value determined by the distribution characteristics of the IN. The block diagram of the proposed impulsive noise compensation method is shown in Fig. 3.10. The proposed calculation method for OT is shown as follows

The real and imaginary distributions of the MCAIN model can be expressed as:

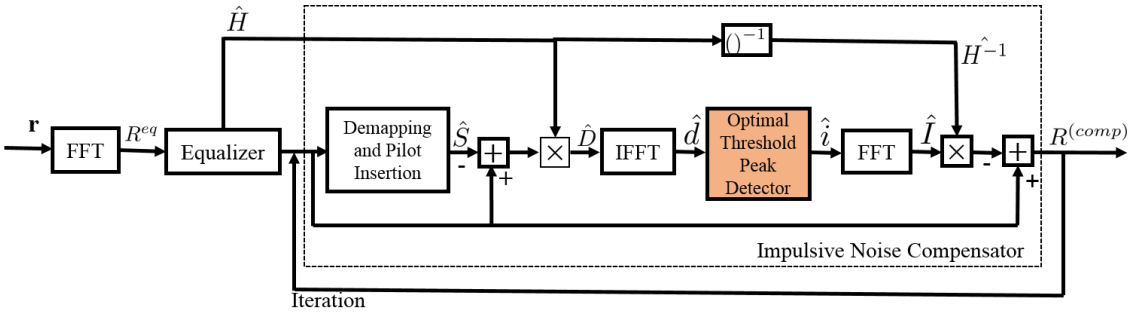

Figure 3.10: The block diagram of the proposed impulsive noise compensation method at the receiver

$$p_A(\hat{d}_n^{\Re}) = \sum_{\ell=0}^{\infty} \frac{e^{-A}A^{\ell}}{\ell!} \frac{1}{\sqrt{2\pi\sigma_{\ell}^2}} e^{\left(-\frac{(\hat{d}_n^{\Re})^2}{2\sigma_{\ell}^2}\right)},$$

$$p_A(\hat{d}_n^{\Im}) = \sum_{\ell=0}^{\infty} \frac{e^{-A}A^{\ell}}{\ell!} \frac{1}{\sqrt{2\pi\sigma_{\ell}^2}} e^{\left(-\frac{(\hat{d}_n^{\Im})^2}{2\sigma_{\ell}^2}\right)}, \tag{3.18}$$

This model can be expressed as mixture of two Gaussian PDFs, each with zero mean but with different variances as presented by the Spaulding and Middleton model in [137]:

$$p_A(\hat{d}_n^{\Re}) = e^{-A}\mathcal{N}(\hat{d}_n^{\Re}, 0, \sigma_w^2) + (1 - e^{-A})\mathcal{N}(\hat{d}_n^{\Re}, 0, \sigma_I^2),$$

$$p_A(\hat{d}_n^{\Im}) = e^{-A}\mathcal{N}(\hat{d}_n^{\Im}, 0, \sigma_w^2) + (1 - e^{-A})\mathcal{N}(\hat{d}_n^{\Im}, 0, \sigma_I^2). \tag{3.19}$$

For complex noise, the magnitude of the simplified IN form in 3.19 exhibits a mixture of two Rayleigh PDFs as:

$$p(|\hat{d}_n|) = \frac{e^{-A}|\hat{d}_n|}{\sigma_w^2} e^{-\frac{|\hat{d}_n|^2}{2\sigma_w^2}} + \frac{(1 - e^{-A})|\hat{d}_n|}{\sigma_I^2} e^{-\frac{|\hat{d}_n|^2}{2\sigma_I^2}}, \tag{3.20}$$

where $(1 - e^{-A})$ is the probability of an impulse occurring, $\sigma_I^2 = \sigma_w^2\left(1 + \frac{1}{A\Gamma}\right)$.

The decision rule based on the ML criterion [138] can be expressed as:

$$\mathrm{ML} = \begin{cases} \hat{i}_n \in \text{impact impulsive}, & \text{if} \quad \dfrac{\frac{|\hat{d}_n|}{\sigma_w^2} e^{-\frac{|\hat{d}_n|^2}{2\sigma_w^2}}}{\frac{|\hat{d}_n|}{\sigma_I^2} e^{-\frac{|\hat{d}_n|^2}{2\sigma_I^2}}} \geq 1 \\ \hat{i}_n \in \text{impulsive free}, & \text{elsewhere} \end{cases}. \tag{3.21}$$

The optimal threshold T_{ML}^{opt} based on the ML criterion threshold must satisfy the following condition

$$\frac{|T_{ML}^{opt}|}{\sigma_w^2} e^{-\frac{|T_{ML}^{opt}|^2}{2\sigma_w^2}} = \frac{|T_{ML}^{opt}|}{\sigma_I^2} e^{-\frac{|T_{ML}^{opt}|^2}{2\sigma_I^2}}, \tag{3.22}$$

We can also simplify Eq. 3.22 as:

$$\frac{\sigma_I^2}{\sigma_w^2} = e^{-\frac{|T_{ML}^{opt}|^2}{2\sigma_I^2} + \frac{|T_{ML}^{opt}|^2}{2\sigma_w^2}},$$

$$\frac{\sigma_I^2}{\sigma_w^2} = e^{|T_{ML}^{opt}|^2 \left(\frac{\sigma_I^2 - \sigma_w^2}{2\sigma_I^2 \sigma_w^2}\right)},$$

$$|T_{ML}^{opt}|^2 = \frac{2\sigma_I^2 \sigma_w^2}{\sigma_I^2 - \sigma_w^2} \ln\left(\frac{\sigma_I^2}{\sigma_w^2}\right),$$

$$|T_{ML}^{opt}| = \sqrt{\frac{2\sigma_I^2 \sigma_w^2}{\sigma_I^2 - \sigma_w^2} \ln\left(\frac{\sigma_I^2}{\sigma_w^2}\right)}$$

$$= \sqrt{2\sigma_w^2 (1 + A\Gamma) \ln\left(1 + \frac{1}{A\Gamma}\right)}. \tag{3.23}$$

While based on Siegert criterion, an additional knowledge of the probability of impulsive noise is required. According to this criterion, the optimal threshold can

be computed as:

$$\frac{e^{-A}|T_{ML}^{opt}|}{\sigma_w^2}e^{-\frac{|T_{ML}^{opt}|^2}{2\sigma_w^2}} = \frac{(1-e^{-A})|T_{ML}^{opt}|}{\sigma_\zeta^2}e^{-\frac{|T_{ML}^{opt}|^2}{2\sigma_\zeta^2}}. \tag{3.24}$$

Following similar previous derivation steps, $|T_{ML}^{opt}|$ can be expressed as:

$$|T_{ML}^{opt}| = \sqrt{2\sigma_w^2(1+A\Gamma)\ln\left(\frac{e^{-A}}{1-e^{-A}}\left(1+\frac{1}{A\Gamma}\right)\right)}. \tag{3.25}$$

Subsequently, the estimated samples are transformed to the FD $\hat{I}_k$ and then divided over the channel frequency response H_k. The signal after the frequency domain IN mitigation method can be expressed as:

$$R_k^{(out)} = R_k^{(eq)} - \frac{\hat{I}_k}{H_k}. \tag{3.26}$$

where the compensated signal $R_k^{(out)}$ is an $N \times 1$ vector represented in the FD by means of the FFT.

3.4 Simulation Results

In this section, the simulation results for a DMT-based G.fast model with the RS+TCM coding scheme are presented. Using MATLAB as the simulation platform, the received signal vector y of a DMT G.fast system over 32-QAM copper channel is given in algorithm 3.1. The G.fast system is implemented firstly over a copper channel using ZF equlaizer at receiver side, with and without the influence of Middleton's class A impulsive noise, as shown in Fig. 3.11 and Fig. 3.12, respectively. It is worth mentioning that, the results illustrated in Fig. 3.11 and Fig. 3.12, were implemented with six different QAM cross-constellations of $M = 32, 128, 512, 2048, 8192$ and $32768 - QAM$ signal points.

Algorithm 3.1 Received signal vector of DMT G.fast system using cross 32-QAM constellation over copper channel and ZF equalizer at receiver side

close all; clear all;

procedure $Input = (M, var, Len - sig, SNRdB, Constl)$

M = 32 ▷ 32-QAM modulation.

L = 1000; ▷ Length of transmit signal.

SNRdB; ▷ SNR in dB.

$SNR = 10.^(SNRdB/10);$

$var = 1./(SNR * log2(M));$

Constl=32 QAM constellation

$Constl = Constl * sqrt(3/(2 * (M - 1)));$

$s = Constl(randint(L, [1M]));$ ▷ Transmitted signal s after modulation.

i = 0;

for u = 1:L

i = i+1;

sbin(i,:) = Constl-bin(find(Constl==s(i,u)),:); ▷ transmitted signal in binary codes.

end

$H = (randn(1, L) + sqrt(-1) * randn(1, L))/sqrt(2);$ ▷ Channel responce.

$n = (randn(1, L) + sqrt(-1) * randn(1, L)) * sqrt(var(in))/sqrt(2);$ ▷ AWGN noise.

$y = H * s + n;$ ▷ Received signal.

$\hat{s}_{zf} = zeros(M, L);$

$kset = zeros(1, L);$

$\tilde{s}_{zf} = (pinv(H' * H + H') * r;$ ▷ ZF equlizer

for $j \leftarrow 1$ *to* $length(Constl)$ **do**

$\hat{s}_{zf}(j,:) = reshape(abs(\tilde{s}_{zf} - Constl(j)).O2, 1, size(r, 1) * size(r, 2));$

end for

end for

for $q = 1 : size(\hat{s}_{zf}, 2)$ **do**

$hatsbin(q,:) = Constl - bin(kset(q),:);$

end for

end for

$[dmin, kset] = min(\hat{s}_{zf});$

$BER = mean(reshape(abs(sbin - hatsbin), 1, L * log2(M)));$

end procedure

Fig. 3.11 shows the BER of G.fast system over copper channel under the the influence of AWGN only. While in Fig. 3.12, we compare the BER performance of G.fast system over copper channel under the effect MCA IN. It is clear that the BER performance of G.fast system in Fig. 3.11 over copper channel under effect of AWGN only exceeds the BER performance of system Fig. 3.12 over copper channel under the effect of IN by at least 10 dB at a BER of 10^{-5} for any of six different QAM cross-constellations signal points.

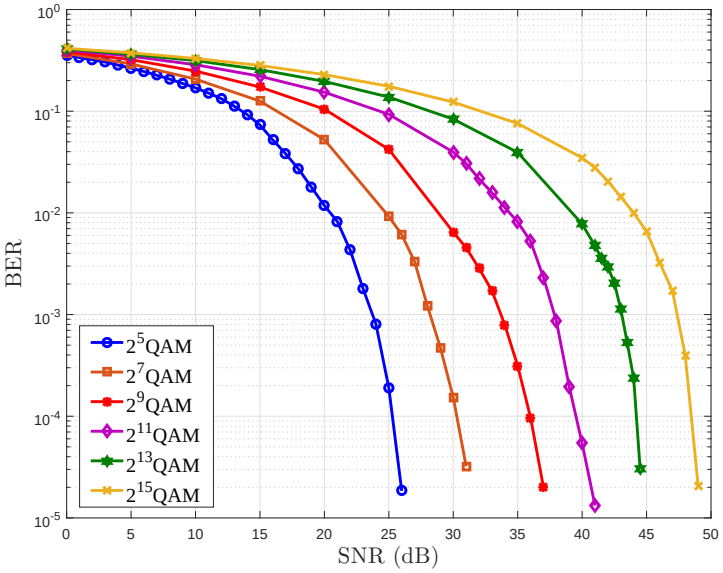

Figure 3.11: BER performance of DMT-based G.fast over copper channel with AWGN only

Fig. 3.13 displays the BER performance comparison between the conventional nonlinear clipping, blanking schemes and the Zhidkov algorithm. The BER performance is evaluated with three different values of impulsive noise index at $A = 0.001, 0.1$ and 1 where the noise ratio Γ is 0.1. It should be noted that, the performance result of the proposed system is obtained for each iteration. However, we only present the results of iterations 1 and 2 in Fig. 3.13, Fig. 3.14 and Fig. 3.15,respectively as there is no change beyond iteration 2.

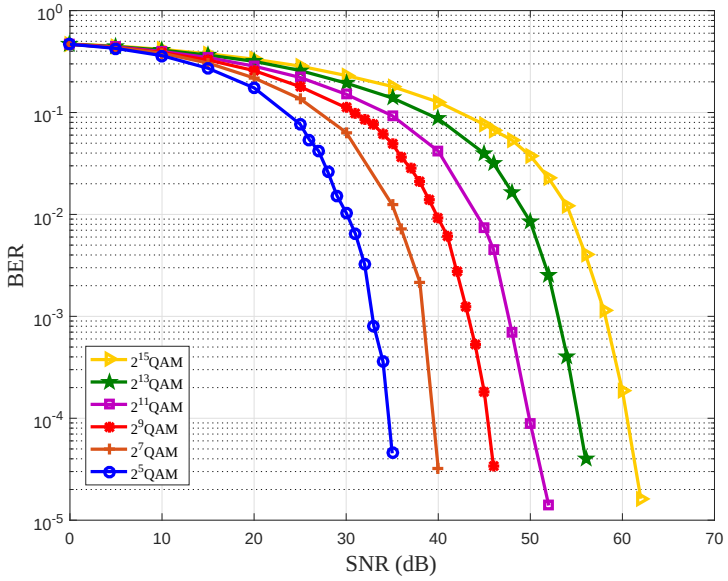

Figure 3.12: BER performance of DMT-based G.fast over copper channel with impulsive noise,A=0.1

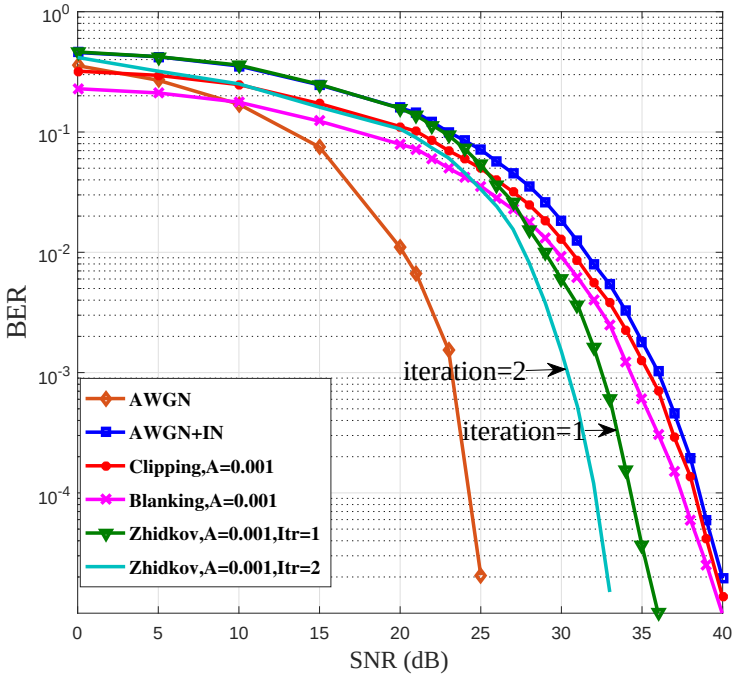

Figure 3.13: BER performance comparison in the presence of impulsive noise of 32QAM G.fast copper channel system with different values of impulsive noise index A=0.001.

As can be observed from Fig. 3.13, the BER curves indicate an additional gain of approximately 3 dB at a BER=10^{-4} during the second iteration. It is interesting to see from Fig. 3.13 that the clipping and blanking methods fail to produce significant

noise mitigation in the G.fast system when utilizing high order QAM constellations, while the Zhidkov algorithm significantly outperforms the clipping and blanking methods at three different values of A, for example, at a BER=10^{-4} there is a gain of 8 dB with $A = 1$, a gain of about 7 dB with $A = 0.1$, and a gain of up to 6 dB with $A = 0.001$. This agrees with the evidence mentioned in a previous study [139] suggesting that conventional nonlinear methods provide insignificant improvements as the constellation size increases.

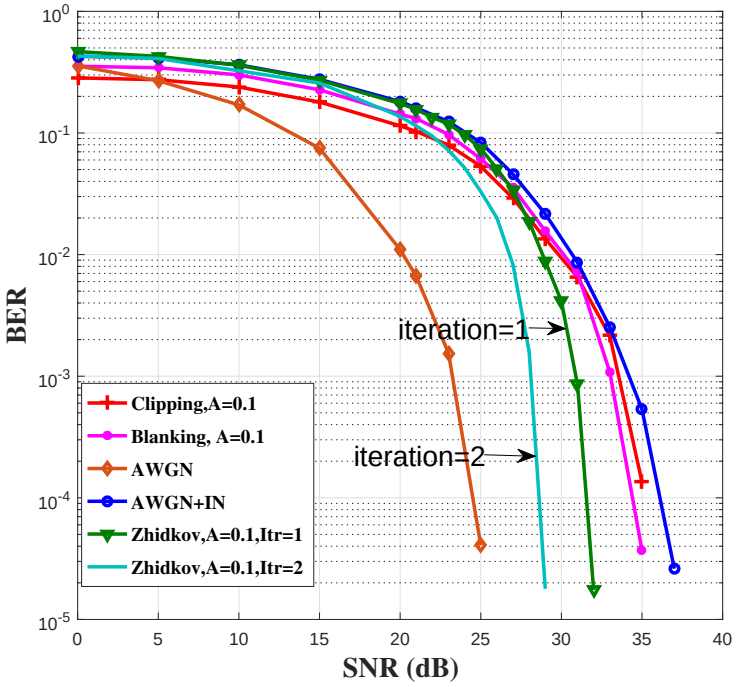

Figure 3.14: BER performance comparison in the presence of impulsive noise of 32QAM G.fast copper channel system with different values of impulsive noise index A=0.1.

Furthermore, it is clearly shown from Fig. 3.14 and Fig. 3.15 that, for higher values of A the noise becomes Gaussian distributed and as a result the noise reduction capability introduced by the system becomes more significant where $A = 1$. Note that 32-QAM cross constellation has been utilized in all simulations.

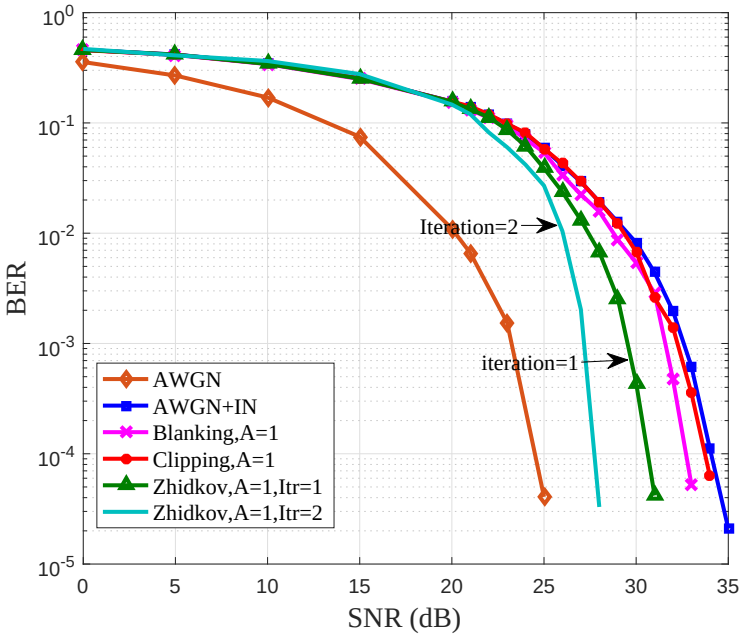

Figure 3.15: BER performance comparison in the presence of impulsive noise of 32QAM G.fast copper channel system with different values of impulsive noise index A=1.

To begin with Fig. 3.16, it is shown that a BER performance comparison between the nonlinearity FD method, which uses a fixed threshold value as presented in [95], and the proposed method of calculating the optimal threshold obtained from Eq. 3.23 as given :

$$= \sqrt{2\sigma_w^2(1 + A\Gamma)\ln\left(1 + \frac{1}{A\Gamma}\right)}.$$

The method presented before in [95] was depend on a fixed threshold value for the whole range of SNR values. Accordingly, it has been tested for the range of all possible threshold values. The five BER performance curves close to AWGN are observed at a FT=[Th1=8.5, Th2=8.9, Th3=9.5, Th4=10.5, Th5=11.3] as depicted in Fig.3.16. It is obvious that the BER performance results from our optimal threshold calculation method outperforms the closest BER performance curve obtained using a fixed threshold value $Th1 = 8.5$ by $1.2dB$ at BER $= 10^{-4}$.

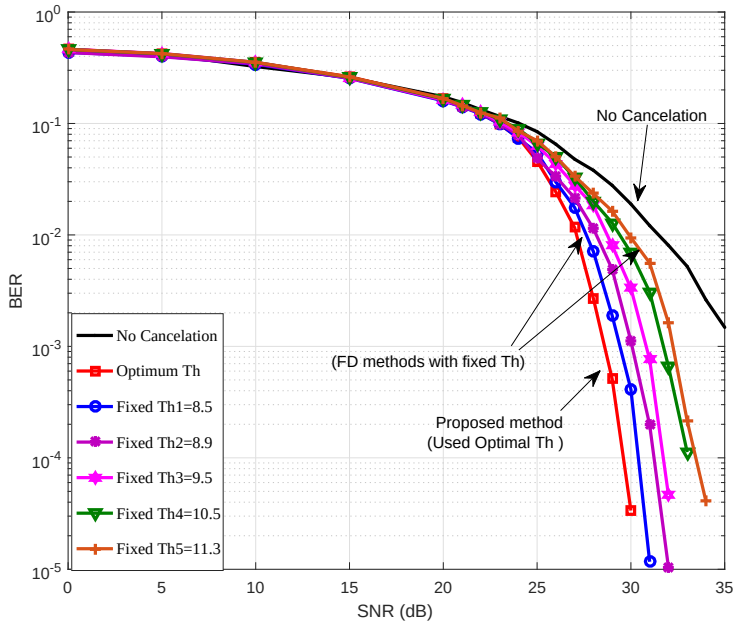

Figure 3.16: BER performance comparison in the presence of IN between the proposed optimal threshold and fixed threshold applied to FD IN mitigation method over 32-QAM G.fast copper channel system

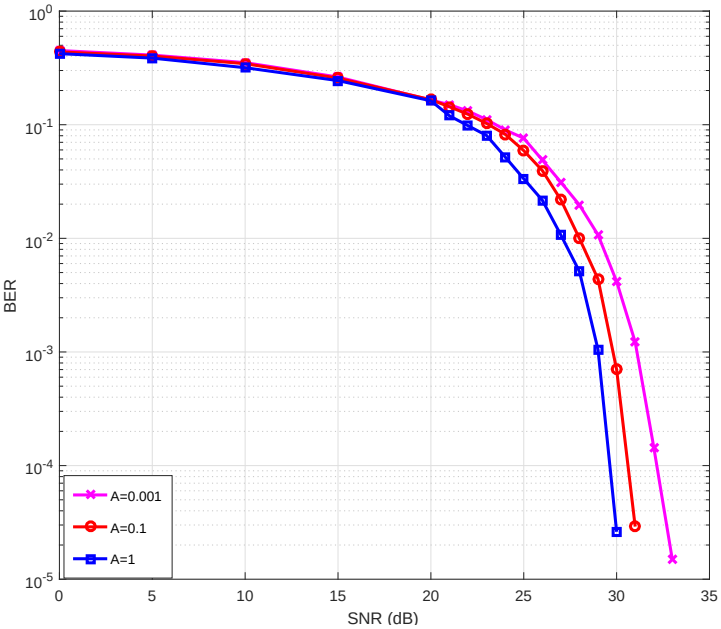

Figure 3.18: BER performance comparison in the presence of IN of the proposed optimal threshold method over 32-QAM G.fast copper channel system with different values of impulsive noise index $A = 0.001, A = 0.1$ and $A = 1$

Additionally, the effect of varying A and Γ on the BER performance is shown in Fig. 3.17 and Fig.3.18, respectively. It is evident that as A and Γ increase the BER performance improves with increasing SNR as shown in Fig. 3.17.

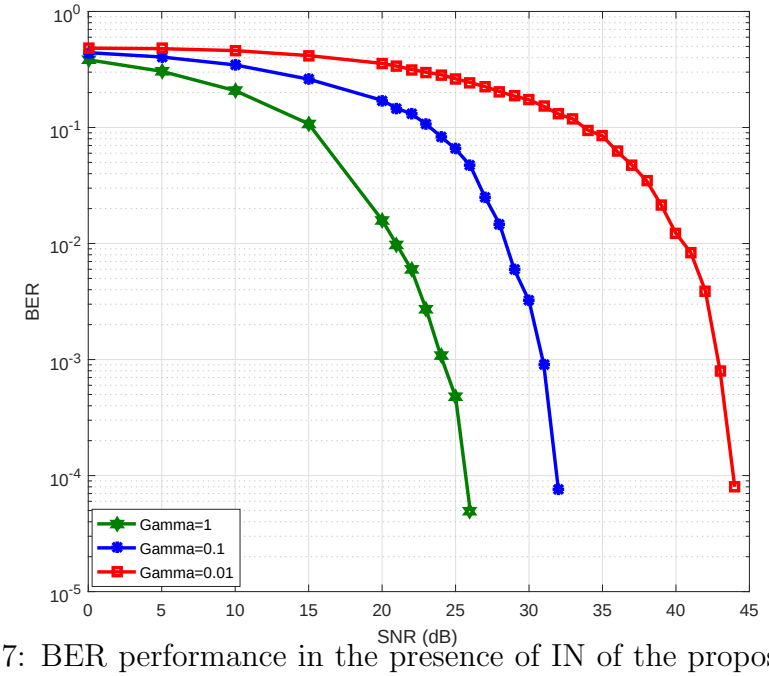

Figure 3.17: BER performance in the presence of IN of the proposed method with three different values of Gamma parameter,simulated results for 32-QAM G.fast copper channel system

3.5 Summary

The effect of IN on a G.fast system investigated in this chapter and different impulse noise mitigation techniques evaluated. A performance comparison between three different IN mitigation schemes, namely Clipping, Blanking, and Zhidkov's algorithm with Middleton Class A impulse noise, presented. However, Clipping and Blanking become less effective when the order of the QAM constellation increases. Performance results showed that Zhidkov's algorithm is very robust and achieves a large gain over conventional nonlinear schemes when utilizing high order QAM constellations in broadband systems such as the G.fast. Therefore, we propose that Zhidkov's algorithm would be a very suitable IN mitigation technique for use in G.fast system.

An optimal threshold expression was derived in this chapter to achieve the optimal performance of IN cancellation methods based in the frequency domain. A direct relationship between the parameters impulsive index A, the noise ratio Γ and optimal threshold is derived in this work. Moreover, the performance of this FD mitigation scheme with OT is compared with FT in terms BER using the MCA IN model. The effect of changing A and Γ was investigated and it was found that varying A and Γ for three different values does cause a significant change in the

BER performance. Results also showed that the proposed scheme is more superior than other existing IN mitigation techniques.

Chapter 4

A Multi-Line Copper Wire Channel Model for a Binder of Twisted Pairs

4.1 Introduction

DSL technology has evolved over generations to face the demand for high bandwidth data transmission over telephone transmission lines. Generally, DSL communication can be referred to as multiple independent system having a single transmitter coupled to a single receiver by a twisted pair [140]. Due to the higher reliability of data transmission it offers and the potential to dramatically increase the capacity of wireless channels, multiple-input multiple-output (MIMO) technology has been identified as one of the most practical methods in wireless communication systems to increase the transmission capacity and improve the link reliability [141]. This technology can be utilized in wire-line communications by considering multiple copper line systems bundled together in the same cable binder [142].

One potential method to achieve a high bit rate is to use a bundle of twisted pairs to transmit the bit stream rather than one pair of wires. Clearly, a system employing a channel as a single MIMO channel (two pairs of wires) with matrix transfer function $\mathbf{H}$ would increase the bit error rate over a system using one set of transceivers assuming that the pairs of wires are treat as two sets of wideband channels [105].

IN has been a limiting factor in DSLs, so the interest in techniques for IN re-

duction has increased and drawn attention [101]. A well-known IN model in communication systems, called Middleton's class A (MCA) noise, has been utilized to model impulse noise in this study. The MCA model is a special case of the popular multi-component Gaussian mixture model [143].

This chapter is organized as follows: Section 4.2 describes the proposed $N_r \times N_t$ G.fast system model and demonstrates the construction and verification of the MLCW channel model. In Section 4.3, the Zhidkov algorithm is presented as a solution to IN on the proposed MLCW G.fast system model. Simulation results are detailed in Section 4.4 and Section 4.5 concludes this chapter.

The contribution of this chapter can be summarized in the following points,

- In this chapter, behaviour of the MIMO-DMT G.fast system under different environments is studied and the effects of increasing the order of cross QAM modulation on the BER performance of the system are presented.

- The performance of G.fast standard is evaluated on the proposed MLCW channel which have been verified and tested with the KS test and displays an independence property between the individual channels. Then, the MIMO copper channel model is compared to a comparable single line G.fast system, which was illustrated in the previous chapter.

- Obtaining the BER performance of the MIMO-DMT G.fast system for different M-ary cross QAM modulations with MIMO copper model and ZFE as a linear equalizer at the receiver side in the presence of IN modelled as the Middleton Class A noise source. Here different MIMO configurations such as such as 2×2, 4×4, 8×8 and 16×16 are used to show the effect in terms of SNR of increasing the number of twisted copper pairs in the same binder over the 1×1configuration.

- Finally, an overview of IN cancellation for a system with multiple pairs as MIMO G.fast is here presented. IN frequency domain cancellation method(as given in chapter 3) is used here as a solution for IN mitigation and it has provided significant performance enhancements to reduce the impact of Middleton Class A noise.

4.2 MLCW G.fast System and Channel Models

Consider a G.fast system with $N_r \times N_t$ receivers and transmitters over MLCW copper channel as shown in Fig. 4.1. The data symbols are generated such that $\mathbf{x} \in \mathrm{GF}(2^s)$, where $\mathrm{GF}(\cdot)$ is a Galois field with s being a positive integer. Then, the data symbols are first encoded with a Reed-Solomon (RS (255,223)) encoder defined in $\mathrm{GF}(2^8)$ as an outer code that produces N = 255 coded symbols from K = 223 information symbols. Then, the coded symbols are interleaved and encoded with the inner four-dimensional trellis-coded modulation (4-D TCM) producing the 4D, 32-QAM signal mapper. Utilizing the constellation mapper from [144], the codewords are mapped into 4-D 32-QAM symbols and fed to the DMT modulator to be transmitted through the MLCW copper channel.

This chapter considers a MLCW channel with a pair of direct lines, i and j, combined with the far-end cross talk (FEXT) effect between the pair of direct lines. The near-end cross-talk (NEXT) effect will not be taken into consideration for this channel since G.fast is concerned with longer cables [145] therefore, the effect of NEXT will be negligible. The direct channels are implemented based on Chen's model, such that [146]:

$$h_{i,i} = e^{-L\gamma(f)}, \tag{4.1}$$

where, L is the cable length in meters, $\gamma(f) = \alpha(f) + j\beta(f)$ is the propagation constant with $\alpha(f)$ and $\beta(f)$, as the attenuation and the phase constants respectively, which can be calculated using:

$$\begin{aligned} \alpha(f) &= k_1\sqrt{f} + k_2 f, \\ \beta(f) &= k_3 f, \end{aligned} \tag{4.2}$$

where, k_1, k_2 and k_3 represent the Chen model constants and f is the frequency [146].

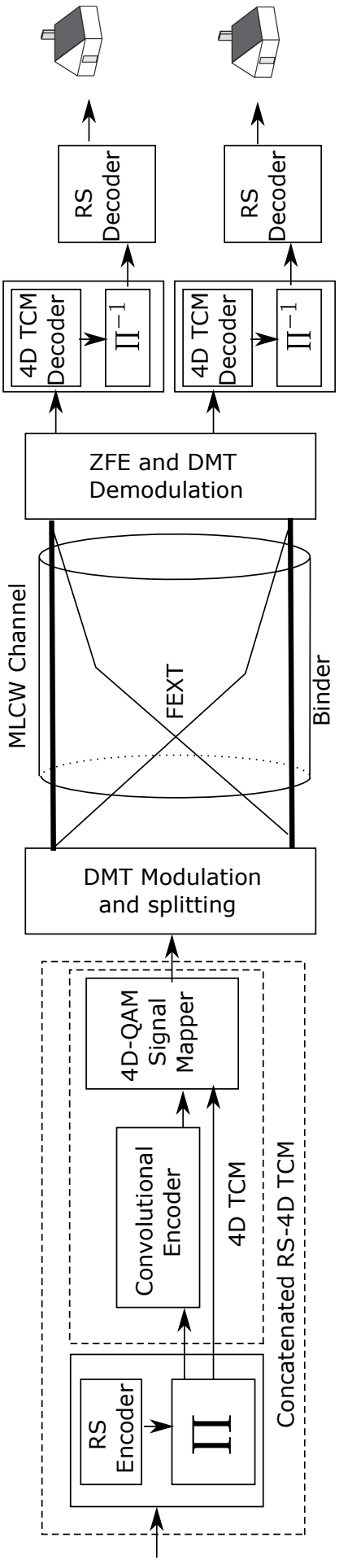

Figure 4.1: $N_r \times N_t$ Multi-line copper wire (MLCW) G.fast system Transceiver

The mutual channels (i.e., between links i and j) are implemented utilizing the FEXT model shown in [145], which represents the American wire gauge (AWG) with a 0.4 mm loop. First, the insertion loss is calculated using:

$$H_{IL}(f, L) = e^{-L/L_m k_{L1}\sqrt{f} + k_{L2} f - jL/L m k_{L3}}, \tag{4.3}$$

where $L_m = 1609.344m$, $k_{L1} = 4.8 \times 10^{-3}$, $k_{L2} = -1.709 \times 10^{-8}$, and $k_{L3} = 4.907 \times 10^{-5}$. Based on (4.3), the FEXT model can be written as:

$$H_{FEXT}(f, l) = k_{xf} f / f_0 \sqrt{L/L_0} H_{IL}(f, l), \tag{4.4}$$

where $f_0 = 1$MHz, $L_0 = 1$km, and $k_{xf} = 10^{-45/20}$.

The channel length was $L_{11} = 100m$ and $L_{22} = 200m$ and the transfer function for the direct channels and the corresponding FEXT channels are presented in Fig. 4.2. It is imperative to check the independence of the individual channels to design the relevant detector. By applying the Kolmogrov-Smirnov (KS) test of independence [147] at a 5% significance level, the result was 0, implying that the null hypothesis shows the two vectors exhibit the same distribution and the channels are independent.

In this chapter, the channel is assumed to be perfectly estimated at the receiver. A zero-forcing detector (ZFE) can then be used to equalize the received signal such that:

$$\mathbf{H}^{\dagger} = (\mathbf{H}^H \mathbf{H})^{-1} \mathbf{H}^H, \tag{4.5}$$

where $\mathbf{H}^{\dagger}$ is the Moore-Penrose pseudo inverse of the channel matrix $\mathbf{H}$.

4.3 DMT-based MLCW G.fast System Over Impulsive Noise Copper Channel

This chapter considers an MLCW system with $N_r \times N_t$ receivers and transmitters with a non-linear IN compensator, as presented in Fig. 4.3. In this work, we consider the same IN model that is used in [139], MCA which has a probability density function (PDF) defined as previously in chapter 3 as:

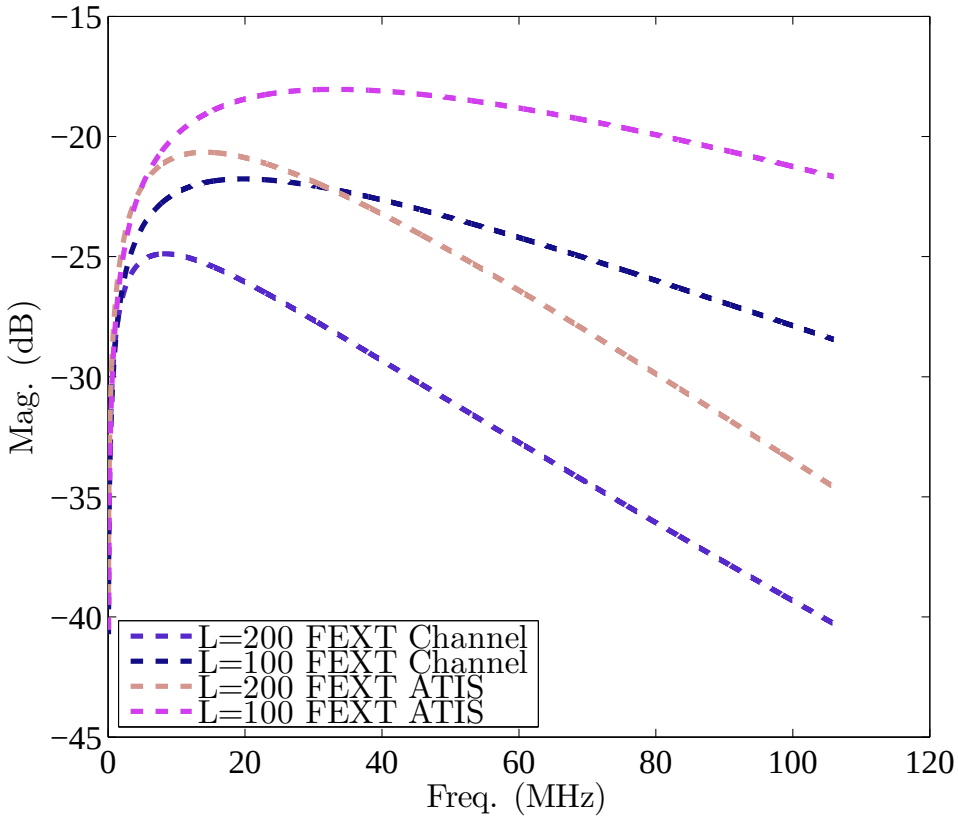

Figure 4.2: Transfer function for the direct channels and the corresponding FEXT channels

$$p(x) = \sum_{s=0}^{\infty} \frac{e^{-A} A^s}{s!} . \frac{1}{\sqrt{2\pi\sigma_s^2}} e^{(-\frac{x^2}{2\sigma^2})}$$

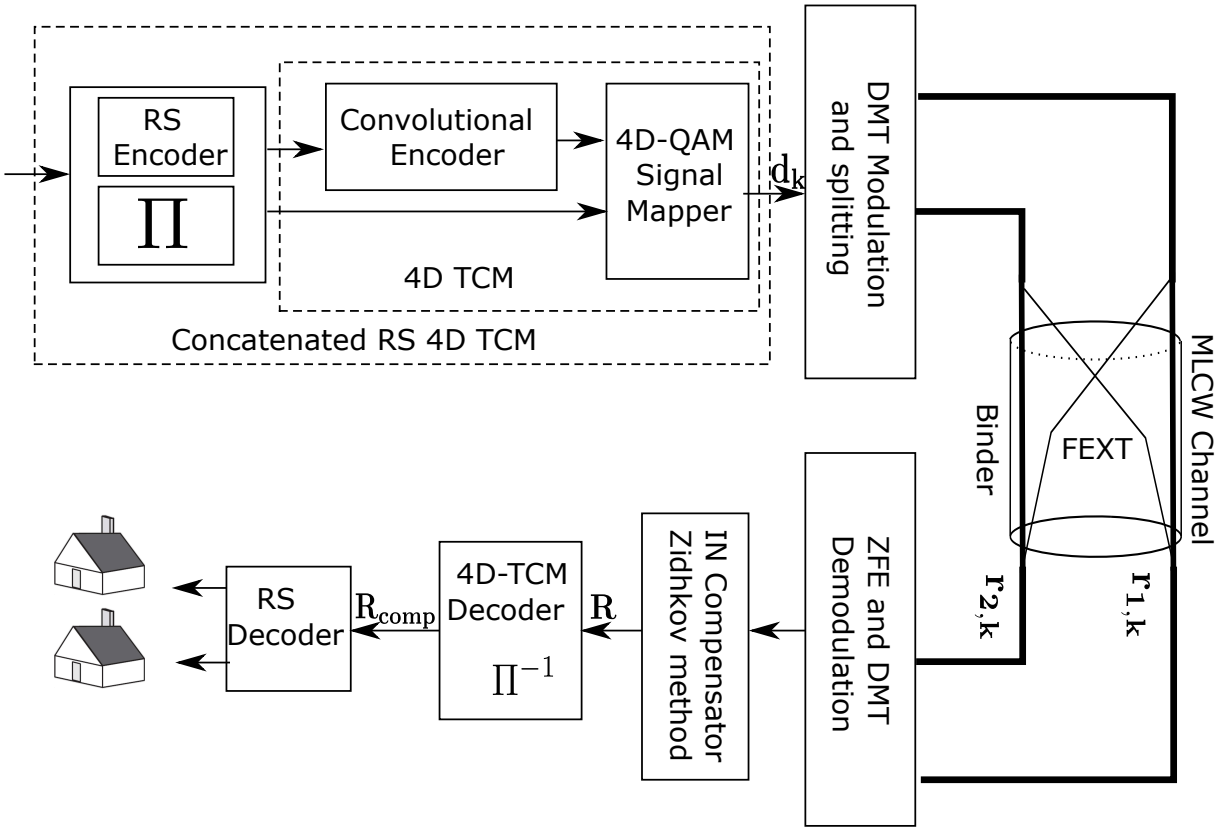

Figure 4.3: $N_r \times N_t$ Multi-line copper wire G.fast system Transceiver with the IN compensator on the receiver

The channel is modelled as two parallel pairs of copper wire line that carries the coded data to the users taking into consideration the effect of the far-end cross-talk (FEXT) effect between the pairs i and j. The received signal per symbol ,$\mathbf{r}_k \in \mathbb{C}^{N_r \times 1}$ in the presence of IN can be written as

$$\mathbf{r}_k = \mathbf{H}_k \mathbf{d}_k + (\mathbf{w}; \mathbf{i} + \mathbf{w}_k), \tag{4.6}$$

where, $\mathbf{H}_k \in \mathbb{C}^{N_r \times N_t}$ represents the channel parameter matrix per symbol, $\mathbf{d}_k \in \mathbb{C}^{N_t \times 1}$ is the transmitted vector per symbol, and $(\mathbf{w}; \mathbf{i} + \mathbf{w}_k) \in \mathbb{C}^{N_r \times 1}$ is the AWGN or the AWGN plus IN vector per symbol, respectively. The subscript k will be dropped from subsequent equations for simplicity. The received signals $\mathbf{r_1}$, $\mathbf{r_2}$ are first equalized based on the ZFE detector and demodulated with DMT demodulator. According to Procedure 4.1, the demodulated vector $\mathbf{R}^{(comp)}$ is achieved by following the algorithm's steps of IN compensator as illustrated in the following IN compensation algorithm.

Algorithm 4.1 : IN compensation algorithm for MLCW G.fast [95]

1: Demapping and pilot estimation $\hat{X}$

2: Estimation of total noise $\hat{D} = \hat{H}(R^{eq} - \hat{X})$

3: $\hat{\mathbf{d}} = \text{IDFT}(\hat{\mathbf{D}})$

4: $\sigma^2 = \frac{1}{M}\sum_{l=0}^{M-1}\left|\hat{d}_l\right|^2$

5: $\hat{\mathbf{i}} = \begin{cases} \hat{d}_l, \text{ if } \left|\hat{d}_l\right| > T_h\hat{\sigma}^2, l = 0, 1, \cdots, M-1, \\ 0, \quad \text{Otherwise} \end{cases}$

6: Samples detection $\hat{\mathbf{I}} = \text{DFT}(\hat{\mathbf{i}})$

7: $\mathbf{R}^{(comp)} = \mathbf{R}^{(eq)} - \hat{\mathbf{I}} \times \hat{\mathbf{H}^{-1}}$

where T_h is used as a threshold value, $\mathbf{R}^{(comp)} = [R_0^{(comp)}, R_1^{(comp)}, \ldots, R_{M-1}^{(comp)}]$ is the compensated signal in the frequency domain by means of a FFT. Procedure 4.1 is repeated for several iterations for better IN cancellation and to improve the BER performance. Following that, each receiver will apply the decoding process on the compensated vector $\mathbf{R}^{(comp)}$ in reverse order to fully reconstruct the transmitted vectors.

4.4 Simulation Results

An outline of IN cancellation for MIMO G.fast system with multiple twisted pairs is presented here. IN frequency domain cancellation method (as illustrated in details in section 2.8.2) is used here to reduce the influence of impulsive noise over MLCW channel. According to comparative study, the simulation results presented in the previous chapter also showed that the proposed scheme is more superior than other existing IN mitigation techniques. As mentioned before that the performance of a mitigation noise method is threshold-dependent. Accordingly, an optimal threshold expression has been derived in subsection 3.3.4 is applied to the MIMO G.fast system here to achieve the optimal performance of IN cancellation methods based in the frequency domain.

Therefore, a number of possible fixed threshold values for FD Impulsive noise cancellation is described. The closest four BER curves to AWGN performance are observed at a $FT = [Th1, Th2, Th3, Th4]$. Then, it is clearly understood that the BER performance results by using optimal threshold-based FD IN mitigation method outperform all BER performance results obtained using a fixed threshold

value. Thus, it is shown from the results in this section that, the OT outperforms FT at higher SNRs than those obtained using a FT. Finally, Simulation results showed that the performance of this proposed FD mitigation scheme (Zhidkov algorithm) with OT can suppress an impulsive noise in copper channel and improve bit-error-rate performance in multi-line copper wire MLCW communication.

In Fig. 4.4, the BER performance of the coded G.fast single-line copper wire system is compared to the G.fast coded MLCW for two cases of with and without IN. It is observed that, G.fast MLCW model has improved performance compared to the single line G.fast scenario regardless of the presence of IN with a gain of 4dB at BER = 10^{-4}. A comparative analysis between the proposed MLCW G.fast and the single-line G.fast system in term of BER performance, utilizing Zhidkov's algorithm as the IN mitigation method as seen in Fig. 4.5. The MLCW G.fast shows an improvement in BER performance of $2dB$ at BER = 10^{-4} after the second iteration compared to the single-line G.fast system. While the performance of the proposed MLCW G.fast system utilizing Zhidkov's algorithm has improved the performance by almost$5dB$ compared to single-line G.fast system at BER = 10^{-4} under the influence of IN.

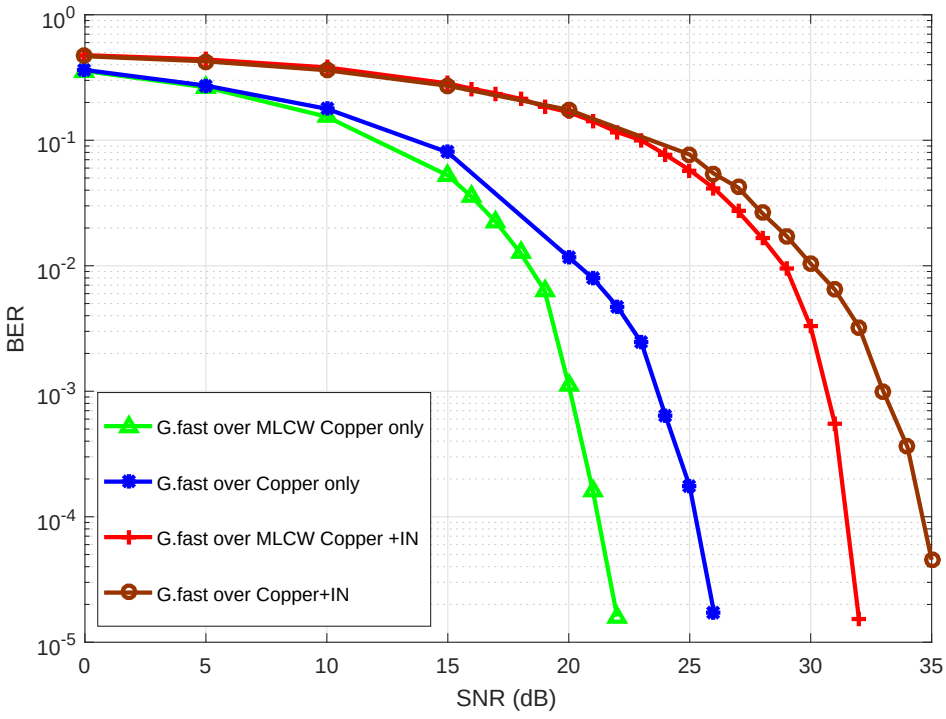

Figure 4.4: The BER performance comparison of the proposed MLCW G.fast vs single-line G.fast over copper channel.

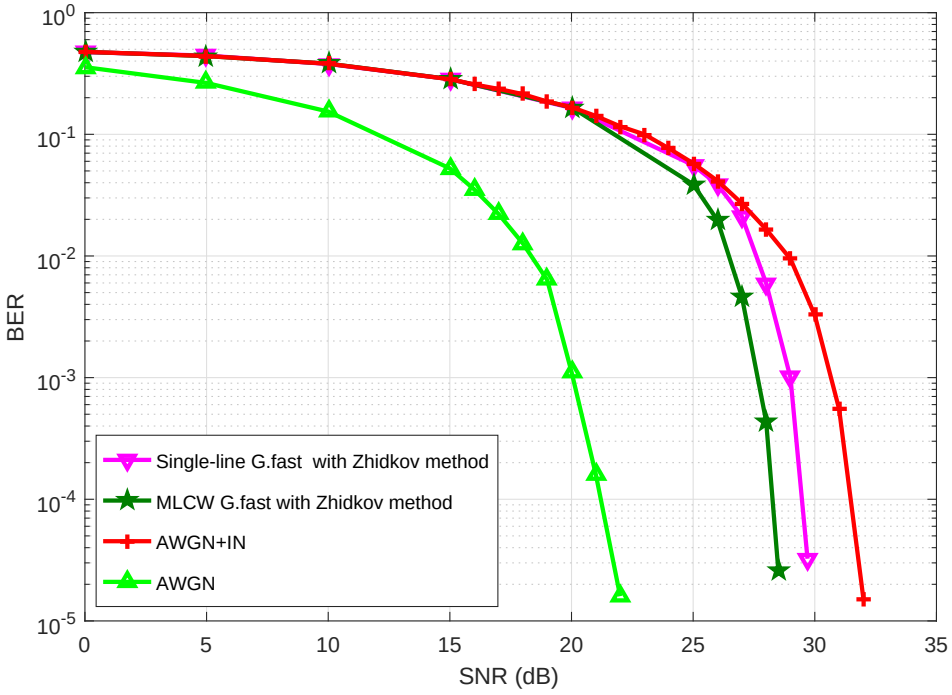

Figure 4.5: The BER performance comparison of the proposed MLCW G.fast vs single-line G.fast utilizing Zhidkov algorithm as an IN mitigation method over copper channel.

Figures 4.6 through 4.9 present the BER performance of 2×2, 4×4, 8×8 and 16×16 MLCW G.fast with six different QAM cross-constellations of $M = 32, 128, 512, 2048, 8192$ and $32768QAM$ signal points affected by AWGN noise only. It can be observed that as the constellation order increases, the capacity of transmission increases while the BER performance decreases.

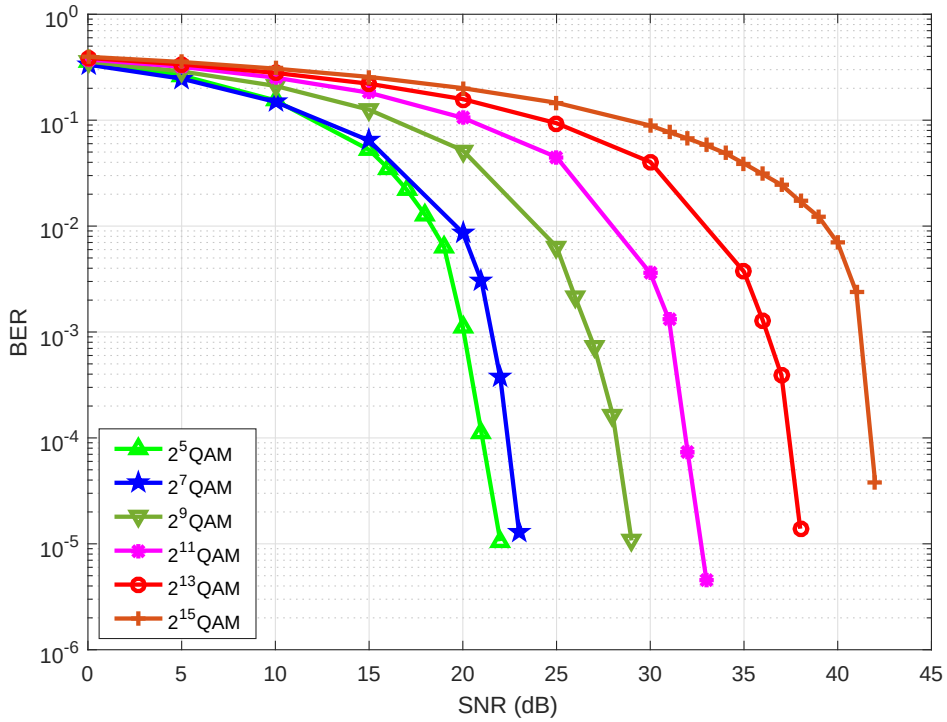

Figure 4.6: The BER performance for the proposed 2×2 MLCW G.fast with six different higher M-QAM signal constellations.

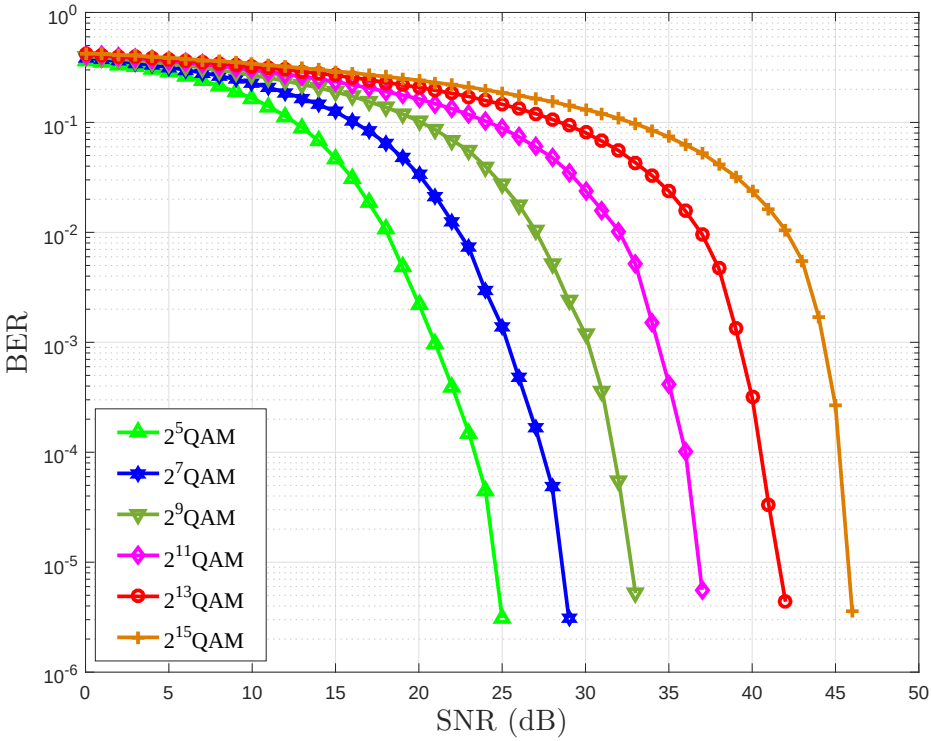

Figure 4.7: The BER performance for the proposed 4×4 MLCW G.fast with six higher M-QAM signal constellations.

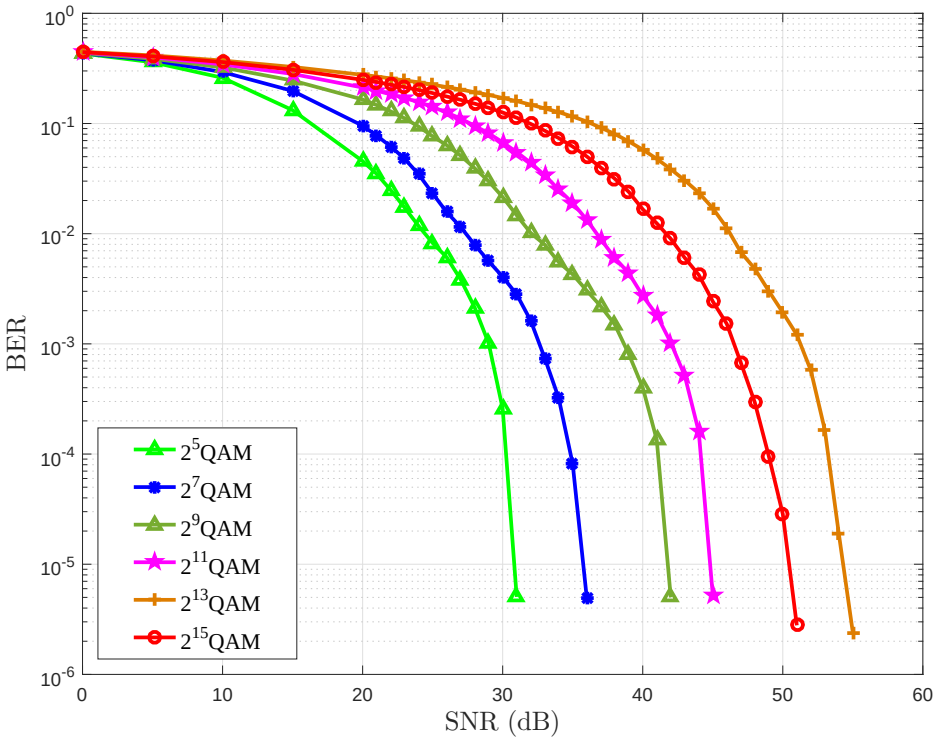

Figure 4.8: The BER performance for the proposed 8×8 MLCW G.fast with six higher M-QAM signal constellations.

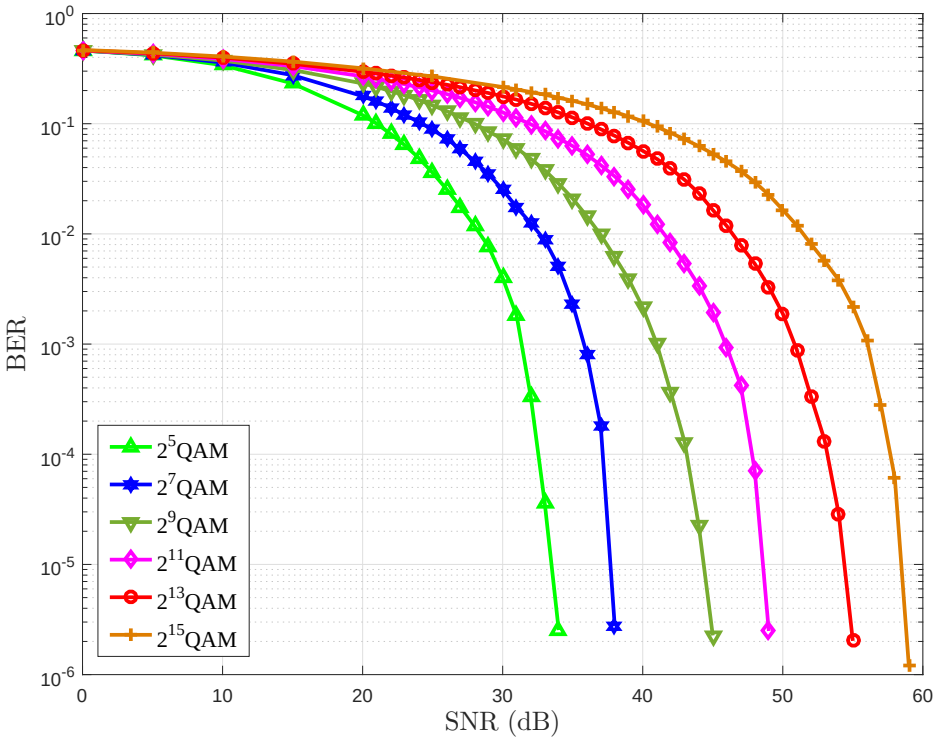

Figure 4.9: The BER performance for the proposed 16×16 MLCW G.fast with six higher M-QAM signal constellations.

More interestingly, The MIMO G.fast system is examined on IN over the proposed MLCW channel throughout Figures 4.10 to 4.13 represent the simulation results in term of BER performance of four different G.fast MIMO configuration such as 2×2, 4×4, 8×8 and 16×16 using 32-QAM modulation and ZFE as a linear equalizer at the receiver side in the presence of IN. Through these figures it is obvious that, the BER performance comparisons between the OT and all fixed thresholds applied to Zhidkov's algorithm for four different MIMO-DMT G.fast configurations outperforms all four BER performance curves obtained using a fixed threshold values, $Th1, Th2, Th3, Th4$ by $1dB$ at BER $= 10^{-4}$.

Additionally, it has been tested for the range of all different MIMO configurations such as 2×2, 4×4, 8×8 and 16×16 through Figures 4.10 to 4.13. It can be seen that, there is no negative effect on BER performance of MIMO G.fast system using OT values applied to FD method when the size of MIMO configurations increased.

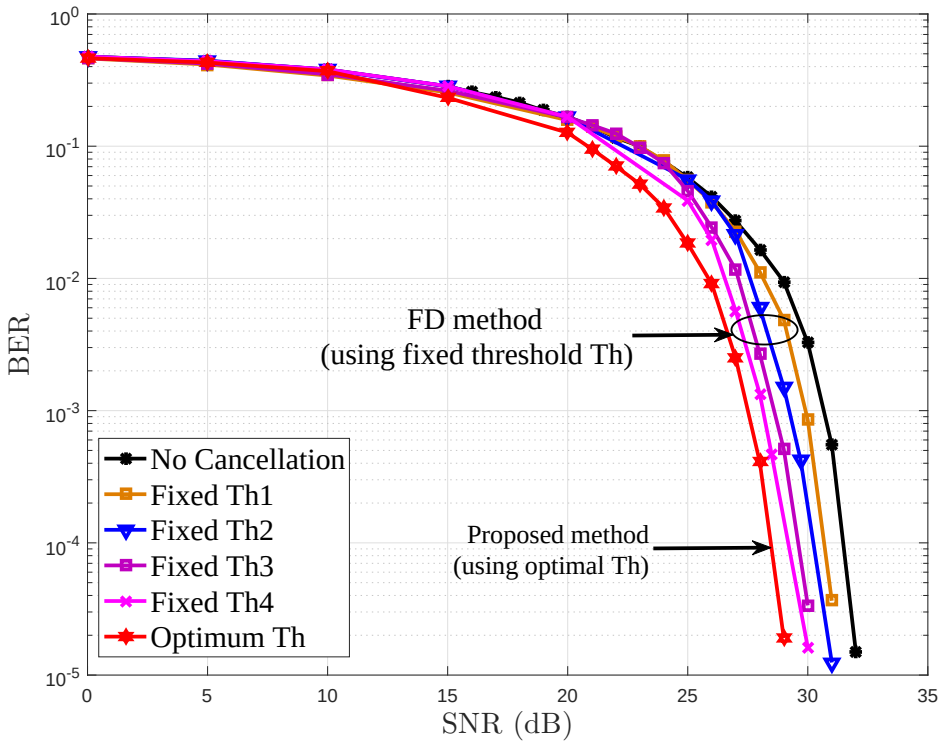

Figure 4.10: BER performance comparison between the optimal and fixed threshold applied to FD IN mitigation method over 32-QAM 2×2 MLCW G.fast system.

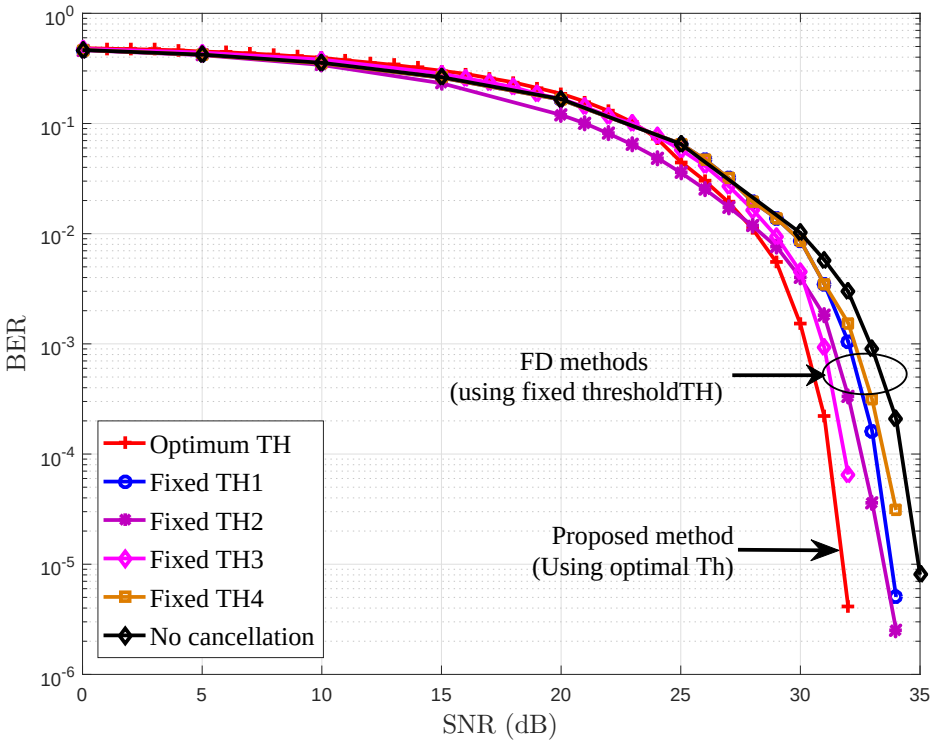

Figure 4.11: BER performance comparison between the optimal and fixed threshold applied to FD IN mitigation method over 32-QAM 4×4 MLCW G.fast system.

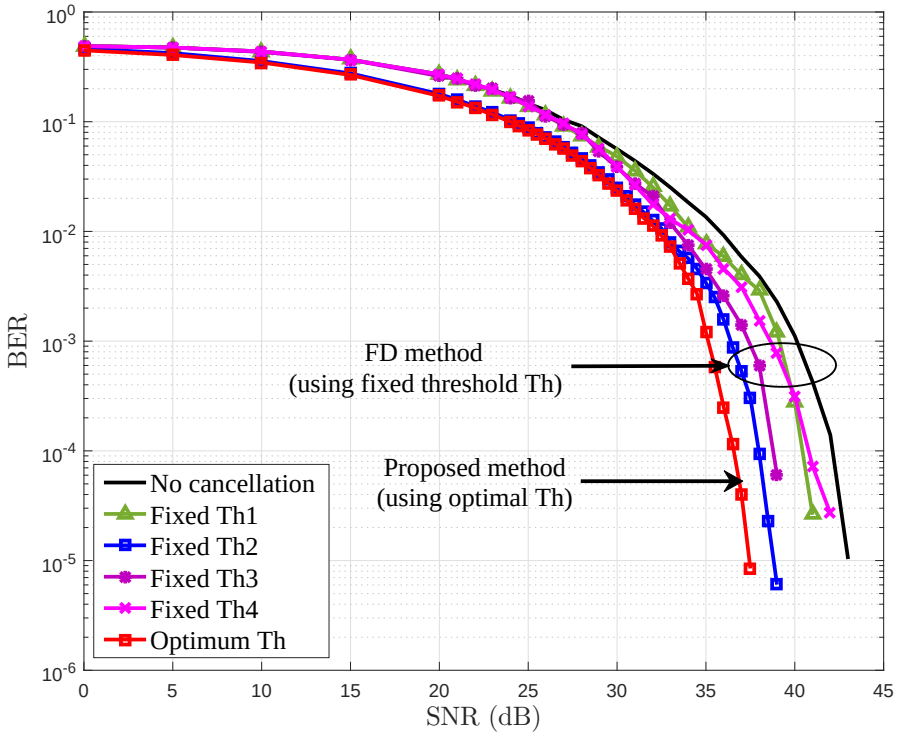

Figure 4.12: BER performance comparison between the optimal and fixed threshold applied to FD IN mitigation method over 32-QAM 8×8 MLCW G.fast system.

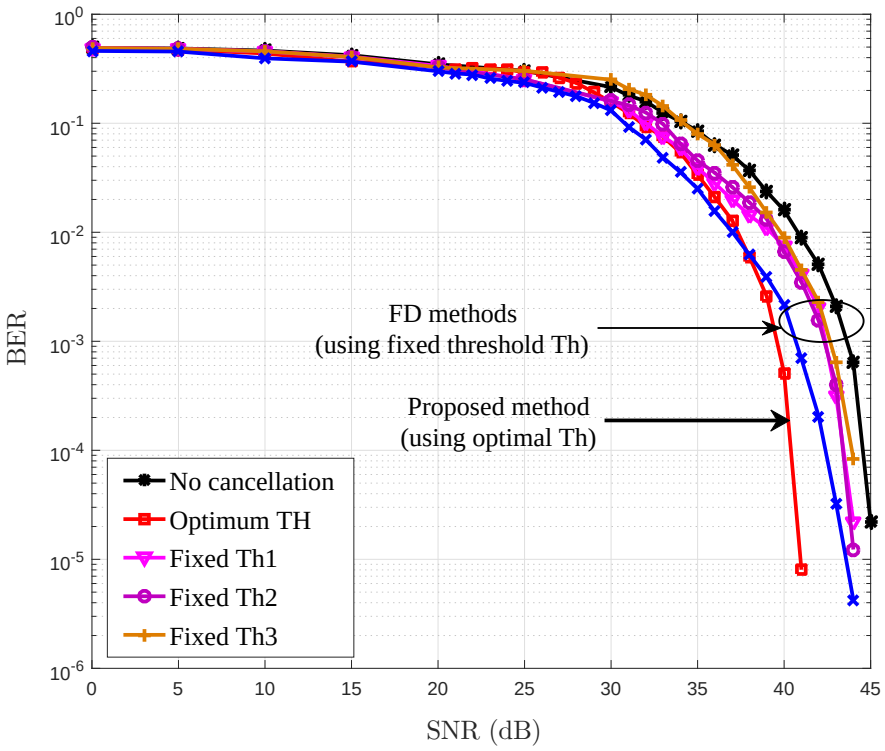

Figure 4.13: BER performance comparison between the optimal and fixed threshold applied to FD IN mitigation method over 32-QAM 16×16 MLCW G.fast system.

4.5 Summary

This chapter presented an evaluation of data transmission using high order QAM, DMT and high frequency MIMO for a G.fast system under the influence of Gaussian and impulsive noise over a copper channel. The goal was the comparative analysis of the BER of MIMO G.fast system using high–order QAM modulation for the two cases of the presence of AWGN only and the presence of AWGN and IN using IN cancellation methods.

Results were also presented for the MLCW channel model affected by Middleton Class A impulsive noise as a class of impulsive noise. In addition, the simulations are verified for different M-QAM cross constellations and for high M values to demonstrate how the proposed system behaves with six different values of QAM cross constellations of $M = 32, 128, 512, 2048, 8192$ and $32768 - QAM$. Finally, the comparative analysis of BER of MIMO DMT G.fast system with IN frequency domain cancellation technique (mentioned in chapter 3 previously) was implemented for all four $M \times N$ MIMO G.fast configurations in this chapter as a solution for IN mitigation.

Chapter 5

Linear and Non-linear Crossstalk cancellation for MLCW Model of G.fast system

5.1 Introduction

Recent wireline G.fast systems use a frequency spectrum from 2MHz to 106 or 212MHz to reach higher data rates. At these frequencies, crosstalk coupling between different copper lines as a electromagnetic coupling of the same binder becomes very strong. These crosstalk coupling can be classified into two categories: near-end crosstalk (NEXT) that arises from DSL transmitters near the receiver, and far-end crosstalk (FEXT) that occurs from transmitters at the far end of the loop as shown in Fig. 5.1.

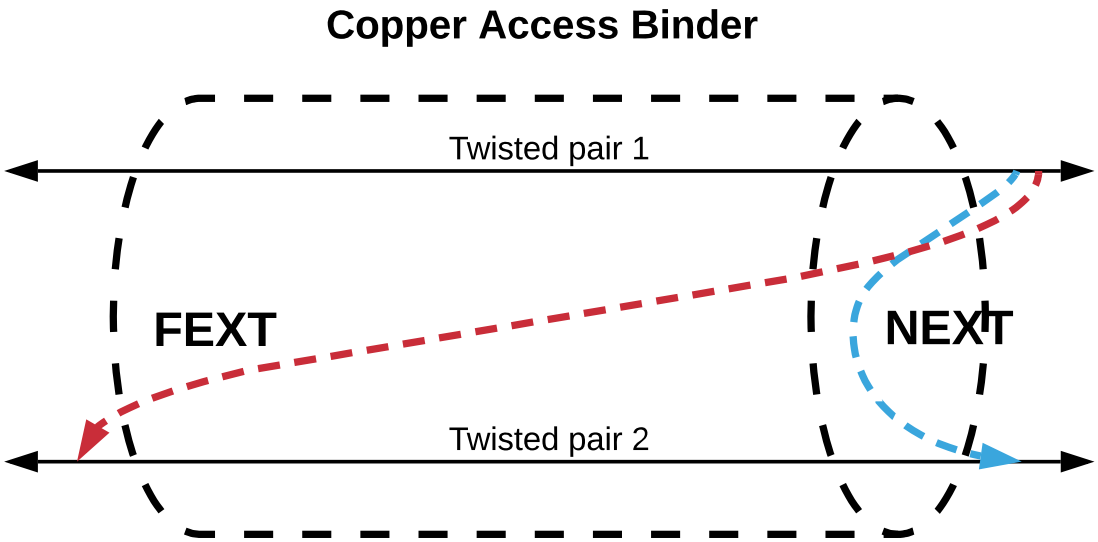

Figure 5.1: NEXT and FEXT interferences in a copper cable binder for 2 the proposed MLCW G.fast system

Consequently, MIMO equalization in the uplink is the key to accomplishing the desired performance of G.fast. This work focuses on MIMO equalization in the uplink. Linear zero-forcing(ZF), nonlinear zero-forcing, linear minimum mean square error (MMSE) and nonlinear MMSE Crosstalk cancellation methods are compared in terms of achievable data rates vs BER performance.

However, to enhance the noise improvement presented by the ZF canceller, the MMSE canceller was introduced, where the noise variance is take into account in the construction of the filtering matrix. The MMSE canceller outperforms the ZF canceller particularly at higher frequency tones. While prior works in [113], [117] showed how crosstalk cancellation of DSL systems could be achieved by more advanced non-linear ZF receivers, simple receivers have been preferred as an operative scheme, mainly in the computationally intensive crosstalk cancellation. With the advance of broadband services, multiple input multiple output (MIMO) has drawn much attention due to its capability of supporting high data rate.

On the other hand, with practical applications, the size of equipment is limited and the complexity for implementation should be moderate and it is difficult to

increase the data transmission rate only through increasing the number of MIMO configurations. Thus, the multiple-input-multiple-output (MIMO) technique combined with multi-level quadrature amplitude modulation (MQAM), such as those used in G.fast system, has been considered an effective scheme for high transmission rate in next generation mobile communication systems [148], [149]. It is worth mentioning that the performance analyses in present literature are mostly focused on MIMO systems under low-order modulation mode. So far, crosstalk cancellation methods for high order QAM constellations, is more challenging. It is necessary to investigate the performance of these schemes which is applicable for DMT-based MIMO G.fast system which uses high order QAM Cross-constellations of $M = 32, 128, 512, 2048, 8192, 32768$ QAM signal points.

The use of a linear structure of crosstalk mitigation is recommended by the ITU-T standard for the G.fast 106 MHz [150]. The various crosstalk cancellation methods have been discussed in the literature and can be evaluated using various trade-offs between performance and computational complexity. Linear cancellation schemes provide inferior error performance with much reduced complexity while Maximum Likelihood Detector (MLD) algorithm provides optimum performance with high complexity. Based on these observations, the comparative study of various cancellation schemes in terms of BER performance and complexity criteria are analysed for different binder configurations. In the following sections, we discuss various crosstalk cancellation schemes for upstream transmission.

The contribution of this chapter can be summarized in the following points,

- The BER performance comparison between linear and nonlinear SIC cancellation schemes are carried out here for cancellation at the downlink receiver in a MIMO-DMT twisted pair G.fast system for the 2×2,4×4, 8×8 and 16×16 MIMO system configurations and also the performance carried out for 32-QAM, 128-QAM, 512-QAM .

- The computational complexities required by each of the linear and nonlinear SIC cancellation methods are compared and tabulated in this chapter.

- Finally, obtaining a BER performance comparison between these schemes for cancellation at the downlink receiver in a MIMO-DMT twisted pair G.fast system in the presence of impact of MCA impulsive noise.

5.2 MIMO Crosstalk Cancellation

The impact of the crosstalk growths with the number of copper lines in the same binder of DSL system. Hence, to challenge this problem crosstalk cancellation can again be considered. The objective of the MIMO canceller is to recover the transmitted symbols, $\hat{s}$, and provides effective approximate solution of the cancellation problem at receiver with the lowest probability of error by utilizing the lowest level of precision in the receiver using different decomposition schemes. Several crosstalk cancellation techniques were proposed in the literature. Through the last two chapters , ZF canceller has been used with G.fast system model. In this chapter, most of crosstalk cancellation techniques are explained and evaluated in terms of predetermined performance and complexity criteria. as shown below in Fig. 5.2, the proposed MLCW G.fast used different four crosstalk cancellation techniques to evaluate the performance of MLCW G.fast system model. Using MATLAB as the simulation platform, received signal vector y of a 4×4 MLCW G.fast system over 32-QAM copper channel is presented in algorithm 5.1.

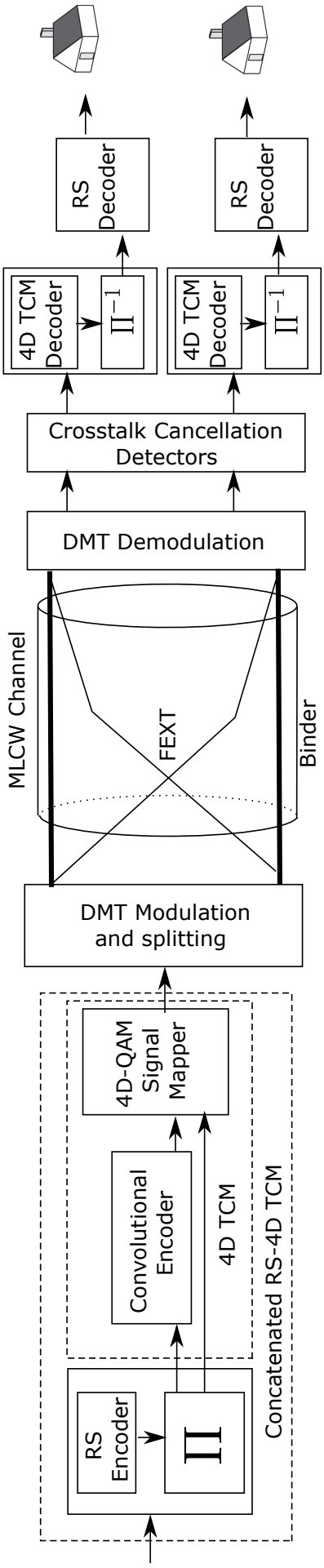

Figure 5.2: The block digram MLCW G.fast system with different crosstalk cancellation techniques.

Algorithm 5.1 Received signal vector of a 4×4 MLCW G.fast system using cross 32-QAM constellation over copper channel

close all;

clear all;

procedure $Input = (Nt, Nr, M, var, Len - sig, SNRdB, Constl)$

Nt = 4; ▷ Number of transmit pair.

Nr =4; ▷ Number of received pair.

M = 32; ▷ 32-QAM modulation.

L = 1000; ▷ Length of transmit signal.

SNRdB; ▷ SNR in dB.

$SNR = 10.^(SNRdB/10)$;

$var = 1./(SNR * log2(M))$;

$Constl = [1+1j1+3j3+1j3+3j1-3j1-1j3-3j3-1j, -3+1j-3+3j-1+1j-1+3j-3-3j-3-1j-1-3j-1-1j, 5+1j5+3j-5+1j-5+3j1+5j1-5j3+5j3-5j, -3+5j-3-5j-1+5j-1-5j5-3j5-1j-5-3j-5-1j]$; ▷ 32 QAM constellation.

$Constl = Constl * sqrt(3/(2 * (M-1)))$;

$s = Constl(randint(Nt, L, [1M]))$; ▷ Transmitted signal s after modulation.

i = 0;

for u = 1:L

for v = 1:Nt

i = i+1;

sbin(i,:) = Constl-bin(find(Constl==s(v,u)),:); ▷ transmitted signal in binary codes.

end

end

$H = (randn(Nr, Nt) + sqrt(-1) * randn(Nr, Nt))/sqrt(2)$; ▷ Channel matrix.

$n = (randn(Nr, L) + sqrt(-1) * randn(Nr, L)) * sqrt(var(in))/sqrt(2)$; ▷ AWGN noise.

$y = H * s + n$; ▷ Received signal.

end procedure

5.2.1 Linear Crosstalk Cancellers

Linear cancellers are simplest cancellers which considered as crosstalk cancellation techniques, used a very simple strategy to achieve partial crosstalk cancellation. So, one of the advantages of using a linear canceller is that the complexity can be effectively reduced by using the linear cancellers. Using the received signal of MIMO channel in algorithm. 5.1, MATLAB programs of BER simulations for the ZF, MMSE crosstalk cancellation techniques in algorithms 5.2 and 5.3, respectively.

5.2.1.1 Zero Forcing Canceller (ZF)

The ZF estimator and the estimated symbol vector are given by the general equation of ZFE canceller can be written as

$$E_{zf} = H(H^H H)^{-1} H^H \tag{5.1}$$

and

$$\begin{aligned} \tilde{d}_{zf} &= E_{zf} r, \\ &= (H^H H)^{-1} H^H r, \\ &= d + (H^H H)^{-1} H^H (W + I) \end{aligned} \tag{5.2}$$

respectively.

The hard decision of d is summarized at the symbol level as follows.

- Step 1. From 5.2, we have $\tilde{d}_{zf} = [\tilde{d_1}, \tilde{d_2}, ..., \tilde{d_K}]^T$.
- Step 2. Let the signal alphabet of M-ary QAM denoting by $Ð = \left\{d^{(1)}, d^{(2)}, ..., d^{(m)}\right\}$, the hard decision of mth signal for d is given by

$$\hat{d_k} = \arg \min_{d^{(m)} \in C} \left| d^{(m)} - \tilde{d_k} \right|, for k = 1, 2, ..., K. \tag{5.3}$$

- Step 3. The hard decision of d is generated as $\hat{d} = \left[\hat{d_1}, \hat{d_2}, ..., \hat{d_K}\right]^T$.

Algorithm 5.2 ZF Canceller

procedure $Input = (r, H, dbin, Nt, L, M, Constl, Constl - bin)$
  $\hat{d}_{zf} = zeros(M, Nt * L);$
  $kset = zeros(Nt, L);$
  $\tilde{d}_{zf} = (pinv(H' * H + H') * r;$
  for $j \leftarrow 1$ *to* $length(Constl)$ **do**
    $\hat{d}_{zf}(j,:) = reshape(abs(\tilde{d}_{zf} - Constl(j)).O2, 1, size(r,1) * size(r,2));$
  end for
  end for
  for $q = 1 : size(\hat{d}_{zf}, 2)$ **do**
    $hatsbin(q,:) = Constl - bin(kset(q),:);$
    end for
  end for
  $[dmin, kset] = min(\hat{d}_{zf});$
  $BER = mean(reshape(abs(dbin - hatdbin), 1, Nt * L * log2(M)));$
end procedure

5.2.1.2 Minimum Mean-Square Error canceller (MMSE)

To reduce the impact from the background noise, the MMSE canceller employs a linear filter that can take into account the noise. The MMSE filter can be found by minimizing the mean-square error (MSE) as 1 The problem of noise enhancement through zero-forcing has already been addressed. An improved performance can be achieved by including the noise term in the design of the linear filter matrix G. This is done by MMSE cancellation schemes, where the filter represents a trade-off between noise amplification and interference suppression. updated by israa To reduce the effect of noise enhancement through ZF cancellation scheme, the MMSE cancellation scheme can be achieved an improved performance by using a linear filter that can take into account the noise. The MMSE filter matrix can be found by minimizing the mean-square error (MSE) between the original transmitted signals and the output of a linear canceller as

$$E_{mmse} = H^H (H^H H + \sigma_n^2 I_{nt})^{-1} \tag{5.4}$$

The resulting estimated symbol vector $\tilde{d}$ is given by

$$\begin{aligned} \tilde{d}_{mmse} &= E_{mmse} r, \\ &= (H^H H + \sigma_n^2 I_{nt})^{-1} H^H r, \end{aligned} \tag{5.5}$$

The MMSE hard decision $\hat{d}$ can be obtained from $\tilde{d}_{mmse}$ by using the method in 5.3

Algorithm 5.3 MMSE Canceller

procedure $Input = (r, H, dbin, var, Nt, L, M, Constl, Constl - bin)$
  $\hat{d}_{mmse} = zeros(M, Nt * L)$;
  $kset = zeros(Nt, L)$;
  $\tilde{d}_{mmse} = (pinv(H' * H + var * eye(Nt)) * H') * r$;
  for $j \leftarrow 1$ *to* $length(Constl)$ **do**
    $\hat{d}_{mmse}(j,:) = reshape(abs(\tilde{d}_{mmse} - Constl(j)).O2, 1, size(r,1) * size(r,2))$;
  end for
  end for
  for $q = 1 : size(\hat{d}_{mmse}, 2)$ **do**
    $hatdbin(q,:) = Constl - bin(kset(q),:)$;
    end for
  end for
  $[dmin, kset] = min(\hat{d}_{mmse})$;
  $BER = mean(reshape(abs(dbin - hatdbin), 1, Nt * L * log2(M)))$;
end procedure

5.2.2 Non-Linear Crosstalk cancellers

To achieve a trade of between the BER performance and computational complexity, Non-linear cancellers are considered. With non-linear crosstalk cancellers, the received signals are not detected in parallel, but one after another. So, the non-linear crosstalk Cancellation process can realize improved performance at relatively high computational complexity. Using the received signal of MIMO channel in algorithm. 5.1, MATLAB programs of BER simulations for the ZF, MMSE crosstalk cancellation techniques in algorithms 5.4 and 5.5, respectively.

5.2.2.1 ZF-Successive Interference Symbol(ZF-SIC) Canceller

For a square matrix H, which $M = N$, the channel matrix H is factorised as

$$\begin{aligned} H &= QR \\ &= Q \begin{bmatrix} r_{1,1} & r_{1,2} & \cdots & r_{1,M} \\ 0 & r_{2,2} & \cdots & r_{2,M} \\ \vdots & \vdots & \ddots & \vdots \\ 0 & 0 & \cdots & r_{M,M} \end{bmatrix} \end{aligned}$$

Algorithm 5.4 ZF-SIC Canceller

procedure $Input = (r, H, dbin, var, Nt, L, M, Constl, Constl - bin)$
  $kset = zeros(Nt, L)$;
  $ibin = 0$;
  $[Q, R] = qr(H)$;
  $\tilde{w}_{zf-sic} = Q' * r$;
  for $u = 1 : L$ **do**
    for $j = 1 : M$ **do**
      $\hat{d2}_{zf-sic}(j) = (abs(Constl(j) - (\tilde{w}_{zf-sic}(2, u)/R(2, 2))))^2$;
    end for
    $[dmin2, kset(2, u)] = min(\tilde{d2}_{zf-sic})$;
    $hatd(2, u) = Constl(kset(2, u))$;
    for $forq = 1 : M$ **do**
      $\tilde{d1}_{zf-sic}(q) = (abs(Constl(q) - (\tilde{w}_{zf-sic}(1, u) - hatd(2, u) * R(1, 2))/R(1, 1)))^2$;
    end for
    $[dmin1, kset(1, u)] = min(\tilde{d1}_{zf-sic})$;
    $hatdbin(ibin + 1, :) = Constl - bin(kset(1, u), :)$;
    $hatdbin(ibin + 2, :) = Constl - bin(kset(2, u), :)$;
    $ibin = ibin + 2$;
  end for
  $BER = mean(reshape(abs(dbin - hatdbin), 1, Nt * L * log2(M)))$;
end procedure

Where the $N \times N$ matrix Q is unitary and R of size $M \times M$ is upper triangular.

Here, $r_{g,j}$ represent the (g,j)th entry of R. By multiplying the received signal vector r with Q^H, the operation of the received vector r is performed by

$$\begin{aligned}\tilde{w}_{zf-sic} &= Q^H r, \\ &= Rd + Q^H n \end{aligned} \tag{5.6}$$

Note that the $Q^H n$ and n have the same statistical properties,5.6 is rewritten as

$$\tilde{w}_{zf-sic} = Rd + n \tag{5.7}$$

$$\begin{bmatrix} w_1 \\ w_2 \\ \vdots \\ w_M \end{bmatrix} = \begin{bmatrix} r_{1,1} & r_{1,2} & \cdots & r_{1,M} \\ 0 & r_{2,2} & \cdots & r_{2,M} \\ \vdots & \vdots & \ddots & \vdots \\ 0 & 0 & \cdots & r_{M,M} \end{bmatrix} \begin{bmatrix} d_1 \\ d_2 \\ \vdots \\ d_M \end{bmatrix} + \begin{bmatrix} n_1 \\ n_2 \\ \vdots \\ n_M \end{bmatrix} \tag{5.8}$$

Where w_m and n_m represent the mth element of $\tilde{w}_{zf-sic}$ and n,respectively.Thus, we have

$$\begin{aligned} w_M &= r_{M,M} d_M + n_M. \\ w_{M-1} &= r_{M-1,M-1} d_{M-1} + n_{M-1}. \\ &\vdots \end{aligned} \tag{5.9}$$

Then, 5.9 results in a sequential cancellation procedure. Firstly, d_M can be detected from w_M as follows:

- Let

$$\begin{aligned}\tilde{d}_K &= \frac{w_K}{r_{K,K}} \\ &= d_K + \frac{n_K}{r_{K,K}}. \end{aligned} \tag{5.10}$$

  From 5.10, we have $\tilde{d}_{zf-sic} = [\tilde{d}_1, \tilde{d}_2, ..., \tilde{d_K}]^T$.

- Denoting by $C = \left\{c^{(1)}, c^{(2)}, ..., c^{(m)}\right\}$ the signal alphabet of M-ary QAM the

hard decision of d given by

$$\hat{d_K} = \arg \min_{d^{(m)} \in C} \left| c^{(m)} - \tilde{d_K} \right| \tag{5.11}$$

for k=1,2,...,K.

Then, sequential cancellation procedure is carried out to detect all the data transmitted symbols of d. The mth symbol of d, dm, can be detected after cancelling $M - m$ data symbols. This procedure is terminated till all the data symbols of d are detected.

$$u_k = w_k - \sum_{j=k+1}^{K} r_{k,j} \hat{d}_j, \ k \epsilon 1, 2, ..., K-1, \tag{5.12}$$

Where $\hat{d}_j$ represents the hard decision estimate of d_j from u_j. Then, the hard decision of the mth symbol of d, dm, can be estimated as

$$\hat{d_k} = \arg \min_{d^{(m)} \in C} \left| c^{(m)} - \tilde{d_k} \right| \tag{5.13}$$

where $\tilde{d_k} = \dfrac{u_k}{r_{k,k}} = d_k + \dfrac{n_k}{r_{k,k}}$.

5.2.2.2 MMSE Successive Interference Symbol (MMSE-SIC) Canceller

Firstly,an extended channel matrix is defined as

$$H_{ex} = \left[H^T \sigma^2 I \right]^T \tag{5.14}$$

While r and n are also extended, where $r_{ex} = \left[r^T 0^T \right]^T$ and $n_{ex} = \left[n^T - \sigma^2 d^T \right]^T$, respectively.

performing the QR factorization on H_{ex}, we have

$$H_{ex} = Q_{ex} R_{ex} \tag{5.15}$$

where Q_{ex} and R_{ex} denote a unitary matrix and un upper triangular matrix,respectively.

In 5.6, let r, H, n, Q and R be replaced by $r_{ex}, H_{ex}, nH_{ex}, Q_{ex}$ and R, respectively. Then,the resulting

$$\begin{aligned} \tilde{w}_{mmse-sic} &= Q_{ex}^{H} r_{ex}, \\ &= R_{ex} d + Q_{ex}^{H} n_{ex} \end{aligned} \tag{5.16}$$

with Eq. 5.16, the MMSE-SIC cancellation is carried out by the sequential cancellation procedure given from 5.6 to 5.13

Algorithm 5.5 MMSE SIC canceller

procedure $Input = (r, H, dbin, var, Nt, L, M, Constl, Constl - bin)$
  $kset = zeros(Nt, L)$;
  $ibin = 0$;
  $Hex = [H; sqrt(var) * eye(Nt)]$;
  $rex = [r; zeros(Nt, L)]$;
  $[Q, R] = qr(Hex)$;
  $\tilde{w}_{mmse-sic} = Q' * rex$; ▷ comment
  for $u = 1 : L$ **do**
    for $j = 1 : M$ **do**
      $\tilde{d2}_{mmse-sic}(j) = (abs(Constl(j) - (\tilde{w}_{mmse-sic}(2, u)/R(2, 2))))^2$;
    end for
    $[dmin2, kset(2, u)] = min(\hat{d2}_{zf-sic})$;
    $hats(2, u) = Constl(kset(2, u))$;
    for $forq = 1 : M$ **do**
      $\hat{d1}_{zf-sic}(q) = (abs(Constl(q) - (\tilde{w}_{mmse-sic}(1, u) - hatd(2, u) * R(1, 2))/R(1, 1)))^2$;
    end for
    $[dmin1, kset(1, u)] = min(\hat{d1}_{zf-sic})$;
    $hatdbin(ibin + 1, :) = Constl - bin(kset(1, u), :)$;
    $hatdbin(ibin + 2, :) = Constl - bin(kset(2, u), :)$;
    $ibin = ibin + 2$;
  end for
  $BER = mean(reshape(abs(dbin - hatdbin), 1, Nt * L * log2(M)))$;
end procedure

5.3 Complexity Analysis

Gaxpy algorithm is presented here to compute an approximate calculation for the complexity required by each MIMO canceller. According to this algorithm, the complexity concept is generally defined as the number of mathematical operations which required to compute the estimate of the transmitted signal. The computational complexities of linear, nonlinear SIC cancellation technique are Compared in this section. Fig. 5.9 presents a comparison of ZF, MMSE, ZF-SIC and MMSE-SIC

cancellation algorithms in terms of computational complexities. Linear cancellers used in this work have a complexity of $O(9N_r+2N_rN_t(N_t-4))$ operations. Referring back to Subsection 5.2.1.1, Zero Forcing algorithm method is depend on calculation of pseudo-inverse of the channel transfer matrix H. Pseudo-inverse of H needs to be calculated only once per transmitted MIMO vector. Non-linear ZF and MMSE cancellers Based on the QR-factorization of the channel matrix H = QR, which has been used as a successive interference cancellation procedure with backward substitution requires calculating MCG procedure and takes $O(N2t(2Nr+1)+NtNr)$ operations.

5.4 Simulation Results

In this chapter the impact of crosstalk on the copper channel is mitigated effectively using linear and non-linear MIMO crosstalk cancellation algorithms. BER performance analysis is performed for comparisons between linear and non-linear ZF and MMSE cancellers are carried out for 4×4, 8×8 and 16×16 MLCW G.fast system using 32, 128 and 512-QAM signal constellations as cleared from Fig. 5.3, Fig. 5.4 and Fig. 5.5, respectively.

Generally, the performance of MMSE algorithm is better than ZF, however more interestingly, it is found that with the increase in the constellation size both of cancellers, ZF and MMSE show the same performance. The reason behind is that with the increase in the constellation size the power of the transmitted signal and the data rate also increase due to this it can be concluded from equation that the BER performance of MMSE becomes weaker and approaches to the performance of ZF.

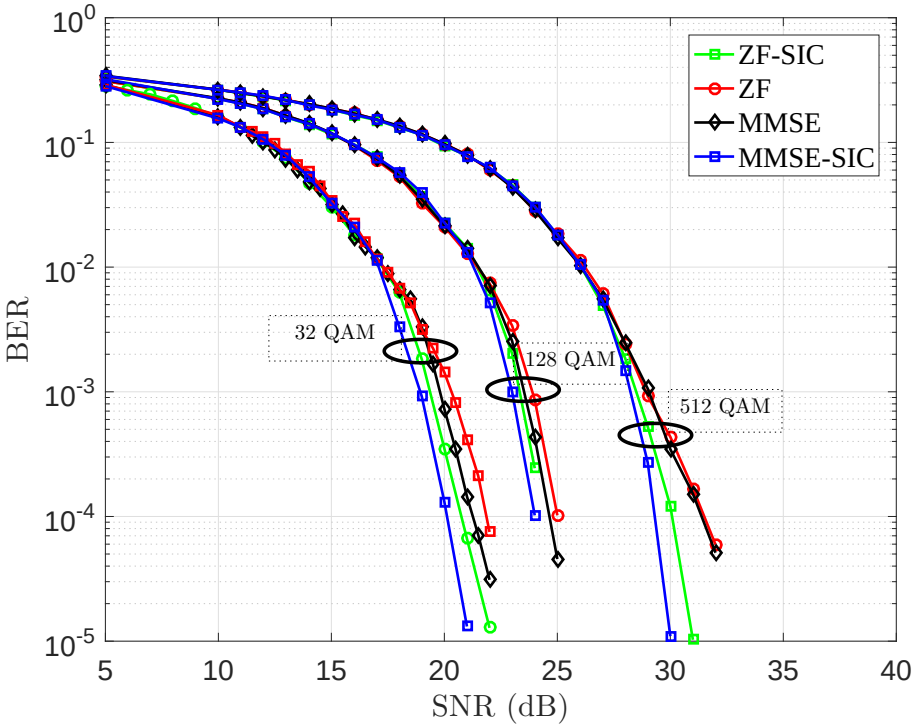

Figure 5.3: BER performance of linear and non-linear crosstalk cancellation techniques for a 4×4 MLCW G.fast system using different value of M-QAM cross constellation(M=32,128 and 512).

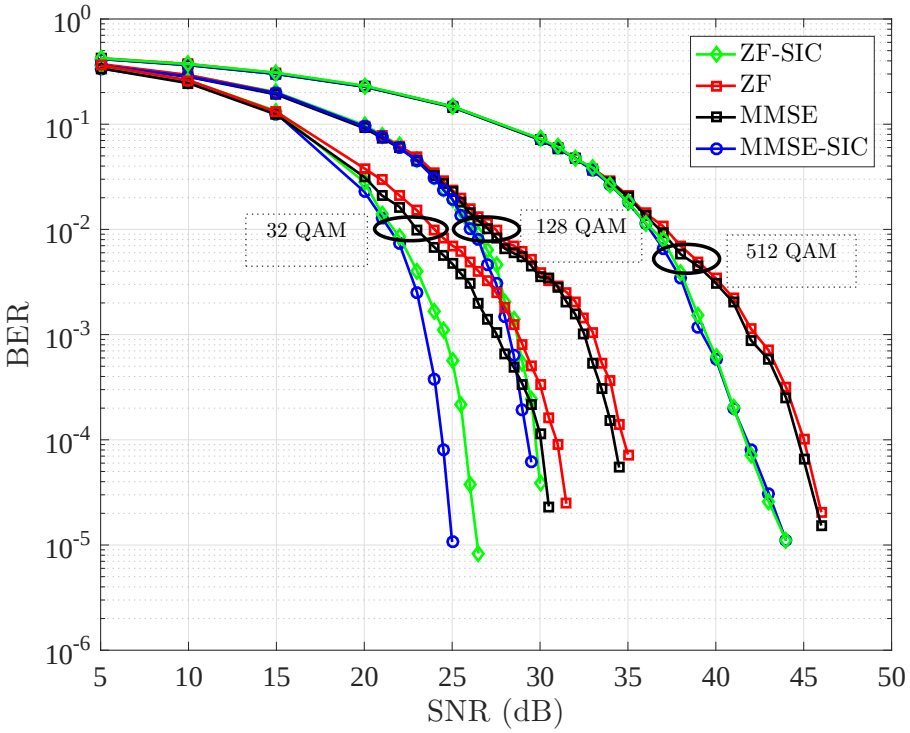

Figure 5.4: BER performance of linear and non-linear crosstalk cancellation techniques for a 8×8 MLCW G.fast system using different value of M-QAM cross constellation(M=32,128 and 512).

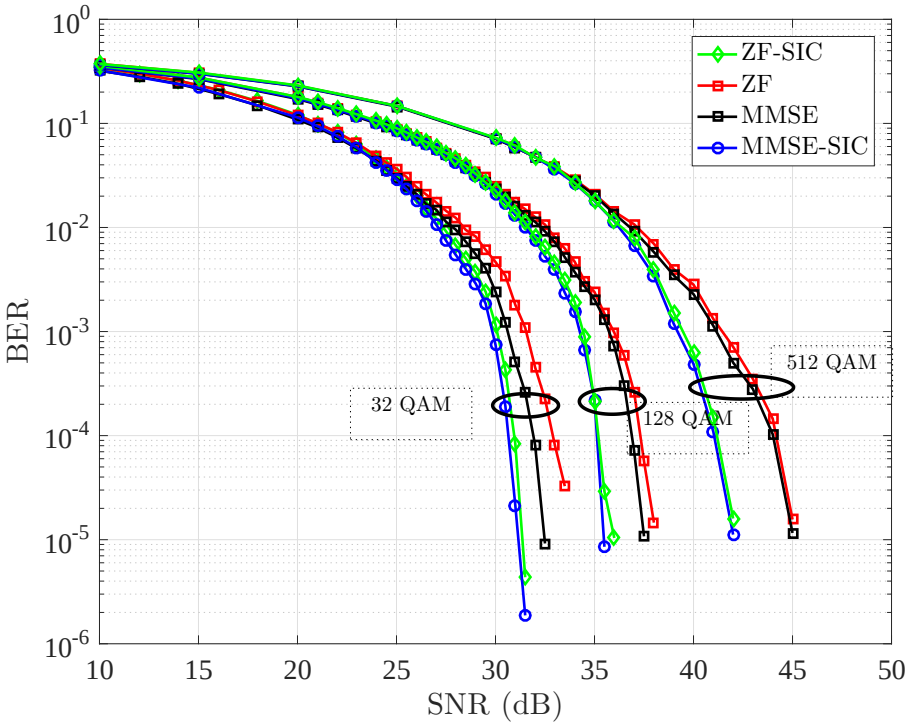

Figure 5.5: BER performance of linear and non-linear crosstalk cancellation techniques for a 16 × 16 MLCW G.fast system using different value of M-QAM cross constellation(M=32,128 and 512).

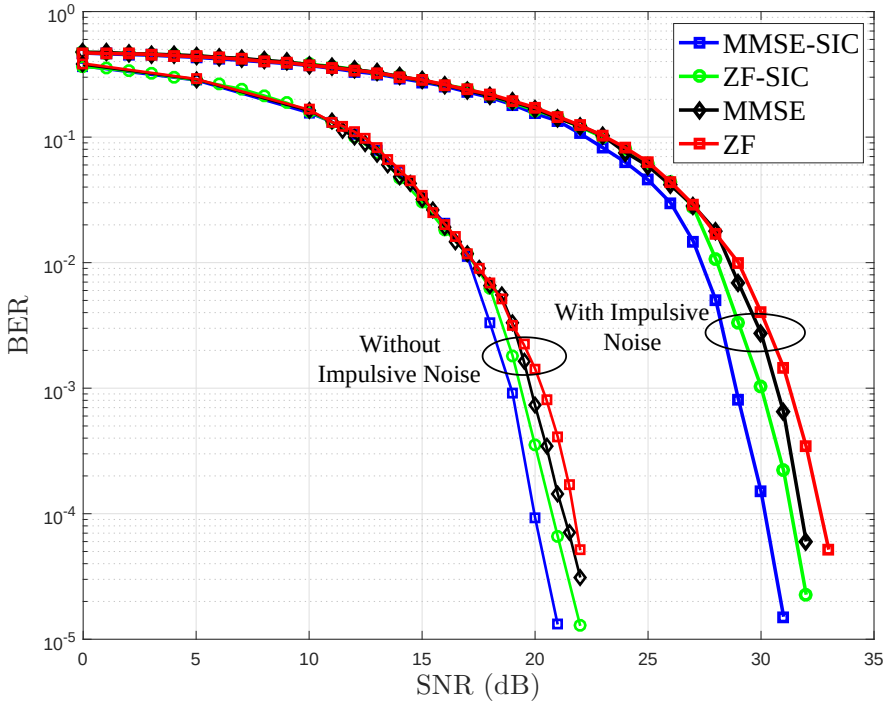

Figure 5.6: BER performance of 4 × 4 MLCW G.fast system with different linear and non-linear crosstalk cancellation methods in the presence of IN using 32-QAM cross constellation

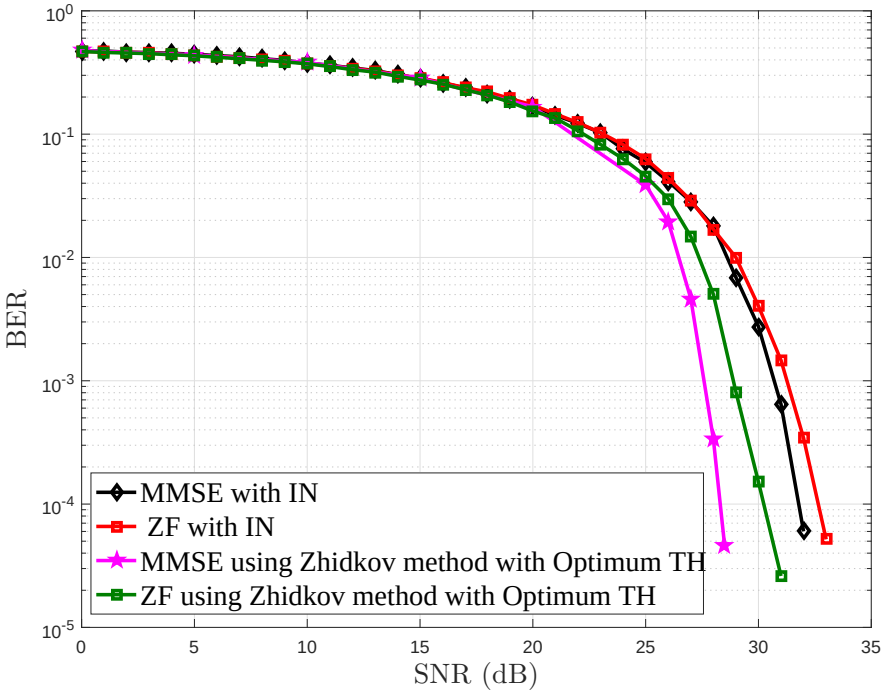

Figure 5.7: BER performance of 4×4 MLCW G.fast system with linear crosstalk cancellation methods utilizing optimal threshold-based Zhidkov algorithm with method 32-QAM cross constellation

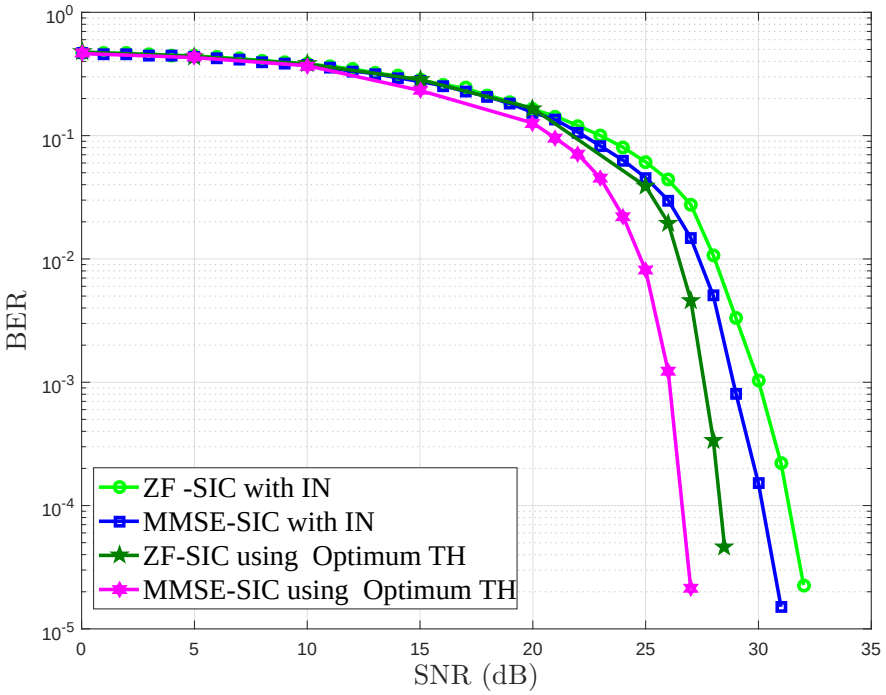

Figure 5.8: BER performance of 4 × 4 MLCW G.fast system with non-linear crosstalk cancellation methods utilizing optimal threshold-based Zhidkov algorithm with method 32-QAM cross constellation

Fig. 5.3 compares the BER performance for four different crosstalk cancellation

methods ZF, ZF-SIC, MMSE and MMSE-SIC. Generally, it can be noticed that the performance improved as the size of QAM constellation decreases. In addition, in each cancellation method (i.e., ZF and MMSE), the gab difference between the linear and non-linear methods decreases as the QAM constellation increases until they coincide at 512-QAM.

Besides, it is clearly understood that the growth in the size of QAM constellation does effect the performance gain of the MMSE canceller, negatively. This effect does not appear in the ZF canceller which explains the coincident of the MMSE and ZF performances at high QAM constellations. This can be accounted as a positive aspect for systems used high-order QAM such as our proposed system design. This simulation results presented here validated the fact that the BER performance can be improved and a large amount of computational effort is maintained by simplify used with ZF as a crosstalk canceller .

More interestingly, by comparing the results in Fig. 5.3 to Fig. 5.5, it can be recognized that an enormous loss in the BER performance in MIMO G.fast system as the size of MIMO configuration increases. For example, for 4×4 MIMO using for 32-QAM, BER is equal to 1e-4 at 20dB SNR. Whereas for 8×8 MIMO using with 32-QAM, BER is close to 2e-2 at 20dB SNR. for 16×16 MIMO using for 32-QAM, BER is worst to 1e-1 at 20dB SNR.

From the above analysis, it is clearly understood that, there is a degradation to the BER performance of the ZF and the MMSE cancellers when the number of twisted pairs in the same binder is increased.

From the results in Fig. 5.3 to Fig. 5.5, it can be noticed that linear and non-linear MMSE cancellers are outperform linear and non-linear ZF cancellers by 2dB at BER $=10^{-3}$ for all three configuration sizes of MIMO G.fast system; 4×4, 8×8 and 16×16.This can be accounted as a positive aspect of the proposed design. the use of ZF will be inevitable to ensure improved rates

As cleared from previous analysis results, the last chapter investigated the effect of IN on the ZF- based MLCW G.fast system model. Ultimately, this chapter enumerates the BER performance of MLCW G.fast system with higher signal constellations such as 32,128 and 512-Quadrature Amplitude Modulation (QAM) using different crosstalk cancellation techniques under the influence of Middleton Class A impulsive noise.

The goal is the comparative analysis of bit error probability of MIMO DMT

G.fast system in two cases: using high–order QAM constellation with different crosstalk cancellation techniques in the presence of Gaussian noise only, and using high–order QAM modulations with different crosstalk cancellation techniques in the presence of Middleton Class A impulsive noise.

Linear and non-linear crosstalk cancellation techniques such as ZF,MMSE ,ZF-SIC and MMSE-SIC are investigated and evaluated here in terms of BER performance in the presence of IN as cleared in Fig. 5.6. Then, it is clear to understood from Fig. 5.7 and Fig. 5.8 that, the BER performance results by using optimal threshold-based IN mitigation method, which has been mentioned in section 4.3, which applied to non-linear cancellation methods, ZF-SIC and MMSE-SIC outperform all BER performance results obtained using OT method applied to linear ZF and MMSE cancellation methods.

By utilizing Zhidkov's algorithm as the IN mitigation method with optimal threshold rather than fixed threshold, the non-linear canceller MMSE confirmation an improvement in BER performance of $2dB$ after the second iteration at BER $=10^{-4}$ compared to the linear canceller MMSE and the same result with linear and non-linear ZF canceller. Referring to Fig. 5.9, note that the complexity curve for ZF-based cancellation is almost the same as the complexity curve for MMSE-based cancellation on different MIMO configurations. More interestingly, as pointed out in Table 5.1, the SIC cancellation schemes has the highest computational complexity compared with linear cancellation schemes. This validates the fact that SIC-based cancellation sustain much computational effort in the calculations of pseudo-inverse of the channel transfer matrix H. Finally, one of the more significant findings to arise from this study that, it is provided an affordable trade-off in term of complexity and BER performance when deployment of broadband copper systems is infeasible or costly.

Table 5.1: Table of operations required by each method at $N_t = N_r$ and $N_r = 4$, 8 and 16 pairs.

Detection Method	**Compixity order**	$N_r = 4$	$N_r = 8$	$N_r = 16$
Linear ZF	$O(9N_r + 2N_rN_t(N_t - 4))$	198	4046	5880
SIC ZF	$O(N2t(2Nr + 1) + NtNr)$	584	6288	8704
Linear MMSE	$O(9N_r + 2N_rN_t(N_t - 4))$	198	4046	5880
SIC MMSE	$O(N2t(2Nr + 1) + NtNr)$	584	6288	8704

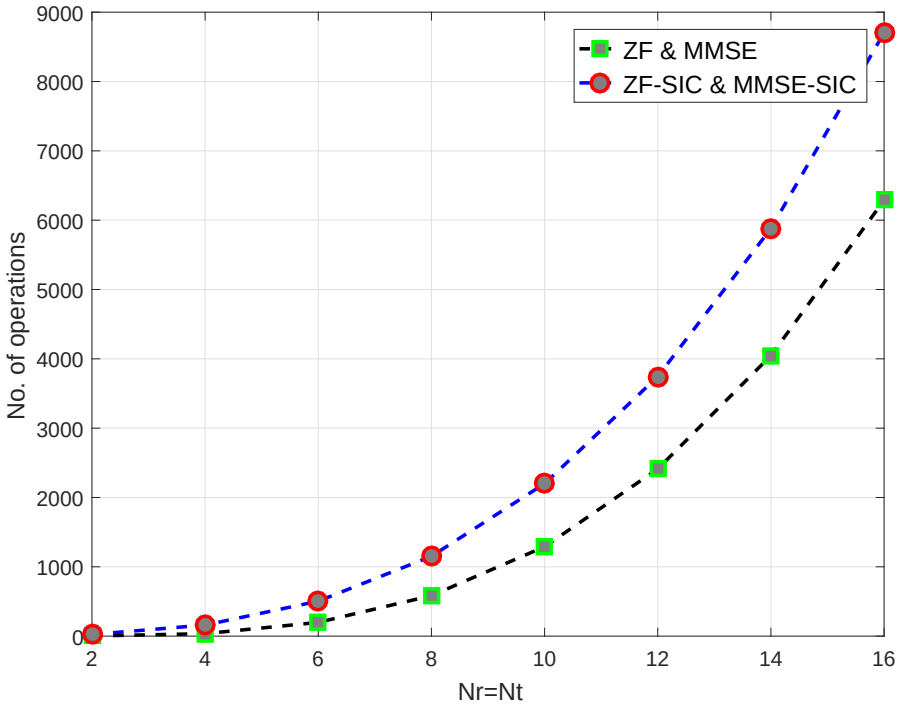

Figure 5.9: A comparison of ZF, MMSE, ZF-SIC and MMSE-SIC crosstalk cancellation methods in terms of computational complexity

5.5 Summary

In this chapter, the performance of linear and non-linear cancellation techniques are analysed for various MIMO system configurations using M-QAM modulation. The comparison between ZF and MMSE cancellers for both linear and SIC techniques is presented for the 2×2 , 4×4 , 8×8 and 16×16 twisted pair G.fast system configurations and also the performance is carried out for 32-QAM, 128-QAM and 512-QAM between ZF and MMSE cancellers.

In this chapter, BER performance of M-QAM MIMO DMT-based G.fast systems

with linear and SIC cancellers is investigated under copper channel [148].

The performance comparison between ZF and MMSE is carried out for the 4×4, 8×8, 16×16 MIMO system configurations and $32 - QAM$, $128 - QAM$ and $512 - QAM$ between ZF and MMSE cancellers. However, performance improvements occur for ZF with an increase in modulation bits/symbol [151]. As the number of pairs in the same binder increases to the order of tens to hundreds, even reduced complexity cancellers becomes very complex. While, with small number of pairs, the full potential of MIMO with high capacities is not achieved.

Chapter 6

Thesis Summary and Future Work

6.1 Thesis Summary

During the last few years, broadband wireline access networks over copper evolved into a viable technology that increases end-user bit rates to meet the rapid growing demand for high data rate communications. One of the major compensations of wireline broadband technology is the use of an existing physical communications infrastructure, namely, the telephone network. The fourth generation of broadband over copper communications infrastructure is known as G.Fast, which was started recently by the International Telecommunication Union (ITU).

Researches in conventional communication systems considered the noise channel as AWGN. However, it is not always the case, due to man-made or natural phenomena that add unwanted noise to the transmitted signal over the channel. For example, AWGN is not suitable to model several applications, such as communication over copper line transmission cables, underwater communications, and power line communication. The principal impairing factor facing the wireline communication systems is IN. Middleton's class A (MCA) noise was considered in this thesis to model IN.

The main contributions offered in this thesis are summarised below:

- Chapter 3 presented a well-designed overview of the G.fast standard, describing the modulation and coding method used for the single line G.fast over copper channel affected by the impact of Gaussian and impulsive noise. This chapter gave an overview on the copper channel model developed for G.fast system, which is the basis of our proposed G.fast channel model. The BER

performance of DMT-based G.fast system over copper channel enumerated for six different higher QAM signal constellations of $M = 32, 128, 512, 2048, 8192$ and $32768 - QAM$ based-DMT with RS+TCM in the presence of IN modelled as the Middleton Class A noise source.

The influence of the Middleton Class A impulsive noise on a G.fast system investigated in this chapter and three different impulse noise mitigation techniques, clipping, blanking, and Zhidkov's algorithm, evaluated along with a fair comparison study in terms of BER performance between these three methods. It can be observed that the frequency domain IN cancellation method achieves a significant BER performance over the traditional TD methods, clipping and blanking, such as, a gain of $8dB$ where $A = 1$, a gain of about $7dB$ with $A = 0.1$, and a gain of up to $6dB$ with $A = 0.001$ at a BER=10^{-4} and Γ is 0.1.

It can be observed that frequency domain IN cancellation method achieved a significant impact on IN compensation process in the G.fast system when utilizing high order QAM constellations, while the traditional TD methods, clipping and blanking underperform to produce a substantial effect on the IN mitigation process. A fixed threshold value used in these three methods for the whole range of SNR values, which was considered as a crucial factor in the impulsive noise compensation process. Because one FT value is not appropriate for all the SNR values, accordingly a novel method of calculating the optimal threshold has been proposed and derived for further improvement of the BER performance of the IN cancellation process based in the frequency domain. In this work, the characteristic parameters of the MCA model, such as impulsive index A and the noise ratio Γ is coupled with optimal threshold value in the derived equation of OT. Moreover, the influence of varying A and Γ investigated and it was found that the changing A and Γ for three different values caused a significant change in the BER performance. Finally, the BER performance results which obtained from the proposed OT calculation equation tested and compared with FT values implemented on the MCA as an IN model. Nonlinearity FD Zhidkov method outperformed all BER performance results achieved using a fixed threshold value by $1.2dB$ at BER = 10^{-4}.

- Attention towards MIMO data transmission systems increased rapidly, thus

G.fast coding system based DMT-MIMO on impulsive noise for broadband wireline applications have been implemented in chapter 4. This chapter focused on a multi-line copper wire model for MLCW G.fast system under the influence of Gaussian and impulsive noise. Using different six QAM signal constellation, $M = 32, 128, 512, 2048, 8192$ and $32768 - QAM$, and under different channel conditions, the BER performance was evaluated and compared for all four different configuration systems 2×2, 4×4, 8×8 and 16×16 MIMO twisted pair G.fast systems.

Moreover, there was an improved performance attained by applying the designed MLCW channel model to the G.fast system compared to the G.fast single-line copper wire system affected by Middleton Class A impulsive noise for all four $M \times N$ MIMO G.fast configurations. The BER performance comparison results between the OT and all fixed thresholds applied to FD method for 2×2, 4×4, 8×8 and 16×16 configurations outperform all four BER performance curves obtained using a fixed threshold values such as, $Th1, Th2, Th3, Th4$ by $1dB$ at BER $= 10^{-4}$.

It recognized, through a comparison of BER performance of MLCW G.fast systems using the IN frequency domain cancellation technique (mentioned in chapter 3 previously) decreases the influence of Middleton Class A noise. The derived OT calculation method achieved a positive effect on performance when it is utilised with Zhidkov's algorithm for all four $M \times N$ MIMO G.fast configurations.

- In chapter 5, the performance of linear and non-linear cancellation techniques analysed for various MIMO system configurations using M-QAM modulation. The comparison between ZF and MMSE cancellers for both linear and SIC techniques presented for the 2×2, 4×4, 8×8 and 16×16 of twisted pair G.fast system configurations and also performance carried out for 32-QAM, 128-QAM and 512-QAM between ZF and MMSE cancellers.

  The simulation results suggested that, the performance of the both non-linear ZF and MMSE cancellers showed good performance compared to the linear ZF MMSE cancellers. From the results, it seen that the non-linear MMSE improved the BER performance of $2dB$ after the second iteration at BER $=10^{-4}$ compared to the linear canceller MMSE and the same result between

linear and non-linear ZF canceller. In addition, by comparing the complexity of the implementation, it observed that the linear algorithms (ZF and MMSE) were computationally simple and almost comparable to SIC techniques. In conclusion, it is clearly understood that there was a degradation to the BER performance of the ZF and the MMSE cancellers when the number of twisted pairs in the same binder increased.

6.2 Future Work

Investigations into the BER performance of DMT-G.fast access network on wired applications over IN environments were the main aspects in this thesis. However, the G.fast system faces new challenges and there are still open problems regarding the enhancement of BER performance. Thus, to completely achieve the aim of accomplishing gigabit date rates over copper channel in G.fast standard, further investigation is still required. In the following, some research points are suggested for future work.

- There is a large amount of research attention towards reduction of impulsive noise influences. The combination of RS code and TCM with interleaving is assumed in the current G.fast standard in chapter 3. It is worth considering the inability of RS codes to the advantage of soft-decisions in their decoding algorithms. The first option is to utilize more advanced FEC codes such as low-density parity-check (LDPC) codes with G.fast standard over copper channel to investigate their behaviour in impulsive noise environments and producing a fair comparison between them to discover robust codes for such harsh environment.

- It is well known that the crosstalk management using MIMO precoding in the downlink and MIMO equalization in the uplink is important to attain the required performance of G.fast system as mentioned before in chapter 4. Therefore, the main considerations for future study would be focus on the MIMO precoding in downlink in the presence of impulsive noise.

- Chapter 5 provided an overview of the most important crosstalk mitigation methods (linear and nonlinear) and explained them through a fair comparison

study. Even so, all these techniques still require high implementation complexity, and more research to reduce the complexity of their mitigation algorithms would be one of the key respects for future study.

References

[1] J. Maes and C. J. Nuzman, "The Past, Present, and Future of Copper Access," *Bell Labs Technical Journal*, vol. 20, pp. 1–10, 2015.

[2] J. H. Van Wyk and L. P. Linde, "Performance evaluation of a gigabit DSL modem using super orthogonal complete complementary codes under practical crosstalk conditions," *SAIEE Africa Research Journal*, vol. 108, no. 4, pp. 144–149, 2017.

[3] P. Golden, H. Dedieu, and K. S. Jacobsen, *Fundamentals of DSL technology*. CRC Press, 2005.

[4] W. Coomans, R. B. Moraes, K. Hooghe, and J. Maes, "The 5th Generation Broadband Copper Access," in *Broadband Coverage in Germany. 9th ITG Symposium. Proceedings*. VDE, 2015, pp. 1–5.

[5] J. Maes and C. J. Nuzman, "The Past, Present, and Future of Copper Access," *Bell Labs Technical Journal*, vol. 20, pp. 1–10, 2015.

[6] C. Sales, R. M. Rodrigues, F. Lindqvist, J. Costa, A. Klautau, K. Ericson, J. R. i Riu, and P. O. Borjesson, "Line topology identification using multi-objective evolutionary computation," *IEEE Transactions on Instrumentation and Measurement*, vol. 59, no. 3, pp. 715–729, 2010.

[7] Y. Ma and Z. Jia, "Evolution and trends of broadband access technologies and fiber-wireless systems," in *Fiber-Wireless Convergence in Next-Generation Communication Networks*. Springer, 2017, pp. 43–75.

[8] B. Li, "Performance Enhancement in Copper Twisted Pair Cable Communications," 2016.

[9] S. Zafaruddin, I. Bergel, and A. Leshem, "Signal processing for gigabit-rate wireline communications: An overview of the state of the art and research challenges," *IEEE Signal Processing Magazine*, vol. 34, no. 5, pp. 141–164, 2017.

[10] M. Nevosad and P. Lafata, "Modelling of Propagation Constant of Twisted Pairs and Its Temperature Dependence at G. fast Frequencies," *Elektronika ir Elektrotechnika*, vol. 22, no. 2, pp. 107–113, 2016.

[11] D. Acatauassu, I. Almeida, F. Muller, A. Klautau, C. Lu, K. Ericson, and B. Dortschy, "Measurement and modeling techniques for the fourth generation broadband over copper," in *Advanced Topics in Measurements*. IntechOpen, 2012.

[12] P. Lafata, "Simple attenauation models of metallic cables suitable for G. fast frequencies," 2015.

[13] D. Acatauassu, S. Höst, C. Lu, M. Berg, A. Klautau, and P. O. Börjesson, "Simple and causal twisted-pair channel models for G.fast Systems," in *2013 IEEE Global Communications Conference (GLOBECOM)*, Dec 2013, pp. 2834–2839.

[14] R. Strobel, *Channel Modeling and Physical Layer Optimization in Copper Line Networks*. Springer, 2019.

[15] S. J. Lee, F. Breyer, S. Randel, H. P. Van Den Boom, and A. M. Koonen, "High-speed transmission over multimode fiber using discrete multitone modulation," *Journal of Optical Networking*, vol. 7, no. 2, pp. 183–196, 2008.

[16] Y. Ruan, *Interference Cancellation Techniques for Multiple-Line Transmission in Modern DSL Systems*. Cuvillier Verlag, 2014.

[17] J. Zhang, S. Chen, R. Zhang, A. F. Al Rawi, and L. Hanzo, "Differential evolution algorithm aided turbo channel estimation and multi-user detection for G.Fast systems in the presence of FEXT," *IEEE Access*, vol. 6, pp. 33 111–33 128, 2018.

[18] A. Ahrens and C. Lange, "Iteratively Detected MIMO-OFDM Twisted-Pair Transmission Schemes," in *International Conference on E-Business and Telecommunications*. Springer, 2008, pp. 281–293.

[19] D. Middleton, I. of Electrical, and E. Engineers, *An introduction to statistical communication theory*. IEEE press Piscataway, NJ, 1996.

[20] D. Middleton, "Statistical-physical models of electromagnetic interference," *IEEE Transactions on Electromagnetic Compatibility*, no. 3, pp. 106–127, 1977.

[21] L. A. Berry, "Understanding Middleton's canonical formula for class A noise," *IEEE Transactions on Electromagnetic compatibility*, no. 4, pp. 337–344, 1981.

[22] K. Vastola, "Threshold detection in narrow-band non-Gaussian noise," *IEEE Transactions on Communications*, vol. 32, no. 2, pp. 134–139, 1984.

[23] S. Miyamoto, M. Katayama, and N. Morinaga, "Performance analysis of QAM systems under class A impulsive noise environment," *IEEE transactions on electromagnetic compatibility*, vol. 37, no. 2, pp. 260–267, 1995.

[24] R. Haring and A. H. Vinck, "Performance bounds for optimum and suboptimum reception under class-A impulsive noise," *IEEE Transactions on Communications*, vol. 50, no. 7, pp. 1130–1136, 2002.

[25] K. Wiklundh, P. Stenumgaard, and H. Tullberg, "Channel capacity of Middleton's class A interference channel," *Electronics letters*, vol. 45, no. 24, pp. 1227–1229, 2009.

[26] T. Shongwey, A. H. Vinck, and H. C. Ferreira, "On impulse noise and its models," in *Power Line Communications and its Applications (ISPLC), 2014 18th IEEE International Symposium on*. IEEE, 2014, pp. 12–17.

[27] Z. Xie, R. T. Short, and C. K. Rushforth, "A family of suboptimum detectors for coherent multiuser communications," *IEEE Journal on Selected Areas in Communications*, vol. 8, no. 4, pp. 683–690, May 1990.

[28] A. Klein, G. K. Kaleh, and P. W. Baier, "Zero forcing and minimum mean-square-error equalization for multiuser detection in code-division multiple-

access channels," *IEEE Transactions on Vehicular Technology*, vol. 45, no. 2, pp. 276–287, May 1996.

[29] A. Duel-Hallen, "A family of multiuser decision-feedback detectors for asynchronous code-division multiple-access channels," *IEEE Transactions on Communications*, vol. 43, no. 2/3/4, pp. 421–434, Feb 1995.

[30] J. Proakis, G. Bauch, and M. Salehi, *Modern Communication Systems Using MATLAB*. Cengage Learning, 2013.

[31] J. Proakis, *Digital Communications*, ser. McGraw-Hill series in electrical and computer engineering : communications and signal processing. McGraw-Hill, 2001.

[32] I. A. Bello, B. Halak, M. El-Hajjar, and M. Zwolinski, "A survey of VLSI implementations of tree search algorithms for MIMO detection," *Circuits, Systems, and Signal Processing*, vol. 35, no. 10, pp. 3644–3674, 2016.

[33] D. Wei, A. Fazlollahi, G. Long, and E. Wang, "G. fast for FTTdp: Enabling gigabit copper access," in *Globecom Workshops (GC Wkshps), 2014*. IEEE, 2014, pp. 668–673.

[34] S. Kumar and R. Gupta, "Bit error rate analysis of Reed-Solomon code for efficient communication system," *International Journal of Computer Applications*, vol. 30, no. 12, pp. 11–15, 2011.

[35] Z. Jianyong and I. B. Djordjevic, "Mapping design of a four-dimensional 32-ary signal constellation over an AWGN channel," *Communications, China*, vol. 11, no. 7, pp. 64–73, 2014.

[36] J. Daniel and J. Costello, "Error control coding, fundamentals and applications," 1983.

[37] M. Timmers, M. Guenach, C. Nuzman, and J. Maes, "G. fast: Evolving the copper access network," *Communications Magazine, IEEE*, vol. 51, no. 8, pp. 74–79, 2013.

[38] L. Gui, Y. Xu, B. Liu, L. Gong, and Y. Li, "An iterative decoding technique and architecture for RS concatenated TCM coding systems," *Consumer Electronics, IEEE Transactions on*, vol. 56, no. 3, pp. 1288–1296, 2010.

[39] H. Lee, "Reed-solomon decoder systems for high speed communication and data storage applications," Sep. 8 2005, uS Patent App. 11/222,435.

[40] R. E. Blahut, "Transform techniques for error control codes," *IBM Journal of Research and development*, vol. 23, no. 3, pp. 299–315, 1979.

[41] A. Agarwal, M. C. Ng, and R. Arvind, "A Comparative Evaluation of High-Level Hardware Synthesis Using Reed–Solomon Decoder," *Embedded Systems Letters, IEEE*, vol. 2, no. 3, pp. 72–76, 2010.

[42] X. Hu, "A novel high-speed trellis-coded modulation encoder/decoder ASIC design," Ph.D. dissertation, University of Saskatchewan Saskatoon, 2003.

[43] G. Ungerboeok, "Signal Sets, Part I: Introduction," *IEEE communications Magazine*, vol. 25, no. 2, 1987.

[44] H. Thune, "Trellis Coded Modulation(TCM) System for Satellite Communication:A Review," *International Engineering Research Journal (IERJ)*, vol. 1, pp. 507–512, 2015.

[45] G. Ungerboeck and I. Csajka, "On improving data-link performance by increasing the channel alphabet and introducing sequence coding," in *IEEE Int'l. Symp. Info. Theory*, 1976.

[46] S. Ten Brink, "Convergence behavior of iteratively decoded parallel concatenated codes," *Communications, IEEE Transactions on*, vol. 49, no. 10, pp. 1727–1737, 2001.

[47] G. Ungerboeck, "Channel coding with multilevel/phase signals," *Information Theory, IEEE Transactions on*, vol. 28, no. 1, pp. 55–67, 1982.

[48] M. Hong *et al.*, "Analysis of the Bit Error Rate of Trellis-coded Modulation," Ph.D. dissertation, Citeseer, 2002.

[49] G. Ungerboeck, "Trellis-coded modulation with redundant signal sets Part II: State of the art," *Communications Magazine, IEEE*, vol. 25, no. 2, pp. 12–21, 1987.

[50] K. J. Hole, H. Holm, and G. E. Øien, "Adaptive multidimensional coded modulation over flat fading channels," *Selected Areas in Communications, IEEE Journal on*, vol. 18, no. 7, pp. 1153–1158, 2000.

[51] R. Fang and W. Lee, "Four-dimensionally coded PSK systems for combatting effects of severe ISI and CCI," in *Globecom'83-Global Telecommunications Conference*, vol. 1, 1983, pp. 1032–1038.

[52] A. Calderbank and N. Sloane, "Four-dimensional modulation with an eight-state trellis code," *AT&T technical journal*, vol. 64, no. 5, pp. 1005–1018, 1985.

[53] M. A. Chishtie, *Viterbi implementation on the TMS320C5x for V. 32 modems*. Texas Instruments Incorporated, 1996.

[54] D. Forney, "Concatenated codes," *Scholarpedia*, vol. 4, no. 2, p. 8374, 2009.

[55] G. Ferland, "Modelling of a Trellis Decoder used as Inner Code in a concatenated coding system," in *Electrical and Computer Engineering, 1993. Canadian Conference on*. IEEE, 1993, pp. 259–261.

[56] O. Aitsab and R. Pyndiah, "Performance of concatenated Reed-Solomon/convolutional codes with iterative decoding," in *Global Telecommunications Conference, 1997. GLOBECOM'97., IEEE*, vol. 2. IEEE, 1997, pp. 934–938.

[57] I. S. Reed and G. Solomon, "Polynomial codes over certain finite fields," *Journal of the society for industrial and applied mathematics*, vol. 8, no. 2, pp. 300–304, 1960.

[58] R. N. Bjørk, H. Ytre-Hauge, E. Rosnes, and A. Vahlin, "COMPARISON OF TCM+ RS CODING AND TURBO CODES FOR SPECTRALLY EFFICIENT LOW-DELAY SYSTEMS."

[59] K.-T. Chen, S.-K. Yang, F.-H. Kuo, and R.-R. Lee, "The evaluation of next-generation copper-wire technology," in *Network Operations and Management Symposium (APNOMS), 2015 17th Asia-Pacific*. IEEE, 2015, pp. 412–415.

[60] M. Peeters and S. Vanhastel, "The Copper Phantom," *OSP Mag*, 2011.

[61] P. Ödling, T. Magesacher, S. Höst, P. O. Börjesson, M. Berg, and E. Areizaga, "The fourth generation broadband concept," *Communications Magazine, IEEE*, vol. 47, no. 1, pp. 62–69, 2009.

[62] R. Strobel and W. Utschick, "Coexistence of G. fast and VDSL in FTTdp and FTTC Deploy-ments."

[63] T. Plückebaum, S. Jay, and K.-H. Neumann, "VDSL and G. fast Vectoring and the impact on VULA," 2014.

[64] F. Mazzenga, R. Giuliano, M. Petracca, M. Vari, and F. Vatalaro, "A downstream power back-off procedure for Mixed FTTC and FTTDp scenarios," *Communications Letters, IEEE*, vol. 18, no. 6, pp. 965–968, 2014.

[65] M. Timmers, K. Hooghe, M. Guenach, and J. Maes, "Digital Complexity in DSL: an Extrapolated Historical Overview," *proceedings of Access*, 2011.

[66] Littelfuse, "Littelfuse Electronics - G.Fast FTTH FTTP FTTdp technology," 2019. [Online]. Available: https://info.littelfuse.com/gfast-solutions

[67] M. Guenach, C. Nuzman, P. Tsiaflakis, and J. Maes, "Power optimization in vectored and non-vectored G. fast transmission," in *Global Communications Conference (GLOBECOM), 2014 IEEE*. IEEE, 2014, pp. 2229–2233.

[68] P. Biyani, A. Mahadevan, S. Prakriya, P. Duvaut, and S. Prasad, "Cooperative alien noise cancellation in upstream VDSL: A new decision directed approach," *Communications, IEEE Transactions on*, vol. 61, no. 8, pp. 3494–3504, 2013.

[69] A. Colmegna, S. Galli, and M. Goldburg, "Methods for supporting vectoring when multiple service providers share the cabinet area," *FASTWEB/ASSIA Vectoring White Paper*, 2012.

[70] G. Ginis and J. M. Cioffi, "Vectored transmission for digital subscriber line systems," *Selected Areas in Communications, IEEE Journal on*, vol. 20, no. 5, pp. 1085–1104, 2002.

[71] K. Kerpez, J. Cioffi, S. Galli, G. Ginis, M. Goldburg, M. Mohseni, and A. Chowdhery, "Compatibility of vectored and non-vectored VDSL2," in *Information Sciences and Systems (CISS), 2012 46th Annual Conference on*. IEEE, 2012, pp. 1–6.

[72] W. Coomans, R. B. Moraes, K. Hooghe, A. Duque, J. Galaro, M. Timmers, A. J. van Wijngaarden, M. Guenach, and J. Maes, "XG-FAST: Towards 10

Gb/s copper access," in *Globecom Workshops (GC Wkshps), 2014.* IEEE, 2014, pp. 630–635.

[73] C. E. Shannon, "A mathematical theory of communication," *ACM SIGMOBILE Mobile Computing and Communications Review*, vol. 5, no. 1, pp. 3–55, 2001.

[74] N. Singh and G. Kaur, "Performance comparison of RSC-RSC and NSC-NSC serially concatenated convolutional code using non-iterative Viterbi decoding technique," in *Communications and Signal Processing (ICCSP), 2015 International Conference on.* IEEE, 2015, pp. 0465–0468.

[75] G. D. Forney and G. D. Forney, *Concatenated codes.* Citeseer, 1966, vol. 11.

[76] J. Hagenauer and P. Hoeher, "Concatenated viterbi decoding," in *Proc. 4th Joint Swedish-Soviet Int. Workshop on Information Theory*, 1989, pp. 29–33.

[77] D. J. MacKay and R. M. Neal, "Near Shannon limit performance of low density parity check codes," *Electronics letters*, vol. 33, no. 6, pp. 457–458, 1997.

[78] S. Benedetto and G. Montorsi, "Serial concatenation of block and convolutional codes," *Electronics Letters*, vol. 32, no. 10, pp. 887–888, 1996.

[79] R. M. Pyndiah, "Near-optimum decoding of product codes: block turbo codes," *Communications, IEEE Transactions on*, vol. 46, no. 8, pp. 1003–1010, 1998.

[80] R. G. Gallager, "Low-density parity-check codes," *Information Theory, IRE Transactions on*, vol. 8, no. 1, pp. 21–28, 1962.

[81] D. J. MacKay, "Good error-correcting codes based on very sparse matrices," *Information Theory, IEEE Transactions on*, vol. 45, no. 2, pp. 399–431, 1999.

[82] T. Flo, P. Orten, and B. Risløv, "Evaluation of coding schemes for spectrally efficient lowdelay radio systems," in *Proc. of 3rd International Symp. on Turbo Codes & Related Topics*, 2003, pp. 387–390.

[83] K. Manish and S. Jyoti, "Performance Comparison of RSC-RSC Concatenated code and RS-RSC Concatenated code using Non-iterative Concatenated

Viterbi Decoding Technique," *Manuscript submitted for publication, IEEE proceedings of ICMIRA*, 2013.

[84] M. Takeda, F. Smith, and A. Klautau, "A comparison between RS+ TCM and LDPC for G. fast channel coding," in *Circuits & Systems (LASCAS), 2015 IEEE 6th Latin American Symposium on.* IEEE, 2015, pp. 1–5.

[85] F. DĂRĂBAN, "Generalization of Wei's construction for the 2N-dimensional TCM encoder and decoder," in *Proceedings of the International Workshop "Trends and Recent Achivements in Information Technology*, pp. 205–213.

[86] G. D. Forney Jr, R. G. Gallager, G. R. Lang, F. M. Longstaff, and S. U. Qureshi, "Efficient modulation for band-limited channels," *Selected Areas in Communications, IEEE Journal on*, vol. 2, no. 5, pp. 632–647, 1984.

[87] A. Calderbank and N. Sloane, "Four-dimensional modulation with eight-state trellis code, AT&T Tech," *Journal*, vol. 64, pp. 1005–1018.

[88] G. D. Forney Jr, "Geometrically uniform codes," *Information Theory, IEEE Transactions on*, vol. 37, no. 5, pp. 1241–1260, 1991.

[89] J. W. Cook, R. H. Kirkby, M. G. Booth, K. T. Foster, D. E. A. Clarke, and G. Young, "The noise and crosstalk environment for adsl and vdsl systems," *IEEE Communications Magazine*, vol. 37, no. 5, pp. 73–78, May 1999.

[90] J. Armstrong and H. A. Suraweera, "Impulse noise mitigation for OFDM using decision directed noise estimation," in *Spread Spectrum Techniques and Applications, 2004 IEEE Eighth International Symposium on.* IEEE, 2004, pp. 174–178.

[91] S. V. Zhidkov, "Analysis and comparison of several simple impulsive noise mitigation schemes for OFDM receivers," *IEEE Transactions on Communications*, vol. 56, no. 1, pp. 5–9, January 2008.

[92] J. Haring and A. H. Vinck, "Iterative decoding of codes over complex numbers for impulsive noise channels," *IEEE Transactions on Information Theory*, vol. 49, no. 5, pp. 1251–1260, 2003.

[93] M. Sliskovic, "Signal processing algorithm for OFDM channel with impulse noise," in *Electronics, Circuits and Systems, 2000. ICECS 2000. The 7th IEEE International Conference on*, vol. 1. IEEE, 2000, pp. 222–225.

[94] F. Abdelkefi, P. Duhamel, and F. Alberge, "On the use of pilot tones for impulse noise cancellation in Hiperlan2," in *Signal Processing and its Applications, Sixth International, Symposium on. 2001*, vol. 2. IEEE, 2001, pp. 591–594.

[95] S. V. Zhidkov, "Impulsive noise suppression in OFDM-based communication systems," *IEEE Transactions on Consumer Electronics*, vol. 49, no. 4, pp. 944–948, Nov 2003.

[96] J. Armstrong and H. A. Suraweera, "Impulse noise mitigation for OFDM using decision directed noise estimation," in *Eighth IEEE International Symposium on Spread Spectrum Techniques and Applications - Programme and Book of Abstracts (IEEE Cat. No.04TH8738)*, Aug 2004, pp. 174–178.

[97] E. Alsusa and K. M. Rabie, "Dynamic Peak-Based Threshold Estimation Method for Mitigating Impulsive Noise in Power-Line Communication Systems," *IEEE Transactions on Power Delivery*, vol. 28, no. 4, pp. 2201–2208, Oct 2013.

[98] K. Rabie, E. Alsusa, A. Familua, and L. Cheng, "Constant envelope OFDM transmission over impulsive noise power-line communication channels," in *Power Line Communications and its Applications (ISPLC), 2015 International Symposium on*. IEEE, 2015, pp. 13–18.

[99] A. G. Olson, A. Chopra, Y. Mortazavi, I. C. Wong, and B. L. Evans, "Real-Time MIMO Discrete Multitone Transceiver Testbed," in *2007 Conference Record of the Forty-First Asilomar Conference on Signals, Systems and Computers*. IEEE, 2007, pp. 126–129.

[100] M. L. Honig, K. Steiglitz, and B. Gopinath, "Multichannel signal processing for data communications in the presence of crosstalk," *IEEE Trans. Commun.*, vol. 38, no. 4, pp. 551–558, 1990.

[101] G. Ginis and C.-N. Peng, "Alien crosstalk cancellation for multipair digital subscriber line systems," *EURASIP J. Adv. Signal Process.*, vol. 2006, no. 1, p. 016828, 2006.

[102] G. Taubock and W. Henkel, "MIMO systems in the subscriber-line network," in *Proc. of the 5th Int. OFDM-Workshop*. Citeseer, 2000, pp. 18–1.

[103] R. Cendrillon, G. Ginis, M. Moonen, and K. Van Acker, "Partial crosstalk precompensation in downstream VDSL," *Signal Process.*, vol. 84, no. 11, pp. 2005–2019, 2004.

[104] R. Cendrillon, M. Moonen, G. Ginis, K. Van Acker, T. Bostoen, and P. Vandaele, "Partial crosstalk cancellation for upstream VDSL," *EURASIP J. Appl. Signal Process.*, vol. 2004, pp. 1520–1535, 2004.

[105] A. G. Olson, A. Chopra, Y. Mortazavi, I. C. Wong, and B. L. Evans, "Real-time MIMO discrete multitone transceiver testbed," in *Forty-First Asilomar Conference Signals, Syst. Comput. ACSSC 2007.* IEEE, 2007, pp. 126–129.

[106] R. Cendrillon, M. Moonen, E. Van den Bogaert, and G. Ginis, "The linear zero-forcing crosstalk canceller is near-optimal in DSL channels," in *IEEE Global Telecommun. Conf. (GLOBECOM)*, 2004, pp. 2334–2338.

[107] R. Cendrillon, M. Moonen, J. Verlinden, T. Bostoen, and G. Ginis, "Improved linear crosstalk precompensation for DSL," in *Proc. IEEE Int. Conf. Acoustics, Speech, and Signal Process. (ICASSP'04).*, vol. 4. IEEE, 2004, pp. iv–1053.

[108] P. K. Pandey, M. Moonen, and L. Deneire, "MMSE-based partial crosstalk cancellation for upstream VDSL," *Signal Processing*, vol. 92, no. 7, pp. 1602–1610, 2012.

[109] A. Ahrens and C. Lange, "Iteratively Detected MIMO-OFDM Twisted-Pair Transmission Schemes," in *International Conference on E-Business and Telecommunications*. Springer, 2008, pp. 281–293.

[110] R. Cendrillon, M. Moonen, R. Suciu, and G. Ginis, "Simplified power allocation and TX/RX structure for MIMO-DSL," in *Global Telecommunications*

Conference, 2003. GLOBECOM'03. IEEE, vol. 4. IEEE, 2003, pp. 1842–1846.

[111] A. Leshem and L. Youming, "A low complexity linear precoding technique for next generation VDSL downstream transmission over copper," *IEEE Transactions on Signal Processing*, vol. 55, no. 11, pp. 5527–5534, 2007.

[112] W. Yu and J. Cioffi, "Multiuser detection in vector multiple access channels using generalized decision feedback equalization," in *Proc. 5th Int. Conf. on Signal Processing, World Computer Congress*, 2000.

[113] V. Oksman, H. Schenk, A. Clausen, J. M. Cioffi, M. Mohseni, G. Ginis, C. Nuzman, J. Maes, M. Peeters, K. Fisher *et al.*, "The ITU-T's new G. vector standard proliferates 100 Mb/s DSL," *IEEE Communications Magazine*, vol. 48, no. 10, 2010.

[114] I. Bergel and A. Leshem, "The performance of zero forcing DSL systems," *IEEE Signal Processing Letters*, vol. 20, no. 5, pp. 527–530, 2013.

[115] R. Cendrillon, G. Ginis, E. Van den Bogaert, and M. Moonen, "A near-optimal linear crosstalk precoder for downstream VDSL," *IEEE Transactions on Communications*, vol. 55, no. 5, pp. 860–863, 2007.

[116] I. Wahibi, M. Ouzzif, J. Le Masson, and S. Saoudi, "Stationary interference cancellation in upstream coordinated DSL using a turbo-MMSE receiver," *International Journal of Digital Multimedia Broadcasting*, vol. 2008, 2008.

[117] C.-Y. Chen, K. Seong, R. Zhang, and J. M. Cioffi, "Optimized resource allocation for upstream vectored DSL systems with zero-forcing generalized decision feedback equalizer," *IEEE Journal of Selected Topics in Signal Processing*, vol. 1, no. 4, pp. 686–699, 2007.

[118] P. Tsiaflakis, J. Vangorp, J. Verlinden, and M. Moonen, "Multiple access channel optimal spectrum balancing for upstream DSL transmission," *IEEE Communications Letters*, vol. 11, no. 4, 2007.

[119] R. Hormis, D. Guo, and X. Wang, "Monte Carlo FEXT cancellers for DSL channels," *IEEE Transactions on Circuits and Systems I: Regular Papers*, vol. 52, no. 9, pp. 1894–1908, 2005.

[120] S. Hu and F. Rusek, "Modulus Zero-Forcing Detection for MIMO Channels," *arXiv preprint arXiv:1801.00947*, 2018.

[121] A. Barthelme, R. Strobel, M. Joham, and W. Utschick, "Weighted MMSE Tomlinson-Harashima precoding for G. fast," in *Global Communications Conference (GLOBECOM), 2016 IEEE*. IEEE, 2016, pp. 1–6.

[122] J. Maes and C. J. Nuzman, "The Past, Present, and Future of Copper Access," *Bell Labs Technical Journal*, vol. 20, pp. 1–10, 2015.

[123] T. Bai, H. Zhang, J. Zhang, C. Xu, A. F. Al Rawi, and L. Hanzo, "Impulsive noise mitigation in digital subscriber lines: The state-of-the-art and research opportunities," *IEEE Communications Magazine*, vol. 57, no. 5, pp. 145–151, 2019.

[124] X. Hu, Z. Chen, and F. Yin, "Impulsive noise cancellation for MIMO power line communications," *Journal of Communications*, vol. 9, no. 3, pp. 241–247, 2014.

[125] Y. Himeur and A. Boukabou, "An adaptive recursive noise compensator for impulsive noise mitigation over OFDM power line communication," *AEU-International Journal of Electronics and Communications*, vol. 70, no. 1, pp. 105–112, 2016.

[126] T. Bai, H. Zhang, R. Zhang, L. L. Yang, A. F. A. Rawi, J. Zhang, and L. Hanzo, "Discrete Multi-Tone Digital Subscriber Loop Performance in the Face of Impulsive Noise," *IEEE Access*, vol. 5, pp. 10 478–10 495, 2017.

[127] R. Pighi, M. Franceschini, G. Ferrari, and R. Raheli, "Fundamental performance limits of communications systems impaired by impulse noise," *IEEE Transactions on Communications*, vol. 57, no. 1, pp. 171–182, January 2009.

[128] S. Laksir and A. Tamtaoui, "Reduction of the effect of impulsive noise on image transmission in OFDM-based power line communications," in *2016 International Conference on Information Technology for Organizations Development (IT4OD)*, March 2016, pp. 1–6.

[129] A. Mengi and A. J. H. Vinck, "Successive impulsive noise suppression in OFDM," in *ISPLC2010*, March 2010, pp. 33–37.

[130] L.-F. Wei, "Trellis-coded modulation with multidimensional constellations," *Information Theory, IEEE Transactions on*, vol. 33, no. 4, pp. 483–501, 1987.

[131] E. Martos-Naya, J. López-Fernández, L. D. del Rio, M. C. Aguayo-Torres, and J. E. Munoz, "Optimized interpolator filters for timing error correction in DMT systems for xDSL applications," *IEEE Journal on Selected Areas in Communications*, vol. 19, no. 12, pp. 2477–2485, 2001.

[132] W. Abd-Alaziz, Z. Mei, M. Johnston, and S. L. Goff, "Non-binary turbo-coded OFDM-PLC system in the presence of impulsive noise," in *2017 25th European Signal Processing Conference (EUSIPCO)*, Aug 2017, pp. 2576–2580.

[133] D. Middleton, "Statistical-Physical Models of Electromagnetic Interference," *IEEE Transactions on Electromagnetic Compatibility*, vol. EMC-19, no. 3, pp. 106–127, Aug 1977.

[134] T. Magesacher, M. Jakovljevic, M. Loiola, P. Odling, P. Borjesson *et al.*, "Measurement and modeling of short copper cables for ultra-wideband communication," in *Proceedings of SPIE-The International Society for Optical Engineering*, 2006.

[135] H. Matsuo, D. Umehara, M. Kawai, and Y. Morihiro, "An iterative detection for OFDM over impulsive noise channel," in *Proceedings of the 6th International Symposium on Power-Line Communications and its Applications (ISPLC)*, 2002, pp. 27–29.

[136] Z. Ali, F. Ayaz, and C.-S. Park, "Optimized threshold calculation for blanking nonlinearity at OFDM receivers based on impulsive noise estimation," *EURASIP Journal on Wireless Communications and Networking*, vol. 2015, no. 1, p. 191, 2015.

[137] A. Spaulding and D. Middleton, "Optimum reception in an impulsive interference environment–part I: coherent detection," *IEEE Trans. Inf. Theory*, vol. 25, no. 9, pp. 910–923, 1977.

[138] J. G. Proakis, "Digital communications. 2008," *McGraw-Hill, New York*.

[139] K. M. Rabie and E. Alsusa, "Performance analysis of adaptive hybrid nonlinear preprocessors for impulsive noise mitigation over power-line channels," in *2015*

IEEE International Conference on Communications (ICC), June 2015, pp. 728–733.

[140] S. Kiykioglu, "Central office interface techniques for digital subscriber lines," Nov. 30 2004, uS Patent 6,826,278.

[141] R. Peng and R.-R. Chen, "Application of nonbinary LDPC cycle codes to MIMO channels," *IEEE Trans. Wireless Commun.*, vol. 7, no. 6, 2008.

[142] T. Magesacher, W. Henkel, G. Tauböck, and T. Nordström, "Cable measurements supporting xDSL technologies," *e&i Elektrotechnik und Informationstechnik*, vol. 119, no. 2, pp. 37–43, 2002.

[143] I. Al-Neami, C. T. Healy, M. Johnston, and C. Tsimenidis, "Investigation into Impulsive Noise Techniques for a G.FAST System," in *2018 11th International Symposium on Communication Systems, Networks Digital Signal Processing (CSNDSP)*, July 2018, pp. 1–5.

[144] G. ITU-T, "9701–Fast access to subscriber terminals (G. fast)-Physical layer specification," *ITU-T recommendation, Series G: Transmission Systems and Media, Digital Systems and Networks*, 2014.

[145] T. Magesacher, W. Henkel, G. Tauböck, and T. Nordström, "Cable measurements supporting xDSL technologies," *e&i Elektrotechnik und Informationstechnik*, vol. 119, no. 2, pp. 37–43, 2002.

[146] W. Y. Chen, "DSL: simulation techniques and standards development for digital subscriber lines," *In: Macmillan Technology Series, Macmillan Technical Publishing, Indianapolis*, 1998.

[147] E. W. M. Coladarci Theodore, Casey D. Cobb and R. C. Clarke, *Fundamentals of statistical reasoning in education.* John Wiley & Sons, 2010.

[148] J. Han, X. Tao, and Q. Cui, "Lower bound of BER in M-QAM MIMO system with ordered ZF-SIC receiver," in *Vehicular Technology Conference, 2009. VTC Spring 2009. IEEE 69th.* IEEE, 2009, pp. 1–5.

[149] P. Zhang, X. Tao, J. Zhang, Y. Wang, L. Li, and Y. Wang, "A vision from the future: beyond 3G TDD," *IEEE Communications Magazine*, vol. 43, no. 1, pp. 38–44, 2005.

[150] S. Zafaruddin, I. Bergel, and A. Leshem, "Signal processing for gigabit-rate wireline communications: An overview of the state of the art and research challenges," *IEEE Signal Processing Magazine*, vol. 34, no. 5, pp. 141–164, 2017.

[151] S. Adnan, N. U. Rehman, and M. I. Zahoor, "Effect of different modulation techniques comparison of linear MIMO receivers," *International Journal of Computer Applications*, vol. 121, no. 20, pp. 36–40, 2015.